Häussinger D, Beuers U, Trauner M (eds): XXII International Bile Acid Meeting – Hepatic and Extrahepatic Targets of Bile Acid Signaling.
Falk Symposium 184, Vienna, 2012, pp 10–18

Molecular Basis and Mechanism of Rotor Syndrome

Viktor Stránecký[a, b] Evita van de Steeg[d] Magdaléna Neřoldová[c]
Ondřej Lukšan[c] A.S. Knisely[e] Stanislav Kmoch[a, b] Alfred H. Schinkel[d]
Milan Jirsa[c]

[a]Center for Applied Genomics and [b]Institute of Inherited Metabolic Diseases, Charles University of Prague, First Faculty of Medicine, and [c]Institute for Clinical and Experimental Medicine, Prague, Czech Republic; [d]Division of Molecular Oncology, The Netherlands Cancer Institute, Amsterdam, The Netherlands; [e]Institute of Liver Studies, King's College Hospital, London, UK

Key Words
Hereditary jaundice · Hyperbilirubinemia · Rotor syndrome · OATP1B1 · OATP1B3

Abstract
Background/Aims: Bilirubin, a breakdown product of heme, is normally glucuronidated and excreted by the liver into bile. Failure of this system can lead to a build up of conjugated bilirubin in the blood, resulting in jaundice. The mechanistic basis of bilirubin excretion and hyperbilirubinemia syndromes is largely understood, but that of Rotor syndrome has remained enigmatic. ***Methods:*** We mapped the genes mutated in 8 Rotor syndrome families and elucidated the mechanism of Rotor hyperbilirubinemia using genetically modified mouse strains. ***Results:*** We found that Rotor subjects carry mutations in *SLCO1B1* and *SLCO1B3* causing complete and simultaneous deficiencies of the organic anion transporting polypeptides OATP1B1 and OATP1B3. These liver-specific proteins mediate uptake of conjugated and unconjugated bilirubin, unconjugated bile salts, xenobiotics, toxins, and countless drugs, drug metabolites, and their conjugates across the sinusoidal membrane of hepatocytes. Using mice deficient in Oatp1a/1b and in the multispecific sinusoidal export pump Mrp3, we found that Mrp3 secretes bilirubin conjugates into the blood, while Oatp1a/1b transporters mediate their hepatic reuptake. Transgenic expression of human OATP1B1 or OATP1B3 restored the function of this detoxification-enhancing liver-blood shuttle in Oatp1a/1b-deficient mice. Within liver lobules, this shuttle may allow transfer of bilirubin (and probably also drug) conjugates formed in upstream hepatocytes to downstream hepatocytes, thereby preventing local saturation of detoxification processes and hepatocyte toxic injury. OATP1B proteins may also be responsible for clearance of bilirubin conjugated in extrahepatic tissues. ***Conclusion:*** Disruption of hepatic uptake of bilirubin glucuronides due to coexisting OATP1B1 and OATP1B3 deficiencies explains Rotor-type hyperbilirubinemia.

Introduction

Unconjugated bilirubin (UCB) bound to albumin in blood is taken up by hepatocytes, bound to cytosolic ligandin, and transported to endoplasmic reticulum, where conjugation with glucuronic acid takes place. Conjugated bilirubin is then translocated back to cytoplasm, from which multidrug resistance-associated protein MRP2 (gene: *ABCC2*) excretes it into bile. In cholestatic liver diseases, conjugated bilirubin flow is redirected to blood by MRP3 (gene: *ABCC3*), which is upregulated at the sinusoidal membrane [1].

Milan Jirsa
Institute for Clinical and Experimental Medicine
Vídeňská 1958/9
CZ–140 21 Praha 4 – Krč (Czech Republic)
E-Mail milan.jirsa@ikem.cz

Two forms of hereditary conjugated jaundice are known as Dubin-Johnson syndrome (DJS; MIM 237500) and Rotor syndrome (RS; MIM 237450). DJS is a rare autosomal recessive predominantly conjugated hyperbilirubinemia without other abnormalities on usual clinical-biochemistry testing and with normal total urinary porphyrin output. Hypercoproporphyrinuria is present, however, with prevalence of isomer I, as is disturbed elimination of bromsulfophthalein, indocyanine green, and radiotracers causing delayed liver visualization and no or late gallbladder visualization on cholescintigraphy. Liver is histologically characterized by hepatocellular accumulation of a dark melanin-like lysosomal pigment. Liver architecture is normal. The disorder is caused by mutations in *ABCC2* leading mostly to absence of MRP2 protein [2].

RS, a rare, benign hereditary conjugated hyperbilirubinemia, clinically resembles DJS; however, three distinctions exist: total urinary porphyrin output is increased [3], liver uptake of anionic dyes and radiotracers is almost absent [4, 5], and liver is histologically normal. RS subjects lack *ABCC2* mutations [6] as well as the hepatocyte pigment deposits typical of DJS.

The aim of our recently published study [7] was to map the gene(s) mutated in RS and to elucidate the mechanism of Rotor hyperbilirubinemia.

Methods

Rotor Syndrome Families. We examined 11 index subjects with RS (8 probands, 3 siblings of probands) – members of 8 families, and 21 clinically well members of 5 of these 8 families. Family members of 3 probands (CE1–CE3) were not available. These and one family (CE4) are Caucasians of Central European ancestry by family report. Three families (A1–A3) are Saudi Arabs and one family (P1) is from the Philippines.

Genotyping. Genotyping was performed using Affymetrix GeneChip Mapping 6.0 Arrays (Affymetrix, Santa Clara, Calif., USA) according to the manufacturer's protocol. Raw feature intensities were extracted from Affymetrix GeneChip Scanner 3000 7G images using GeneChip Control Console Software 2.01. Individual SNP calls were generated using Affymetrix Genotyping Console Software 3.02.

Homozygosity Mapping. Extended homozygosity regions were identified in Affymetrix Genotyping Console Software version 3.02 using the algorithm comparing values from the user's sample set and SNP-specific distributions derived from a reference set of 200 ethnically diverse individuals. Copy number changes and quantitative PCR assay for copy number changes was carried out as described [7].

Mutation Analysis. Long-range PCR encompassing the genomic regions of the deletion breakpoint boundaries was performed using an Expand Long Range dNTPack (Roche Applied Science). PCR products were gel-purified and sequenced using a primer walking approach. DNA sequencing of PCR products and genomic fragments covering 1 kb of the promoter regions and all of the exons, with their corresponding exon-intron boundaries, of *SLCO1B1*, *SLCO1B3*, and *SLCO1A2* was performed using a version 3.1 Dye Terminator cycle sequencing kit (Applied Biosystems, Foster City, Calif., USA) and electrophoresis on an ABI 3100 Avant Genetic Analyzer (Applied Biosystems).

Histology and Immunohistochemistry. Archival liver-biopsy specimens were available from 5 unrelated RS index subjects (probands, Families CE1, CE2, CE3, and P1; brother [A3 II.9] of proband from Family A3). Sections of paraffin-embedded material were routinely stained with hematoxylin-eosin and PAS techniques. OATP1B1 and OATP1B3 were detected with mouse anti-OATP1B antibody, clone MDQ (GeneTex, Irvine, Calif., USA), recognizing the N-terminus of both OATP1B1 and OATP1B3 [8]. Bound antibody was visualized with horseradish peroxidase/diaminobenzidine (EnVision; Dako, Glostrup, Denmark), with hematoxylin counterstaining. Adult human livers without cholestasis served as positive controls; for negative controls, the primary antibody was replaced by buffer. Immunostaining for MRP2 was performed as described [6].

Mouse Strains and Conditions. *Slco1a/1b–/–*, *Abcc2–/–*, *Abcc3–/–*, and *Abcc2;Abcc3–/–* mice have been described [9–12]. All mice were of identical genetic background (99% FVB) and between 9 and 14 weeks of age. *Slco1a/1b;Abcc2–/–*, *Slco1a/1b;Abcc3–/–*, *and Slco1a/1b;Abcc2;Abcc3–/–* combination knockout mice were obtained by crossbreeding of the existing single knockout strains (all FVB background). *Slco1a/1b–/–* and *Slco1a/1b;Abcc2–/–* mice, but not the two *Abcc3*-deficient strains, developed marked jaundice. *Slco1a/1b–/–;1B1^{tg} and Slco1a/1b–/–;1B3^{tg}* transgenic rescue mice were generated using an ApoE promoter to drive liver-specific expression of transgenic OATPs [13]. Liver levels of transgenic OATP1B1 and OATP1B3 were similar to those seen in pooled human liver samples. No jaundice was seen in these strains.

Clinical-Chemical Analysis of Mouse Plasma. Blood samples were isolated by cardiac puncture from isoflurane-anesthetized mice. Standard clinical-chemical analyses of EDTA plasma were performed on a Roche Hitachi 917 analyzer.

Analysis of Bilirubin in Mouse Plasma, Bile and Urine. Gallbladder cannulations and collection of bile in male wild-type, *Abcc2–/–*, *Abcc3–/–*, *Abcc2;Abcc3–/–*, *Slco1a/1b–/–*, *Slco1a/1b;Abcc2–/–*, *Slco1a/1b;Abcc3–/–*, and *Slco1a/1b;Abcc2;Abcc3–/–* mice (n = 4–7) were performed as described [9, 14]. We also collected urine (spot collection beforehand) and heparin plasma (cardiac puncture afterwards) from these mice. Concentrations of bilirubin monoglucuronides (BMG), bilirubin diglucuronide (BDG), and UCB in plasma, bile, and urine were determined as described [15].

Statistical Analysis for Mouse Experiments. One-way ANOVA followed by Tukey's multiple comparison test was used throughout the study to assess the statistical significance of differences between sets of data.

Results

Homozygosity mapping performed in 9 affected individuals identified a single genomic region on chromosome 12 for which 8 tested index subjects and no healthy siblings or parents were homozygous (fig. 1a), suggesting inheritance of both alleles from a common ancestor. Three distinct homo-

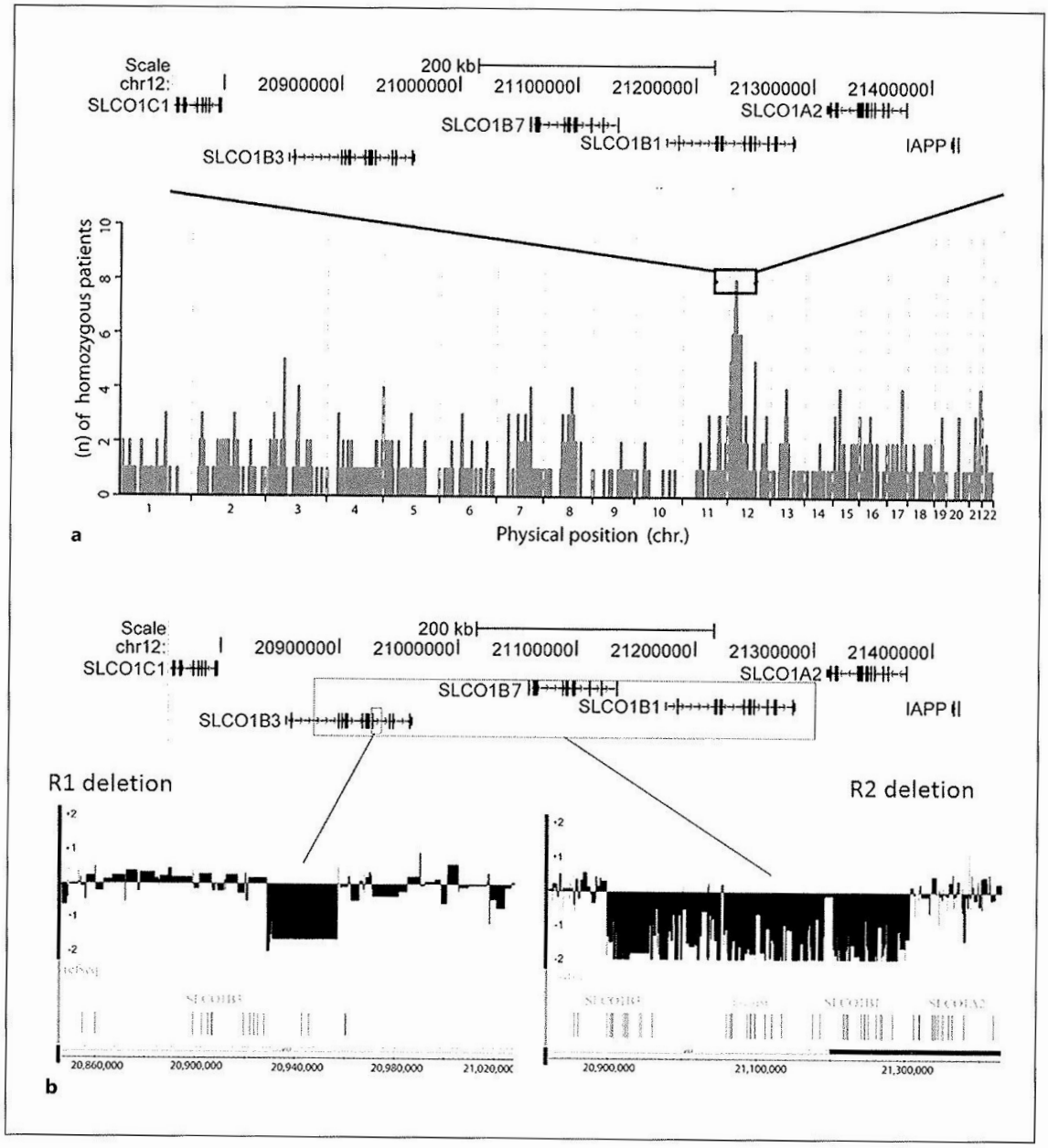

Fig. 1. Rotor families display deficiencies in *SLCO1B1* and *SLCO1B3*. **a** Homozygosity regions in 9 RS index subjects and overview of detected mutations and polymorphisms. The genome map shows number and location of overlapping homozygosity regions in RS index subjects, and gene content of the top candidate region on chromosome 12. **b** Mapping of deletions in the *SLCO1B* locus. The graphs show $\log_2$ of fluorescence intensity ratios for microarray probes distributed along the RS candidate locus in approximately 10-kb intervals for haplotypes R1 and R2, respectively. The value 0 indicates the presence of two copies of the genomic sequence complementary to the probe sequence. Regions with a large rectangular drop (R1) or with multiple irregular rectangular drops (R2) to the baseline noise value –2 indicate loss of two copies due to homozygous deletions in probands CE1 (R1 haplotype) and CE3 (R2 haplotype), respectively. The discrepancy between the results of the microarray-based low-resolution mapping of the R1 deletion (3 exons deleted in *SLCO1B3*) and sequencing-based exact mapping of the deletion breakpoints (1 exon deleted) is explained by long physical distances between the variations genotyped with the microarray probes. Modified with permission from [7].

zygous haplotypes (R1–3) in this genomic region segregated with RS: R1 in Families CE1, CE2, and CE4; R2 in Families CE3, A1, A2, and A3, and R3 in Family P1. Intersection of these haplotypes defined a candidate genomic region spanning *SLCO1C1, SLCO1B3, SLCO1B7, SLCO1B1, SLCO1A2,* and *IAPP* (fig. 1a). A parallel genome-wide copy number analysis detected a homozygous deletion within the *SLCO1B3* gene in the R1 haplotype and a homozygous ~405-kb deletion encompassing *SLCO1B3, SLCO1B7,* and *SLCO1B1* in the R2 haplotype (fig. 1b). Sequence analysis revealed pathogenic mutations affecting both *SLCO1B3* and *SLCO1B1* in each of the haplotypes (table 1). No *SLCO1A2* sequence variation was found in probands representing the three haplotypes, rendering involvement of OATP1A2 in RS unlikely.

SLCO1B7 is supposed to be a non-functional pseudogene lacking the first two exons of but otherwise homologous with *SLCO1B1/3.* Sequence homology of *SLCO1B7* exons 1–13 with exons 3–15 of *SLCO1B3* and *SLCO1B1* is 87 and 83%, respectively. A mouse sequence homologue of *SLCO1B7* (and *SLCO1B1* and *SLCO1B3*) named *Slco1b2* represents the only functional member of the mouse *Slco1b* gene family. In addition to *SLCO1B7,* two spliced *SLCO1B3–SLC01B7* fusion variants are reported in the spliced EST library: AY442325 (*SLCO1B3* exon 4 > *SLCO1B7* exon 3) and AY442326 (*SLCO1B3* exon 14 > *SLCO1B7* exon 11).

In silico analysis based on sequence homology with *SLCO1B1/3* revealed an upstream exon of *SLCO1B7* corresponding with exon 2 of *SLCO1B1/3* and containing the initiation codon followed by two stop codons (fig. 2). Moreover, we found a 5′-upstream 57-bp extension of the original first exon in reference sequence NC_000012 (fig. 2).

The presence of both stop codons was confirmed by direct sequencing of PCR-amplified gDNA fragments. By contrast, no fragment corresponding to the newly identified *SLCO1B7* exon was amplified either by direct PCR from human liver cDNA or by rapid amplification of cDNA ends (RACE) and only a small amount of cDNA corresponding to the 57-bp extension of the original first exon was obtained. Fusion variants AY442325 and AY442326 could not be detected in human liver cDNA using primer sets encompassing potential *SLCO1B3* > *SLCO1B7* sequence shifts. On the other hand, trace amounts of *SLCO1B7* cDNA was identified by detection of fragments corresponding to exons 2–4 and exons 10–11 (numbered according to NC_000012) (fig. 2). The data strongly suggest that *SLCO1B7* is a non-functional gene whose mRNA is quickly degraded probably due to nonsense-mediated decay. Mutations or complete deletion of *SLCO1B7* can thus hardly play any role in causing RS.

Immunostaining of liver biopsies showed absence of detectable staining of OATP1B1 and OATP1B3 in probands representing each haplotype (not shown). In controls, basolateral membranes of centrilobular hepatocytes stained crisply. Thus, the *SLCO1B1* and *SLCO1B3* mutations in each haplotype result in absence of detectable OATP1B1 and OATP1B3 protein from liver.

In Family A2, co-occurrence of the heterozygous splice donor site mutation c.481+1G>T in intron 5 of *SLCO1B1* with the 405-kb R2 deletion in two asymptomatic family members, A2 I.2 and A2 II.3 (table 1), indicates that a single functional *SLCO1B3* allele prevents RS. One individual of >1,000 examined Czech population controls without cholestasis, heterozygous for the R1-haplotype-associated c.1738C>T (p.R580X) mutation in *SLCO1B1,* was also homozygous for the R1-haplotype-associated deletion in *SLCO1B3.* Thus, a single functional *SLCO1B1* allele also prevents RS.

Our findings in Rotor families indicate that lack of bilirubin-glucuronide uptake from plasma is the molecular mechanism underlying RS. This would be possible only when a substantial fraction of bilirubin glucuronide synthesized in hepatocytes is secreted into plasma and not into bile. *Slco1a/1b–/–* mice, which lack the sinusoidal Oatp1a/1b proteins that are functionally homologous to human OATP1B1 and OATP1B3, also display marked conjugated hyperbilirubinemia. We therefore hypothesized that sinusoidal OATPs in the normal liver function in tandem with the sinusoidal efflux transporter MRP3 to mediate substantial hepatic secretion and re-uptake of bilirubin glucuronides and other conjugated compounds [9].

To test the involvement of Mrp3 in this sinusoidal cycling of bilirubin glucuronides, and possible interplay between Mrp3 and Mrp2, we generated *Slco1a/1b;Abcc3–/–, Slco1a/1b;Abcc2–/–,* and *Slco1a/1b;Abcc2;Abcc3–/–* mice. The markedly increased plasma BMG and BDG levels observed in *Slco1a/1b–/–* mice were substantially reduced in *Slco1a/1b;Abcc3–/–* mice, demonstrating that Mrp3 is necessary for this increase (fig. 3a, b). Plasma BMG levels in *Slco1a/1b;Abcc2–/–* mice, even further increased owing to strongly reduced biliary BMG excretion, were similarly decreased in *Slco1a/1b;Abcc2;Abcc3–/–* mice (fig. 3a, b). Thus, Mrp3 secretes bilirubin glucuronides back into blood, and Oatp1a/1b proteins mediate their efficient hepatic re-uptake. The incomplete reversion of plasma bilirubin glucuronide levels in the Oatp1a/1b/Mrp3-deficient strains (fig. 3a, b) suggests that additional sinusoidal exporter(s) partly take over this Mrp3 function.

Table 1. Mutations in *SLCO1B* genes detected in RS subjects and their family members

Haplotype R1			
Subject[a]		*SLCO1B3* **7.2-kb deletion**	*SLCO1B1* **c.1738C>T p.R580X** rs71581941
CE1	**Proband**	del/del	T/T
CE2	**Proband**	del/del	T/T
CE4 I.1	Father	del/wt	T/C
CE4 I.2	Mother	del/wt	T/C
CE4 II.1	**Proband**	del/del	T/T
Haplotype R2			
Subject[a]		*SLCO1B* **locus 405-kb deletion**	*SLCO1B1* **c.481+1G>T splice site mutation**
CE3	**Proband**	del/del	–/–
A1 I.1	Father	del/wt	–/G
A1 I.2	Mother	del/wt	–/G
A1 II.1	**Proband**	del/del	–/–
A1 II.2	Brother	wt/wt	G/G
A2 I.1	Father	del/wt	–/G
A2 I.2	Mother	del/wt	–/T
A2 II.1	**Brother**	del/del	–/–
A2 II.2	**Proband**	del/del	–/–
A2 II.3	Sister	del/wt	–/T
A2 II.4	Sister	del/wt	–/G
A2 II.5	Brother	wt/wt	G/T
A3 I.1	Father	del/wt	–/G
A3 I.2	Mother	del/wt	–/G
A3 II.1	Sister	wt/wt	G/G
A3 II.2	**Proband**	del/del	–/–
A3 II.3	Sister	del/wt	–/G
A3 II.4	Sister	del/wt	–/G
A3 II.5	Sister	del/wt	–/G
A3 II.6	**Brother**	del/del	–/–
A3 II.7	Brother	del/wt	–/G
A3 II.8	Sister	del/wt	–/G
A3 II.9	**Brother**	del/del	–/–
A3 II.10	Brother	wt/wt	G/G
Haplotype R3			
Subject[a]		*SLCO1B3* **c.1747+1G>A splice site mutation**	*SLCO1B1* **c.757C>T p.R253X**
P1 I.1	Father	G/A	C/T
P1 I.2	Mother	G/A	C/T
P1 II.1	**Proband**	A/A	T/T

[a] Subject: family identifier, generation number, subject number, family status. Bold-faced subject identifiers – index subjects with RS (n = 11; 8 probands, 3 affected siblings). 405-kb deletion (assembly NCBI36/hg18) – g.(20898911)_(21303509)del(CA)ins. 7.2-kb deletion (assembly NCBI36/hg18) – g.(20927077)_(20934292)del(N205)ins. wt = Wild-type sequence, i.e. sequence with no detected deletion from which all exons of *SLCO1B1* and *SLCO1B3* could be amplified.

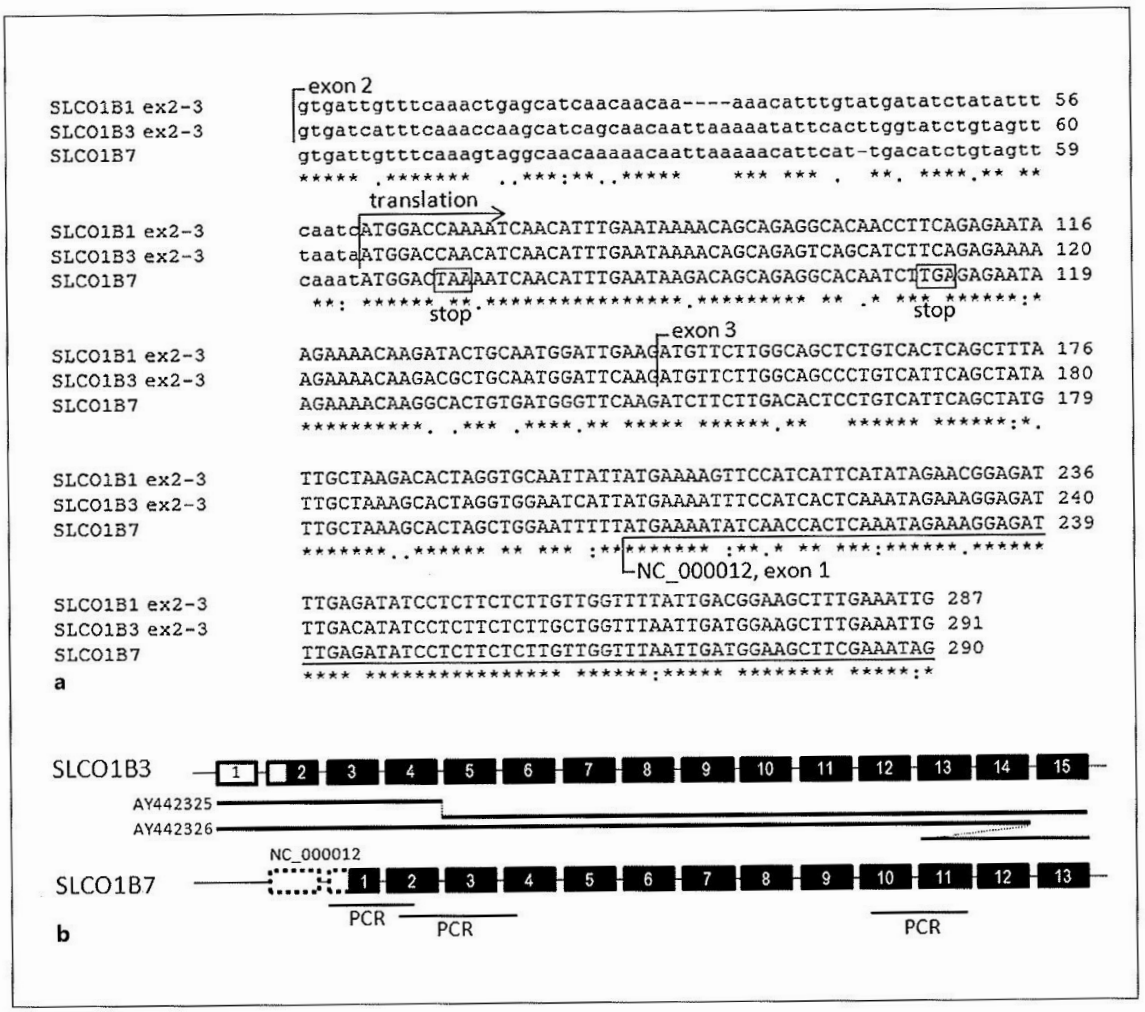

Fig. 2. Sequence alignment of *SLCO1B1*, *SLCO1B3* (exons 2 and 3) and *SLCO1B7* (**a**), and fusion transcripts of *SLCO1B3* and *SLCO1B7* recorded in the spliced EST library (**b**). Coding regions are in capitals. NC_000012 reference sequence of *SLCO1B7* is underlined. Origins of exons 2 and 3 are marked. Boxes in *SLCO1B7* sequence represent stop codons. Bars indicate fragments of *SLCO1B7* amplified from human liver cDNA.

The biliary output of bilirubin glucuronides in the single and combination knockout mice showed that, as long as Oatp1a/1b was functional, Mrp3 improved the efficiency of biliary bilirubin glucuronide excretion, even though it transports its substrates from liver into blood, not bile (data not shown). However, when Oatp1a/1b was absent, Mrp3 instead decreased biliary bilirubin glucuronide excretion, and redirected excretion towards urine via increased plasma bilirubin glucuronide. Thus, both components of the Mrp3 and Oatp1a/1b shuttling loop are necessary to improve hepatobiliary excretion efficiency.

Human hepatocytes express only two OATP1A/1B proteins at the sinusoidal membrane, OATP1B1 and OATP1B3 [16]. To test whether these could mediate the identified Oatp1a/1b functions, and in a liver-specific manner, we generated *Slco1a/1b-/-* mice with liver-specific expression of human OATP1B1 or OATP1B3. These strains displayed a virtually complete reversal of increases in plasma (and urine, data not shown) levels of BMG and BDG in *Slco1a/1b-/-* mice (fig. 3d, e), indicating that both human OATP1B1 and OATP1B3 effectively reabsorb bilirubin glucuronides from plasma into the liver. The modest increase in plasma UCB in *Slco1a/1b-/-* mice was also reduced in the rescue strains (fig. 3c, f), suggesting an ancillary role of these proteins in hepatic UCB uptake.

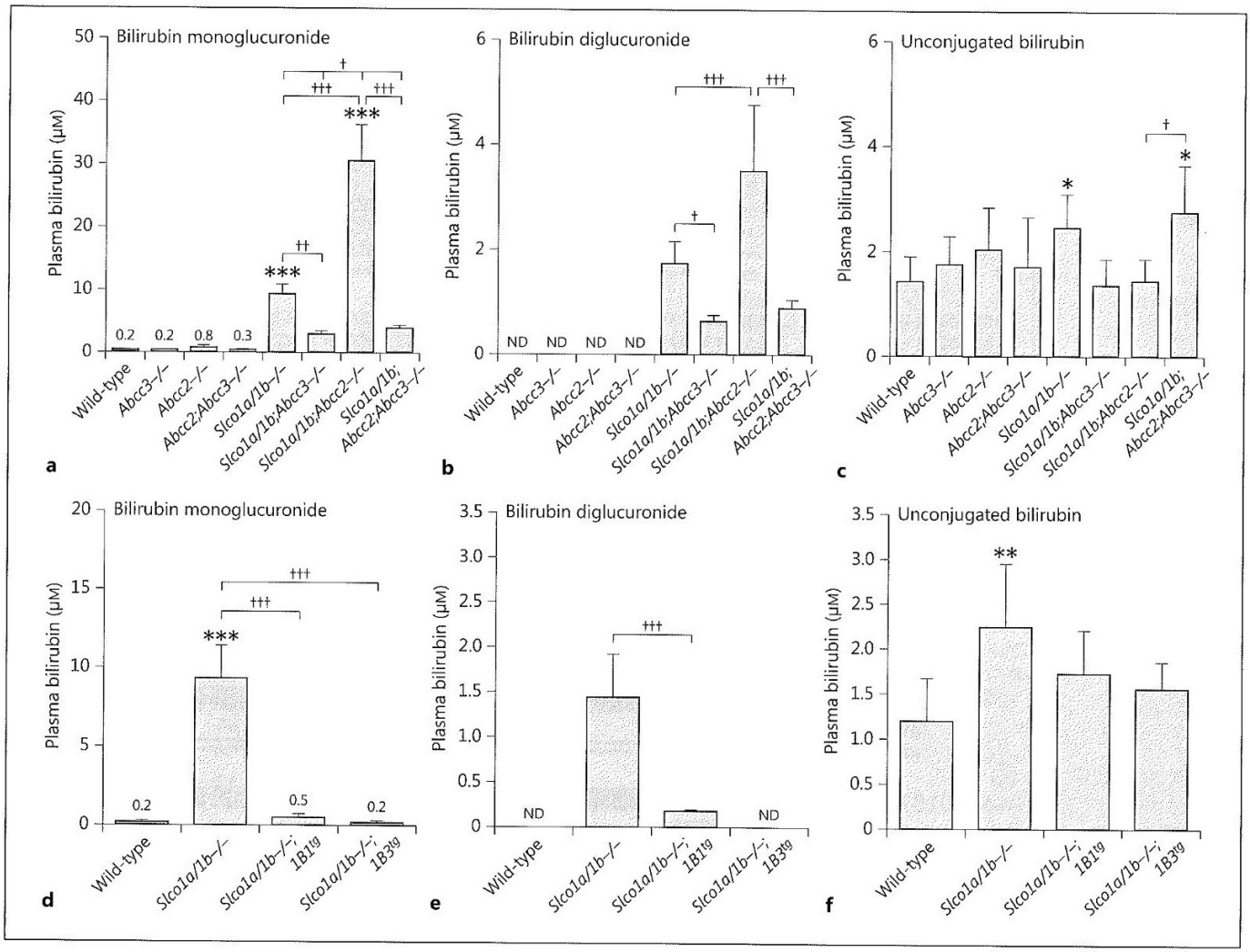

Fig. 3. Increased plasma bilirubin glucuronide in *Slco1a/1b−/−* mice is dependent on Mrp3 and reversed by human OATP1B1 and OATP1B3. **a** BMG. **b** BDG. **c** UCB levels in plasma of male wild-type, *Abcc3−/−*, *Abcc2−/−*, *Abcc2;Abcc3−/−*, *Slco1a/1b−/−*, *Slco1a/1b;Abcc3−/−*, *Slco1a/1b;Abcc2−/−*, and *Slco1a/1b;Abcc2;Abcc3−/−* mice (n = 4–7). **d** BMG. **e** BDG. **f** UCB levels in plasma of male wild-type, *Slco1a/1b−/−*, *Slco1a/1b−/−;1B1^{tg}*, and *Slco1a/1b−/−;1B3^{tg}* mice (n = 5–8). Data are means ± SD, * $p < 0.05$; ** $p < 0.01$; *** $p < 0.001$ when compared with wild-type mice. Bracketed comparisons: † $p < 0.05$; †† $p < 0.01$; ††† $p < 0.001$. ND = Not detectable; detection limit was 0.1 μM. Modified with permission from [7].

Discussion

We demonstrate here that RS is a digenic disorder, caused by a complete deficiency of the major hepatic drug uptake transporters OATP1B1 and OATP1B3. Our data imply that in the normal human liver MRP3, OATP1B1, and OATP1B3 form a liver-blood shuttling loop for bilirubin glucuronide (fig. 4): a substantial fraction of bilirubin conjugated in hepatocytes is secreted back into the blood by MRP3 and subsequently reabsorbed in downstream hepatocytes by OATP1B1 and OATP1B3. In RS this re-uptake is hampered, causing increased plasma bilirubin glucuronide levels and jaundice. The flexible 'hepatocyte-hopping' afforded by this loop facilitates efficient detoxification, presumably by circumventing saturation of further detoxification processes in upstream hepatocytes, including – but not limited to – excretion into bile. This process may also enhance hepatic detoxification of many drugs and drug conjugates. Additional sinusoidal efflux and uptake transporters (MRP4, OATP2B1, NTCP) will further enhance its scope.

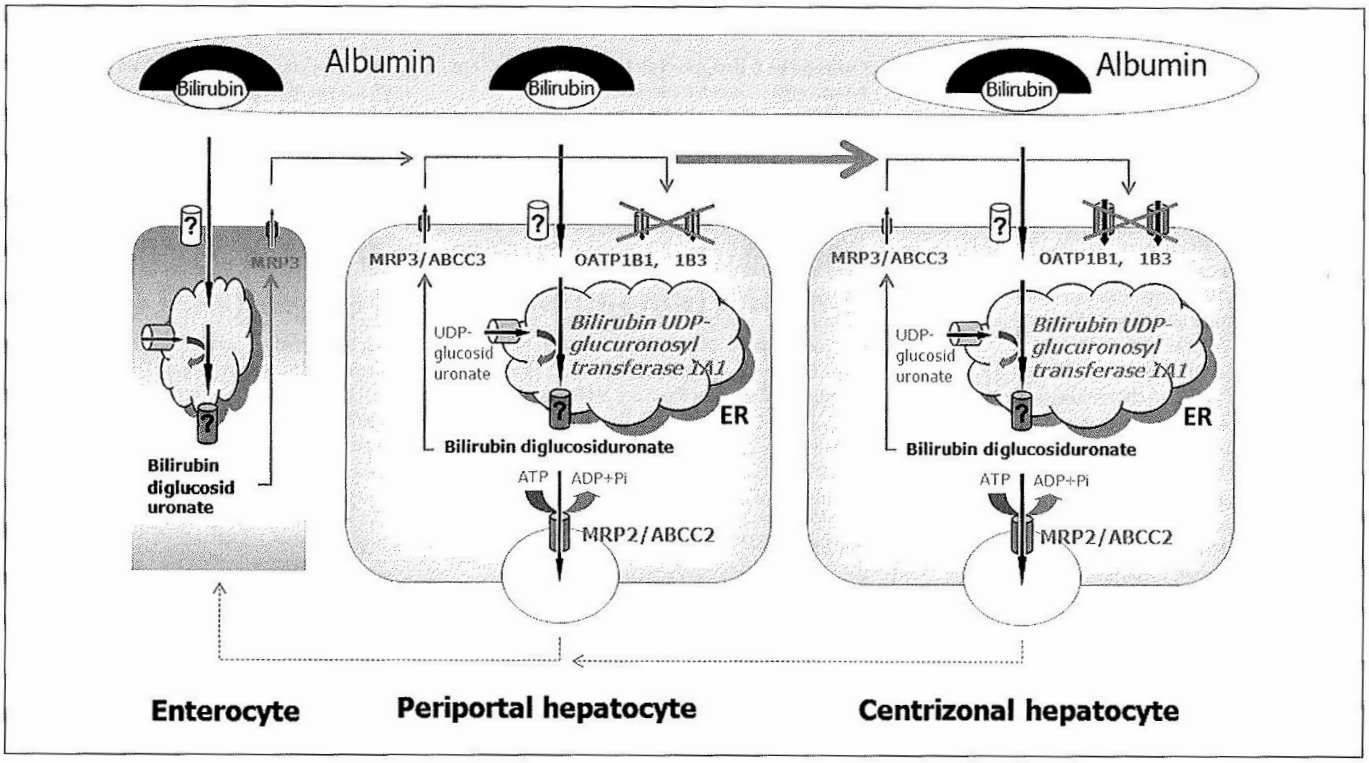

Fig. 4. Molecular mechanism of liver bilirubin handling and RS. A substantial fraction of conjugated bilirubin normally is secreted into blood and not into bile. The MRP3-OATP1B liver-blood shuttle may take place in both periportal and centrizonal hepatocytes (in the latter, expression of OATP1B proteins is higher). The most important point is, however, the ability of this system to shift conjugated bilirubin and other MRP3/OATP1B substrates from periportal to centrizonal hepatocytes, a process also called 'hepatocyte hopping'. This shifting may not only enhance the overall secretory function of the liver but it may also prevent periportal hepatocytes from potential toxicity of ingested xenobiotics or drugs and their conjugates. OAT1Bs are also responsible for liver clearance of bilirubin conjugated in splanchnic organs; intestinal conjugation followed by liver uptake of conjugated compounds may represent an alternative pathway of enterohepatic circulation. Absence of OATP1Bs is the molecular basis of RS.

Preventing accumulation of drug-glucuronides may be particularly important, since protein adduction by acyl-glucuronides is a well-established cause of drug toxicity [17].

OATP1B1 and OATP1B3 deficiency explains the poor liver uptake in RS of anionic diagnostic tracers such as bromosulfophthalein, ^{99m}Tc-HIDA, and related compounds [3–5, 18]. Reduced hepatic (re-)uptake of coproporphyrin isomers probably underlies the increased urinary excretion of coproporphyrins in RS. Surprisingly, phenotypic abnormalities in Rotor subjects are only moderate. Perhaps OATP1B1 and OATP1B3 functions are partly taken over by other sinusoidal uptake transporters, such as OATP2B1. Nevertheless, since even reduced-activity OATP1B1 polymorphisms can result in life-threatening drug toxicities [19–21], the risk of such complications is likely increased substantially in Rotor subjects. That such complications are not widely reported may owe to Rotor subjects' evident jaundice, which may have been a warning sign to prescribe drugs with caution.

The obligatory deficiency in two different, medium-sized genes explains the rarity of RS. Complete deficiency of either OATP1B1 or OATP1B3 alone will occur more frequently, but will not cause jaundice. Carriers of deleterious mutations in *SLCO1B1* might demonstrate idiosyncratic hypersensitivity to OATP1B1 substrate drugs, including statins.

Collectively, our findings explain the molecular basis of RS and demonstrate that MRP3, OATP1B1, and OATP1B3 drive a detoxification-enhancing liver-blood shuttling loop for bilirubin glucuronide which is interrupted in RS.

Disclosure Statement

The research group of A.H. Schinkel receives revenues from commercial distribution of some of the mouse strains used in this study.

References

1 Konig J, Rost D, Cui Y, Keppler D: Characterization of the human multidrug resistance protein isoform MRP3 localized to the basolateral hepatocyte membrane. Hepatology 1999;29:1156–1163.

2 Paulusma CC, Kool M, Bosma PJ, et al: A mutation in the human canalicular multispecific organic anion transporter gene causes the Dubin-Johnson syndrome. Hepatology 1997;25:1539–1542.

3 Wolpert E, Pascasio FM, Wolkoff AW, Arias IM: Abnormal sulfobromophthalein metabolism in Rotor's syndrome and obligate heterozygotes. N Engl J Med 1977;296:1099–1101.

4 Bar-Meir S, Baron J, Seligson U, Gottesfeld F, Levy R, Gilat T: ^{99m}Tc-HIDA cholescintigraphy in Dubin-Johnson and Rotor syndromes. Radiology 1982;142:743–746.

5 LeBouthillier G, Morais J, Picard M, Picard D, Chartrand R, Pomier G: Scintigraphic aspect of Rotor's disease with technetium-99m-mebrofenin. J Nucl Med 1992;33:1550–1551.

6 Hrebicek M, Jirasek T, Hartmannova H, et al: Rotor-type hyperbilirubinaemia has no defect in the canalicular bilirubin export pump. Liver Int 2007; 27:485–491.

7 Van de Steeg E, Stranecky V, Hartmannova H, et al: Complete OATP1B1 and OATP1B3 deficiency causes human Rotor syndrome by interrupting conjugated bilirubin reuptake into the liver. J Clin Invest 2012;122:519–528.

8 Cui Y, Konig J, Nies AT, et al: Detection of the human organic anion transporters SLC21A6 (OATP2) and SLC21A8 (OATP8) in liver and hepatocellular carcinoma. Lab Invest 2003;83:527–538.

9 Van de Steeg E, Wagenaar E, van der Kruijssen CM, et al: Organic anion transporting polypeptide 1a/1b-knockout mice provide insights into hepatic handling of bilirubin, bile acids, and drugs. J Clin Invest 2010;120:2942–2952.

10 Vlaming ML, Mohrmann K, Wagenaar E, et al: Carcinogen and anticancer drug transport by Mrp2 in vivo: studies using Mrp2 (Abcc2) knockout mice. J Pharmacol Exp Ther 2006;318:319–327.

11 Vlaming ML, Pala Z, van Esch A, et al: Impact of Abcc2 (Mrp2) and Abcc3 (Mrp3) on the in vivo elimination of methotrexate and its main toxic metabolite 7-hydroxymethotrexate. Clin Cancer Res 2008;14:8152–8160.

12 Zelcer N, van de Wetering K, de Waart R, et al: Mice lacking Mrp3 (Abcc3) have normal bile salt transport, but altered hepatic transport of endogenous glucuronides. J Hepatol 2006;44:768–775.

13 Van de Steeg E, van der Kruijssen CM, Wagenaar E, et al: Methotrexate pharmacokinetics in transgenic mice with liver-specific expression of human organic anion-transporting polypeptide 1B1 (SLCO1B1). Drug Metab Dispos 2009;37:277–281.

14 Van Herwaarden AE, Jonker JW, Wagenaar E, et al: The breast cancer resistance protein (Bcrp1/Abcg2) restricts exposure to the dietary carcinogen 2-amino-1-methyl-6-phenylimidazo[4, 5-b] pyridine. Cancer Res 2003;63:6447–6452.

15 Spivak W, Carey MC: Reverse-phase h.p.l.c. separation, quantification and preparation of bilirubin and its conjugates from native bile. Quantitative analysis of the intact tetrapyrroles based on h.p.l.c. of their ethyl anthranilate azo derivatives. Biochem J 1985;225:787–805.

16 Hagenbuch B, Gui C: Xenobiotic transporters of the human organic anion transporting polypeptides (OATP) family. Xenobiotica 2008;38:778–801.

17 Zhou S, Chan E, Duan W, Huang M, Chen YZ: Drug bioactivation, covalent binding to target proteins and toxicity relevance. Drug Metab Rev 2005;37:41–213.

18 Hagenbuch B, Meier PJ: Organic anion transporting polypeptides of the OATP/SLC21 family: phylogenetic classification as OATP/SLCO superfamily, new nomenclature and molecular/functional properties. Pflügers Arch 2004;447:653–665.

19 Kalliokoski A, Niemi M: Impact of OATP transporters on pharmacokinetics. Br J Pharmacol 2009;158:693–705.

20 Link E, Parish S, Armitage J, et al: SLCO1B1 variants and statin-induced myopathy – a genome-wide study. N Engl J Med 2008;359:789–799.

21 Takane H, Kawamoto K, Sasaki T, et al: Life-threatening toxicities in a patient with UGT1A1*6/*28 and SLCO1B1*15/*15 genotypes after irinotecan-based chemotherapy. Cancer Chemother Pharmacol 2009;63:1165–1169.

Research Article

For reprint orders, please contact: reprints@futuremedicine.com

Pharmacogenomics

Rare variants in known and novel candidate genes predisposing to statin-associated myopathy

Aim: Genetic variants affecting statin uptake, metabolism or predisposing to muscular diseases may confer susceptibility to statin-induced myopathy. Besides the *SLCO1B1* rs4149056 genotype, common genetic variants do not seem to determine statin-associated myopathy. Here we aimed to address the potential role of rare variants. **Patients & methods:** We performed whole exome sequencing in 88 individuals suffering from statin-associated myopathy and assessed the burden of rare variants using candidate-gene and exome-wide association analysis. **Results:** In the novel candidate gene *CLCN1*, we identified a heterozygote truncating mutation p.R894* in four patients. In addition, we detected predictably pathogenic case-specific variants in *MYOT*, *CYP3A5*, *SH3TC2*, *FBXO32 and RBM20.* **Conclusion:** These findings support the role of rare variants and nominate loci for follow-up studies.

First draft submitted: 21 April 2016; Accepted for publication: 23 May 2016; Pubilshed online: 14 June 2016

Keywords: atorvastatin • *CLCN1* • gene • myopathy • rosuvastatin • simvastatin • statin

Magdaléna Neřoldová*[1], Viktor Stránecký[2], Kateřina Hodaňová[2], Hana Hartmannová[2], Lenka Piherová[2], Anna Přistoupilová[2], Lenka Mrázová[3], Michal Vrablík[4], Věra Adámková[5], Jaroslav A Hubáček[3], Milan Jirsa[1] & Stanislav Kmoch[2]

[1]Laboratory of Experimental Hepatology, Center for Experimental Medicine, Institute for Clinical & Experimental Medicine, Prague, Czech Republic

[2]Institute of Inherited Metabolic Diseases, First Medical Faculty, Charles University, Prague, Czech Republic

[3]Laboratory for Atherosclerosis Research, Center for Experimental Medicine, Institute for Clinical & Experimental Medicine, Prague, Czech Republic

[4]Third Medical Department, First Faculty of Medicine, Charles University & General Faculty Hospital, Prague, Czech Republic

[5]Preventive Cardiology Department, Institute for Clinical & Experimental Medicine, Prague, Czech Republic

*Author for correspondence:
Tel.: +420 261 362 273
magdalena.neroldova@ikem.cz

Statins are 3-hydroxy-3-methyl-glutaryl-coenzyme A (HMG-CoA) reductase inhibitors that decrease serum total and low density lipoprotein (LDL) cholesterol. Although these medications are generally well tolerated, a significant number of patients suffer from acute myopathy after starting statin therapy. Mechanisms contributing to statin-associated myopathy (SAM) include decreased cholesterol content in muscle cell membranes, decreased production of ubiquinon, decreased prenylation of proteins, increased uptake of cholesterol and plant sterols, impaired metabolism of calcium and decreased production of selenoproteins [1–3]. SAM is also caused by genetic variants in enzymes (mostly from the cytochrome P450 family) that metabolize statins. Similarly, SAM may be caused by genetic variants in statin transporters (namely liver and intestinal OATP1B proteins and liver and myocyte ATP-binding cassette transporters) that affect the concentration of statins and their metabolites in blood cells and myocytes. Administration of statins may also unmask the carrier state for a number of genetic myopathies [4].

Family studies have suggested a strong genetic component to SAM susceptibility [5]. Genetic factors predisposing to SAM have recently been reviewed by Ghatak *et al.* [6] and Mosshammer *et al.* [7]. Common genetic variants do not seem to be important determinants of statin-induced muscle toxicity [8], with the exception of the *SLCO1B1* rs4149056 genotype in simvastatin users [9].

In this investigation we aimed to identify additional variants that might place individuals at risk for SAM. We performed whole exome sequencing in 88 individuals suffering from SAM, assessed the burden of rare variants in the known SAM genes, and performed genome-wide rare variant association study to identify novel candidate SAM loci.

Future Medicine part of fsg

Methods

Study subjects

Central European patients of Czech origin treated with simvastatin, atorvastatin or rosuvastatin for hypercholesterolemia who fulfilled the consensual definition of the American College of Cardiology (ACC)/American Heart Association (AHA) for SAM [10] were considered. individuals with other causes of muscle symptoms, such as excessive physical activity, an endocrine disorder, trauma or infection, were excluded. None of the enrolled patients had been administered known inhibitors of OATP1B1, including cyclosporine, rifampin, other antibiotics, anticancer drugs, estrogens or oral contraceptives for at least 1 month prior to the onset of myopathy. Eligible participants were also not taking medications that increased the likelihood of SAM due to inhibition of cytochrome P450 isoenzymes (amiodarone, verapamil, antifungal drugs, among others), except for fenofibrate which does not increase the risk of muscle side effects of statins [11]. Pregnancy was ruled out in fertile women.

Written informed consent was obtained from all study participants prior to blood sampling for genomic DNA analysis. The retrospective observational study protocol was approved by the local ethics committee and followed the rules of the Declaration of Helsinki of 1975.

Comparisons were made with the publicly available genotype data from subjects of European origin sequenced in the 1000 Genomes Project [12], Exome Sequencing Project (ESP) [13] and Exome Aggregation Consortium (ExAC) [14].

Additional comparisons were made with the in-house collection of more than 800 exomes analyzed at the Institute for Inherited Metabolic Disorders, Charles University in Prague, Czech Republic, from which we selected 121 biologically unrelated healthy individuals of Czech origin, mostly parents identified in projects aimed at the characterization of various rare genetic diseases of pediatric onset. Association of candidate variants with SAM was validated by comparison with more than 2000 Czech population controls from the MONICA study [15].

DNA genotyping

Genomic DNA was extracted from whole blood samples using the Qiagen DNA micro kit (Qiagen, Hilden, Germany). The quantity and quality of the isolated DNA was verified spectrophotometrically using the NanoDrop 2000 (Thermo Fisher Scientific, Praha, Czech Republic). Genotyping was performed using the Illumina HumanOmni2.5 Exome BeadChips (CA, USA) at The Microarray Facility of The Centre of Applied Genomics of The Hospital for Sick Children in Toronto according to the manufacturer's protocol.

Whole-exome sequencing

DNA was fragmented by sonication performed on a Covaris S2 system (Covaris, MA, USA). Sequencing libraries were constructed using the New England BioLabs NEBNext® Ultra™ DNA Library Prep Kit (NEB, MA, USA). Exomes were captured by the SeqCap Kit V3 (Roche NimbleGen, WI, USA)) according to the manufacturer's protocol. Libraries were sequenced on an Illumina HiSeq 1500 (Illumina, CA, USA) system at the University Hospital in Motol (Prague, Czech Republic) as described [16]. The resulting FASTQ files were aligned to the human reference genome (hg19) using Novoalign v.2.08.03 (Novocraft Technologies, Selangor, Malaysia). After genome alignment, conversion of SAM format to BAM and duplicate removal were performed with Picard Tools v.1.129 [17]. The Genome Analysis Toolkit (GATK v.3.3) was used for local realignment around indels, base recalibration and variant recalibration and genotyping. All processed BAM files (cases and controls) were jointly genotyped using GATK Unified Genotyper. Variants were annotated with SnpEff [18] and GEMINI [19], and CNVs were identified from exome read counts with CONTRA (v. 2.0.6) [20] and CNVkit (v. 0.7.4). Genetic ancestry of participants and controls was estimated from obtained genotypes using principal component analysis.

Selection of candidate variants

All variants that were predicted to be protein-altering (i.e., missense, nonsense, frameshift or canonical splice site changes) and not present in segmental duplication regions were selected for association analysis.

Screening for pathogenic mutations in 156 known functionally annotated candidate genes

Screening for predictably pathogenic mutations was performed in ten genes affecting blood concentration and hepatic metabolism of statins (Figure 1), 17 genes affecting statin concentration, calcium homeostasis in myocytes, energy metabolism, production of coenzyme Q10 and muscle vascularization. Screening was also performed in four genes important in vitamin D metabolism and 125 known myopathy genes (Table 1).

Association testing

Significant differences between genotype frequencies in the patient cohort and control groups were assessed by the chi-square test. A p-value of <0.05 was considered statistically significant.

The single-variant genome-wide association test was performed using standard allelic testing implemented

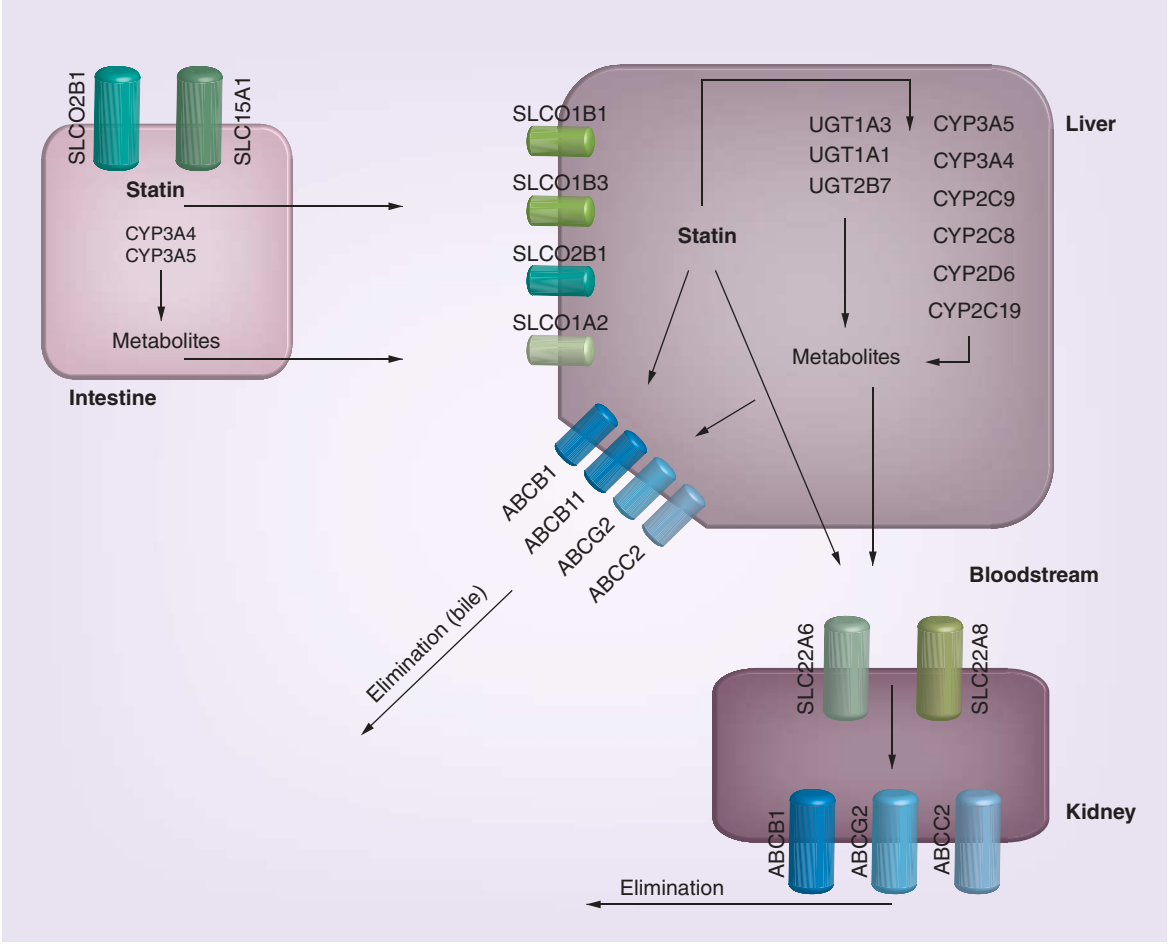

Figure 1. Schematic representation of simva-, atorva- and rosuvastatin metabolism pathways.

in PLINK [33]. For multiple variant testing, the C-alpha variance-component test [34] implemented in GEMINI was used with multiple allele frequencies thresholds. To relax the stringency of the exome-wide significance thresholds, only the genes with detected variation were included in the analysis [35]. Number of genes then suggested Bonferroni correction threshold (eg., 0.05/number of genes with variation). The significance for each test was assessed by permutation testing.

Identification of additional candidate genes by functional annotation

Genes showing a statistically significant burden of rare variants or containing recurrent unique mutations were annotated in GeneDistiller [36], DAVID [37] and using the GeneRIF [38] data. Candidate genes were prioritized through keyword and keyphrase analysis and individual expert evaluation.

Validation of prioritized variants by alternative genotyping methods

When possible, prioritized genetic variants were validated using corresponding genotypes from HumanOmni2.5 Exome BeadChips. Alternatively, Sanger sequencing using the Applied Biosystems ABI 3130 genetic analyzer was performed. Other methods used for targeted detection of variants in subjects participating in the cross-sectional study of the Czech population [15] were PCR-RFLP and TaqMan genotyping using the ABI 7300 system (Applied Biosystems) with standard kits supplied by the same manufacturer.

Results

Clinical & laboratory findings in SAM subjects

Eighty-eight patients (31 males and 57 females) aged 29–84 years (median 64.5 years, interquartile range 13.0 years) with clinically and biochemically documented SAM were enrolled. Fifty-four patients (22 males and 32 females) fulfilled published clinical and laboratory criteria [39] for definitive diagnosis of SAM, whereas in 34 patients (9 males and 25 females) SAM was classified as probable.

Fifty-three patients were treated with atorvastatin 10–40 mg daily, 21 patients with simvastatin in daily dose of 20–40 mg, and 14 patients with rosuvastatin, 10–40 mg daily. The median time between

Table 1. List of 156 candidate genes associated or potentially associated with statin myopathy.

Candidate genes	Ref.
Statin transport, blood concentration: *ABCB1*, *ABCG2*, *CYP2C8*, *CYP2D9*, *CYP3A4*, *CYP3A5*, *SLC15A1*, *SLCO1B1*, *SLCO1B3*, *SLCO2B1*	[6–7,9]
Concentration of statins in muscle cells: *ABCC1*, *ABCC4*, *ABCC5*	[7]
Factors affecting calcium homeostasis: *ATP1A1*, *ATP1A2*, *ATP1B1*, *ATP1G1*, *ATP2A1*, *RYR1*	[6]
Cell energy metabolism: *AMPD1*, *CPT2*, *GAA*, *PYGM*	[6]
Variants affecting production of coenzyme Q10: *COQ10A*, *COQ10B*	[6,7]
Muscle vascularization: *AGTR1*, *NOS3*	[6]
Metabolism of vitamin D: *CYP2R1*, *CYP27B1*, *CYP24A1*, *VDR*	[21]
Centronuclear/core myopathies: *BIN1*, *CCDC78*, *CNTN1*, *DNM2*, *MEGF10*, *MTM1*, *MTMR14*, *MYH2*, *MYF6*, *MYH7*, *STIM1*, *TNNT1*	[22–25]
Congenital muscular dystrophies: *LAMA2*, *BAG3*, *CAV3*, *CNBP*, *COL6A1*, *COL6A2*, *COL6A3*, *CRYAB*, *DMD*, *DPM2*, *DMPK*, *FKRP*, *FKTN*, *FLNC*, *GTDC2*, *HSPG2*, *CHKB*, *ISPD*, *ITGA7*, *LARGE*, *LDB3*, *LMNA*, *MYOT*, *POMT1*, *POMT2*, *SEPN1*	[25,26]
Congenital myopathies with prominent contractures: *EMD*, *FHL1*, *SEPN1*, *SYNE1*, *SYNE2*, *TMEM43*	[25,27]
Limb-girdle muscular dystrophies: *ANO5*, *CAPN3*, *DAG1*, *DES*, *DNAJB6*, *DPM3*, *DUX4*, *DYSF*, *PABPN1*, *PLEC*, *POMGNT1*, *PTRF*, *SGCA*, *SGCB*, *SGCD*, *SGCG*, *TCAP*, *TNPO3*, *TRAPPC11*, *TRIM3*, *TRIM32*, *TTN*	[25,28]
Nemaline myopathies: *ACTA1*, *CFL2*, *KBTBD13*, *KLHL40*, *KLHL41*, *LMOD3*, *NEB*, *TNNT*, *TPM2*, *TPM3*	[25,29]
Congenital myasthenic syndromes: *AGRN*, *CACNA15*, *COLQ*, *DOK7*, *DPAGT1*, *GFPT1*, *CHAT*, *CHRNA1*, *CHRNB1*, *CHRND*, *CHRNE*, *CHRNG*, *LAMB2*, *MUSK*, *RAPSN*, *SCN4A*	[25,30]
Metabolic myopathies: *ACADVL*, *ACAD9*, *AGL*, *C10orf2*, *CPT1B*, *ENO3*, *GBE1*, *GYG1*, *GYS1*, *HADHA*, *HADHB*, *LDHA*, *LPIN1*, *OPA1*, *PFKM*, *PGAM2*, *PGK1*, *PGM1*, *PHKA1*, *PNPLA2*, *POLG*, *POLG2*, *RRM2B*, *SLC22A5/OCTN2*, *SLC25A20*, *SUCLA2*, *TK2*, *TYMP*	[31,32]
Vacuolar myopathies: *EPG5*, *GNE*, *LAMP2*, *VCP*, *VMA21*	[25]

Deficiency in some of the listed genes may cause variable clinical, biochemical and histological phenotype. Therefore, genetic classification of myopathies is not unambiguous.

introduction of statin therapy and symptoms of SAM was 1 month in data available from 79 patients. In 10 of these 79 patients, symptoms developed between 4 and 10 months after the onset of statin therapy. The median time between statin withdrawal and disappearance of muscle symptoms was 10 days, with a maximum of 30 days. The symptoms did not disappear in two patients.

Complete data on serum creatine kinase (CK) activity obtained before the onset of statin therapy, at the onset of muscle symptoms and after their decline were available from 59 patients. The highest CK activity was recorded at the onset of symptoms and reached on average 4.54-times (±standard deviation: 8.92) the upper normal limit (Table 2). The peak CK activity did not exceed the upper normal limit in 9 of the 59 patients; however, maximum CK values in these patients were also recorded at the onset of clinical symptoms. The CK activity values measured at the onset of muscle symptoms were unavailable from 29 patients who came to the physician after drug withdrawal. None of the studied patients underwent muscle biopsy.

Only about 22% of the studied SAM patients used fenofibrate together with statins prior to the occurrence of muscle problems. The fraction of fenofibrate users did not differ between patients with normal, mildly elevated and severely elevated CK levels (Table 2).

Population stratification

We used genotype data from SAM patients, controls and 1000 genomes and performed PCA analysis. This showed that all patients and controls cluster together with CEU (northern Europeans from Utah) and TSI (Tuscans from Italy) populations (Supplementary Figure 1).

Variants detected by exome sequencing

In total, we detected 634,429 variants in the SAM patient group. From this set, we removed all variants that were localized in regions of segmental duplications or had a Hardy–Weinberg equilibrium p-value less than 0.001. We extracted all missense, nonsense, frameshift or canonical splice site changing variants. The final set contained 91,353 protein-coding variants.

Pathogenic mutations in *SLCO1B1* & *SLCO1B3*

The known mutation p.V174A (the **5* allele, rs4149056 c.521T>C) in *SLCO1B1* [9] was found in 40 of 88 patients, with two patients being homozygotes. The finding was validated by Sanger sequencing with no discrepancy. The frequency of the **5* allele carriers was significantly higher in our cohort than in Europeans analyzed within the 1000 Genomes project (*5 carriers/wildtype homozygotes ratio 152/351; odds ratio (OR): 1.92; 95% CI: 1.21–3.05; p = 0.005), ExAC (9793/23,545; OR: 2.0; 95% CI: 1.32–3.05; p = 0.0009), ESP (1217/3083; OR: 2.11; 95% CI: 1.38–3.23; p = 0.0004) and in our own exome database (33/121; OR: 2.22; 95% CI: 1.24–3.97; p = 0.01). However, the difference between the frequency 0.455 of the **5* allele carriers in our cohort and the published frequency 0.355 found in 467 Czech individuals tolerating statin therapy [40] (166 carriers, OR: 1.51; 95% CI: 0.95–2.39; p = 0.08) did not reach statistical significance and similar result was obtained by comparing with the frequency 0.359 reported in 2499 Czech volunteers participating in the MONICA study (897 carriers, OR: 1.49; 95% CI: 0.97–2.28; p = 0.07) [40]. We also performed similar calculations for each statin separately and for the pooled cohort of simvastatin and atorvastatin users (34 carriers of 74 users). Although the results for individual statins were inconclusive, we found association of *SLCO1B1*5* with SAM against both MONICA controls (OR: 1.64; 95% CI: 1.02–2.63; p = 0.04) and statin tolerant controls (OR: 1.67; 95% CI: 1.01–2.75; p = 0.04).

There were three patients with heterozygous frameshift mutations that introduced a premature stop codon in *SLCO1B3* (p.D70Efs). No carrier of this mutation was found among Europeans participating in the 1000 Genomes and ESP projects; however, no frequency difference was found between our cohort and the European cohort studied in the ExAC project (OR: 2.83; 95% CI: 0.89–9.00; p = 0.07) or 461 Czech population controls from the MONICA study (OR: 1.77; 95% CI: 0.47–6.68; p = 0.39).

In addition to the above-listed mutations, we found only known polymorphisms in *SLCO1B1* (rs2306283 p.N130D, rs11045819 p.P155T, rs34671512 p.L643F) discussed in [41] and in *SLCO1B3* (rs4149117 p.S112A, rs140353351 p.C162G, rs7311358 p.M233I, rs60140950 p.G256A, rs144378120 p.T550A). None of these variants were either significantly over-represented or under-represented in the studied cohort.

Pathogenic mutations in the additional 154 known candidate genes

We then searched in the remaining 154 functionally annotated candidate genes listed in Table 1 for statistically significantly over-represented variations with an OR > 1.75 (p <0.05) compared with Europeans participating in any of the 1000 Genomes, ExAC, ESP databases and to our in-house population samples. Using these criteria, we identified the four variants in *SLC15A* (rs4646227 p.G419A), *ABCC4* (rs11568694 p. V854F), *AMPD1* (rs139582106 p.Q189H) and *CYP24A1* (rs6068812 p.L409S) listed in the upper section of Supplementary Table 1. We also found a known mutation rs2229291 p.F352C in *CPT2,* listed as pathogenic in Human Gene Mutation Database (CM065101), with a minor allele frequency (MAF) <5% in all three databases (Supplementary Table 1, middle section).

Rare variants over-represented or unique in SAM patients

Application of the same approach on all detected gene variants led to identification of a new candidate gene *CLCN1* encoding the chloride channel (Supplementary Table 1 [bottom section] & Table 3 [upper section]). Mutations in *CLCN1* causes dominant (Thomsen) or recessive (Becker) myotonia. The

Table 2. Clinical and laboratory data of the studied patients with statin-associated myopathy.

Serum CK activity	Number of patients	Sex (m/f)	Median age (IQR)	Susp/proven diagnosis	Atorva/Simva/ Rosuva (%)	Feno-fibrate users	SAM type [39]
>4 × ULN	13	10/3	61 (52–68)	all 13 polygenic	46/31/23	4 (31%)	11 (85%) defin 2 (15%) prob
1–4 × ULN	37	14/23	66 (60–71)	2 hFH 35 polygenic	68/22/10	7 (19%)	25 (68%) defin 12 (32%) prob
<ULN	9	3/6	67 (57–74)	1 hFH 8 polygenic	78/11/11	2 (22%)	6 (67%) defin 3 (33%) prob
Not available	29	4/25	63 (57–68)	All 29 polygenic	51/25/25	6 (21%)	12 (41%) defin 17 (59%) prob

defin: Definitive; hFH: Heterozygous familial hypercholesterolaemia; IQR: Interquartile range, prob: Probable; Pt: patient; Susp: Suspect; ULN: Upper limit of normal.

heterozygous truncating mutation p.R894* found in four SAM individuals with only mild CK elevation is considered to be the most frequent *CLCN1* pathogenic mutation found in both forms of myotonia. Since mutations in *CLCN1* have not been associated with SAM to our best knowledge, we validated the finding by TaqMan genotyping of 2438 Czech volunteers from the MONICA study. The mutation p.R984* was found in 41 of 2438 control subjects and the p.R984* carrier frequency difference between the SAM subjects and population controls was nearly significant (OR: 2.83; 95% CI: 0.99–8.09; p = 0.04).

In addition to *CLCN1*, we found a known pathogenic mutation in *CYP2C19*. Since *CYP2C19* is not directly involved in statin metabolism, this finding has probably little significance for SAM.

We also searched in the known 156 candidate genes for novel variants present neither in the in-house controls nor in any of the database controls. A complete list of such rare variants is presented in Supplementary Table 2. Two of these rare variants compiled based on their predicTable pathogenicity (with prediction score for missense variations calculated by PredictSNP as >70%) are presented in the bottom section of Table 3.

Exome-wide association analysis: single-variant association test

To identify novel candidate variants and genes that might be involved in SAM, we first selected from the initial set of 91,353 protein-coding variants only the variants that had higher frequencies in cases than in the in-house controls and performed single variant association testing. This filter identified 40,874 variants. Using the single-variant exome-wide significance test threshold $p < 1.2 \times 10^{-6}$ (0.05/40,874 variants), we identified 12 candidate variants. Most of these variants were probably spurious signals, as they were localized in genes that have notoriously high false positive variant calls (e.g., mucins, olfactory receptors, keratins, interleukin receptors).

Exome-wide association analysis: gene-based association test

Single-variant association tests are not powerful enough to identify relevant rare variants in patient cohorts with less than 100 individuals. Therefore, we employed C-alpha variance component testing, which is more powerful than standard burden tests in situations where the majority of the identified variants have no effect. Initially we performed the test selecting the genes having at least one variants with MAF less than 1% from the complete set of 91,353 protein-coding variants. This step identified 13,492 genes and defined the burden exome-wide significance test threshold $p < 3.7 \times 10^{-6}$ (0.05/13,492 genes). Using this threshold, we identified 24 genes with significantly increased burden of rare variants. Functional annotation and classification of contributing variants revealed an increased burden of rare variants in *LDLR* ($p = 5.6 \times 10^{-8}$) that might be causal for primary hypercholesterolemia rather than SAM. Statin-induced muscle toxicity might be associated with variants in *CYP3A5* ($p = 2.6 \times 10^{-6}$) that are known to underlie interindividual differences in response to statins and variants in *SH3TC2* ($p = 1.2 \times 10^{-20}$) that might lead even in heterozygous state to neuropathy [42]. Less plausible candidates included variants in *SLC19A1* ($p = 2.6 \times 10^{-6}$) encoding the intestinal folate transporter, variants in *CACNA1H* ($p = 2.6 \times 10^{-6}$) encoding voltage-dependent calcium channel complex.

Case-specific rare variants

To identify rare and potentially highly penetrant mutations in functionally relevant genes that may be below the set exome-wide significance threshold, we extracted all variants that were present only in cases but not in controls and had a maximal MAF in any population in ExAC database (max_aaf_all) <0.1%. In total we identified 11,055 variants in 7072 genes. In this dataset, we searched only for those genes that contained at least three unique mutations in SAM patients, had individual gene-based C-alpha variance component

Table 3. Pathogenic and predictably pathogenic mutations found in known and potential SAM candidate genes.

Gene	Variant	dbSNP accession number	Allele count	Selection criterion	HGMD accession number	ClinVar	PredictSNP
CLCN1	R894*	rs55960271	4	OR > 1.75	CM940286	Pathogenic	–
CYP2C19	M1V	rs28399504	1	MAF < 5%	CM983291	Pathogenic	Not tested
ABCC4	N823fs	–	1	Rare	–	–	–
MYOT	I11T	–	1	Rare	–	–	72%

Upper section presents mutations in potential novel candidate genes. Rare pathogenic mutations in known candidates are shown in the bottom section.

Table 4. Predictably pathogenic case-specific variants.

Gene	Variant	dbSNP access number	Allele count	PredictSNP
CYP3A5	L32Tfs	rs200579169	1	–
SH3TC2	R954*	rs80338933	1	–
FBXO32	R189*	–	1	–
RBM20	R761W	–	1	72%

test $p < 0.05$ and were relevant to SAM according to their functional annotation.

This analysis revealed just four candidate genes: *FBXO32, CLU, FLNC* and *RBM20*. A full set of all variations found in these genes in SAM patients is presented in Supplementary Table 3, a subset of predictably pathogenic mutations (PredictSNP score >70% for missense mutations) is shown in Table 4.

In *FBXO32*, we identified four cases with unique heterozygous mutations (R209Q; R189*; E168K and K151R), whereas no unique variant was found in the in-house controls (C-alpha p value = 1.6×10^{-4}). In four other SAM patients, we detected unique heterozygous mutations in *CLU* (V195I, Q10R, T203I, M172V); with no such variants found in controls (C-alpha p = 1.6×10^{-4}). In *FLNC* we identified a unique homozygous mutation p.E534K in one patient and seven other patients were heterozygous for this or other unique mutations. In addition to this, we identified one heterozygous *FLNC* variant p.R2331H, which was present in one patient and one control, and five other heterozygous *FLNC* variants (splice site, p.I1849V, p.V2026M, p.R478H and p.E536K) that were present exclusively in eight controls (C-alpha p = 0.01).

Finally, we identified five patients carrying five unique heterozygous mutations in *RBM20;* (Q568L, R761W, G817D, A818S and E1125K). Moreover, we detected one heterozygous *RBM20* variant p.S1195Y present in one patient and one control and one other heterozygous *RBM20* variant p.R755H present exclusively in one control (C-alpha p = 0.01).

Discussion

In the first part of our study, we analyzed the known loci influencing statin metabolism and pharmacokinetics, muscle metabolism and muscle function. Despite the low proportion of patients taking simvastatin (22.7%) and the low daily doses of administered statins, we found a significantly higher frequency of the *SLCO1B1*5* allele in our SAM patients than in the in-house, 1000 Genomes, ExAC and ESP databases. These data are consistent with the role of the **5* allele observed in the go-DARTS study [11]; however, the difference between the frequency 0.455 of the **5* allele carriers in our cohort and the published frequencies 0.355 found in 467 Czech individuals tolerating statin therapy and 0.359 reported in 2499 Czech volunteers participating in the MONICA study [40] did not reach statistical significance. Significance was reached only in a subgroup of 74 simvastatin and atorvastatin users. This can be attributed to the decreasing effect of *SLCO1B1*5* on the exposure to simvastatin, atorvastatin and rosuvastatin. In this context, we found it interesting that the frequency of *SLCO1B1*5* reported in the Czech population [40] is significantly higher than in any of the European population samples analyzed in 1000 Genomes, ExAC and ESP.

Contrary to our initial expectations, we found no significant contribution of rare null and splice site mutations in *SLCO1B1* or *SLCO1B3* representing the molecular basis of rotor hyperbilirubinemia [43].

Analysis of the remaining 154 known candidate genes revealed two pathogenic or predictably pathogenic mutations in *CYP24A1*, one mutation in *ABCC4* encoding the muscle statin efflux transporter and in three myopathy genes *AMPD1, CPT2* and *MYOT*. Relevance of the rare mutations found in *AMPD1* and *CPT2* Is questionable. The frequency of the *AMPD1* null mutation rs17602729 p.Q45X is high (>8% in ExAC and ESP, 21% in our controls and 14% in our SAM patient group). Similarly, the *CPT2* variant p.F352C is too common in frequency to be pathogenic. The novel variation p.I11T found in *MYOT* thus remains the only relevant myopathy candidate variant found by this approach.

The potential role of sarcolemmal ABCC transporters in SAM has been suggested by Knauer *et al.* [44]; however, neither association of mutations in *ABCC4* with SAM, nor phenotype of complete *ABCC4* deficiency has ever been reported. Therefore, we could not ascertain the importance of *ABCC4* haploinsufficiency found in one SAM subject as genetic predisposition to this condition.

Contribution of low vitamin D levels to SAM is of clinical interest because vitamin D supplementation could potentially reduce the risk of SAM [45,46]. Since variations in *VDR* encoding the vitamin D receptor have recently been reported in SAM patients [47], we looked specifically at *VDR* and genes encoding vitamin D hydroxylases. To our surprise, we found that two of our SAM patients carry a known pathogenic missense variation in *CYP24A1* encoding the 1,25alpha-

dihydroxyvitamin D3 24-hydroxylase that is responsible for inactivation of vitamin D3. Mutations in *CYP24A1* are linked with autosomal recessive infantile hypercalcemia (OMIM #126065). Since heterozygous mutations in *CYP24A1* could increase but not decrease the levels of vitamin D3, relevance of our findings as a factor predisposing to SAM is unlikely.

The most surprising finding presented in Table 3 is that of the four cases with truncating mutations in *CLCN1* encoding the muscle chloride channel CLC-1. Mutations in *CLCN1* have never been linked with SAM, although statins have been shown to downregulate ClC-1 protein function in rats [48]. Since the increase of the p.R984* frequency in our SAM patients almost reached statistical significance when compared with the corresponding large population control group and the relatively rare pathogenic mutations in *CLCN1* could be missed in large GWAS studies, we believe this finding needs to be validated in a large genetic association study.

The gene-based association testing and the search for case-specific rare variants in the second part of our study identified several potential candidates. Although the increased burden of rare variants identified in *LDLR* represents part of the genetic architecture of hypercholesterolemia that is treated with statins, *CYP3A5* is a known candidate gene for SAM. Mutations in *SH3TC2* lead to neuropathy [42] but their role in SAM is uncertain. The functional effect of rare variants in *SLC19A1* and *CACNA1H* is unclear as well; however, their potential contribution to increased intestinal statin uptake or calcium metabolism deserves further attention.

The finding of recurrent mutations in *FBXO32, FLNC* and *RBM20* are of particular interest. *FBXO32* encodes atrogin-1 which acts as the muscle-specific ubiquitin ligase, a key protein upregulated in muscle atrophy. Atrogin-1 is upregulated in SAM, and its downregulation prevents myocytes from developing statin toxicity [49]. The presence of inactivation mutations rather contradicts their association with SAM. On the other hand, *FLNC* and *RBM20* mutations may represent genetic predisposition to myofibrillar myopathy that may be exacerbated by statin usage.

Conclusion

We found rare pathogenic variants in some of the known statin myopathy genes and identified rare variants in several other genes involved in muscle function. From these *CLCN1* seems to be the most promising novel candidate for follow-up studies.

Supplementary data

To view the supplementary data that accompany this paper, please visit the journal website at: www.futuremedicine.com/doi/full/10.2217/pgs-2016-0071

Acknowledgements

We thank the Genomic facility in Motol University Hospital in Prague (OPPK.CZ.2.16/3.100/24022) and The National Center for Medical Genomics (LM2015091) for their instrumental and technical support.

Financial & competing interests disclosure

The study was supported by the grant number NT-14025-3/2013 from the Internal Grant Agency, Ministry of Health of the Czech Republic and by the project for development of research organization 00023001 (IKEM, Prague, Czech Republic) – Institutional support. The authors have no other relevant affiliations or financial involvement with any organization or entity with a financial interest in or financial conflict with the subject matter or materials discussed in the manuscript apart from those disclosed.

No writing assistance was utilized in the production of this manuscript.

Executive summary

- Eighty-eight patients who developed statin myopathy were screened for rare pathogenic variants by whole exome sequencing.
- A known rare myotonia-related truncating mutation p.R894* in *CLCN1* was found in four patients.
- Additional case-specific pathogenic mutations were found in *MYOT, CYP3A5, SH3TC2, FBXO32 and RBM20.*
- Rare variants contribute to the genetic architecture of susceptibility to statin myopathy.

References

Papers of special note have been highlighted as:
•• of considerable interest

1 Mammen AL, Amato AA. Statin myopathy: a review of recent progress. *Curr. Opin. Rheumatol.* 22(6), 644–650 (2010).

2 Thompson PD, Clarkson P, Karas RH. Statin-associated myopathy. *JAMA* 289(13), 1681–1690 (2003).

3 Ucar M, Mjorndal T, Dahlqvist R. HMG-CoA reductase inhibitors and myotoxicity. *Drug Saf.* 22(6), 441–457 (2000).

4 Argov Z. Statins and the neuromuscular system: a neurologist's perspective. *Eur. J. Neurol.* 22(1), 31–36 (2015).

5 Hedenmalm K, Granberg AG, Dahl ML. Statin-induced muscle toxicity and susceptibility to malignant hyperthermia and other muscle diseases: a population-based case–control

study including 1st and 2nd degree relatives. *Eur. J. Clin. Pharmacol.* 71(1), 117–124 (2015).

6 Ghatak A, Faheem O, Thompson PD. The genetics of statin-induced myopathy. *Atherosclerosis* 210(2), 337–343 (2010).

7 Mosshammer D, Schaeffeler E, Schwab M, Morike K. Mechanisms and assessment of statin-related muscular adverse effects. *Br. J. Clin. Pharmacol.* 78(3), 454–466 (2014).

8 Hopewell JC, Reith C, Armitage J. Pharmacogenomics of statin therapy: any new insights in efficacy or safety? *Curr. Opin. Lipidol.* 25(6), 438–445 (2014).

9 Link E, Parish S, Armitage J *et al.* SLCO1B1 variants and statin-induced myopathy – a genomewide study. *N. Engl. J. Med.* 359(8), 789–799 (2008).

•• **Reports the association of the *SLCO1B1*5* allele with high dose simvastatin-associated myopathy. The **5* allele is the only known frequent genetic variation associated with SAM confirmed in validation studies.**

10 Pasternak RC, Smith SC Jr, Bairey-Merz CN, Grundy SM, Cleeman JI, Lenfant C. ACC/AHA/NHLBI Clinical Advisory on the use and safety of statins. *Stroke* 33(9), 2337–2341 (2002).

11 Donnelly LA, Doney AS, Tavendale R *et al.* Common nonsynonymous substitutions in SLCO1B1 predispose to statin intolerance in routinely treated individuals with Type 2 diabetes: a go-DARTS study. *Clin. Pharmacol. Ther.* 89(2), 210–216 (2011).

12 1000 Genomes. A deep catalog of human genetic variation. http://browser.1000genomes.org/index.html

13 NHLBI Exome Sequencing Project (ESP). Exome variant server. http://evs.gs.washington.edu/EVS/

14 ExAC Browser (Beta) | Exome Aggregation Consortium. http://exac.broadinstitute.org/

15 Cifkova R, Skodova Z, Bruthans J *et al.* Longitudinal trends in major cardiovascular risk factors in the Czech population between 1985 and 2007/8. Czech MONICA and Czech post-MONICA. *Atherosclerosis* 211(2), 676–681 (2010).

16 Kmoch S, Majewski J, Ramamurthy V *et al.* Mutations in *PNPLA6* are linked to photoreceptor degeneration and various forms of childhood blindness. *Nature Commun.* 6, 5614 (2015).

17 Picard. http://broadinstitute.github.io/picard/

18 Cingolani P, Platts A, Wang Le L *et al.* A program for annotating and predicting the effects of single nucleotide polymorphisms, SnpEff: SNPs in the genome of Drosophila melanogaster strain w1118; iso-2; iso-3. *Fly* (*Austin*) 6(2), 80–92 (2012).

19 Paila U, Chapman BA, Kirchner R, Quinlan AR. GEMINI: integrative exploration of genetic variation and genome annotations. *PLoS Comput. Biol.* 9(7), e1003153 (2013).

20 Li J, Lupat R, Amarasinghe KC *et al.* CONTRA: copy number analysis for targeted resequencing. *Bioinformatics* 28(10), 1307–1313 (2012).

21 Girgis CM, Clifton-Bligh RJ, Hamrick MW, Holick MF, Gunton JE. The roles of vitamin D in skeletal muscle: form, function, and metabolism. *Endocr. Rev.* 34(1), 33–83 (2013).

22 Kerst B, Mennerich D, Schuelke M *et al.* Heterozygous myogenic factor 6 mutation associated with myopathy and severe course of Becker muscular dystrophy. *Neuromuscul. Disord.* 10(8), 572–577 (2000).

23 Majczenko K, Davidson AE, Camelo-Piragua S *et al.* Dominant mutation of CCDC78 in a unique congenital myopathy with prominent internal nuclei and atypical cores. *Am. J. Hum. Genet.* 91(2), 365–371 (2012).

24 Malicdan MCV, Nishino I. Central core disease. In: *GeneReviews(R)*. Pagon RA, Adam MP, Ardinger HH *et al.* (Eds). University of Washington, WA, USA (1993).

25 Abath Neto O, Tassy O, Biancalana V, Zanoteli E, Pourquie O, Laporte J. Integrative data mining highlights candidate genes for monogenic myopathies. *PLoS ONE* 9(10), e110888 (2014).

26 Clarke NF, Maugenre S, Vandebrouck A *et al.* Congenital muscular dystrophy type 1D (MDC1D) due to a large intragenic insertion/deletion, involving intron 10 of the LARGE gene. *Eur. J. Hum. Genet.* 19(4), 452–457 (2011).

27 Bonne G, Leturcq F, Ben Yaou R. Emery-Dreifuss muscular dystrophy. In: *GeneReviews(R).* Pagon RA, Adam MP, Ardinger HH *et al.* (Eds). University of Washington, WA, USA (1993).

28 Pegoraro E, Hoffman EP. Limb-girdle muscular dystrophy overview. In: *GeneReviews (Internet)*. Pagon RA, Adam MP, Ardinger HH (Eds). University of Washington Seattle, WA, USA (2012).

29 North KN, Ryan MN. Nemaline myopathy. In: *GeneReviews (Internet)*. Pagon RA, Adam MP, Ardinger HH (Eds). University of Washington Seattle, WA, USA(2015).

30 Abicht A, Muller JS, Lochmuller H. Congenital myasthenic syndromes. In: *GeneReviews (Internet)*. Pagon RA, Adam MP, Ardinger HH (Eds). University of Washington Seattle, WA, USA (2012).

31 Chinnery PF. Mitochondrial disorders overview. In: *GeneReviews(R)*. Pagon RA, Adam MP, Ardinger HH *et al.* WA, USA (1993).

32 Adler M, Shieh PB. Metabolic myopathies. *Semin. Neurol.* 35(4), 385–397 (2015).

33 Purcell S, Neale B, Todd-Brown K *et al.* PLINK: a tool set for whole-genome association and population-based linkage analyses. *Am. J. Hum. Genet.* 81(3), 559–575 (2007).

34 Neale BM, Rivas MA, Voight BF *et al.* Testing for an unusual distribution of rare variants. *PLoS Genet.* 7(3), e1001322 (2011).

35 Kiezun A, Garimella K, Do R *et al.* Exome sequencing and the genetic basis of complex traits. *Nat. Genet.* 44(6), 623–630 (2012).

36 Seelow D, Schwarz JM, Schuelke M. GeneDistiller – distilling candidate genes from linkage intervals. *PLoS ONE* 3(12), e3874 (2008).

37 Dennis G Jr, Sherman BT, Hosack DA *et al.* DAVID: Database for Annotation, Visualization, and Integrated Discovery. *Genome Biol.* 4(5), P3 (2003).

38 GeneRIF: Gene Reference into Function. www.ncbi.nlm.nih.gov/gene/about-generif

39 Vrablik M, Zlatohlavek L, Stulc T *et al.* Statin-associated myopathy: from genetic predisposition to clinical management. *Physiol. Res.* 63(Suppl. 3), S327–S334 (2014).

40 Hubacek JA, Dlouha D, Adamkova V, Lanska V, Ceska R, Vrablik M. Possible gene–gender interaction between the *SLCO1B1* polymorphism and statin treatment efficacy. *Neuro. Endocrinol. Lett.* 33(Suppl. 2), 22–25 (2012).

41 Niemi M, Pasanen MK, Neuvonen PJ. Organic anion transporting polypeptide 1B1: a genetically polymorphic transporter of major importance for hepatic drug uptake. *Pharmacol. Rev.* 63(1), 157–181 (2011).

42 Lupski JR, Reid JG, Gonzaga-Jauregui C *et al.* Whole-genome sequencing in a patient with Charcot–Marie–Tooth neuropathy. *N. Engl. J. Med.* 362(13), 1181–1191 (2010).

43 Van De Steeg E, Stranecky V, Hartmannova H *et al.* Complete *OATP1B1* and *OATP1B3* deficiency causes human Rotor syndrome by interrupting conjugated bilirubin reuptake into the liver. *J. Clin. Invest.* 122(2), 519–528 (2012).

44 Knauer MJ, Urquhart BL, Meyer Zu Schwabedissen HE *et al.* Human skeletal muscle drug transporters determine local exposure and toxicity of statins. *Circ. Res.* 106(2), 297–306 (2010).

45 Michalska-Kasiczak M, Sahebkar A, Mikhailidis DP *et al.* Analysis of vitamin D levels in patients with and without statin-associated myalgia – a systematic review and meta-analysis of 7 studies with 2420 patients. *Int. J. Cardiol.* 178 111–116 (2015).

46 Mergenhagen K, Ott M, Heckman K, Rubin LM, Kellick K. Low vitamin D as a risk factor for the development of myalgia in patients taking high-dose simvastatin: a retrospective review. *Clin. Ther.* 36(5), 770–777 (2014).

47 Ovesjo ML, Skilving I, Bergman P, Rane A, Ekstrom L, Bjorkhem-Bergman L. Low vitamin D levels and genetic polymorphism in the vitamin D receptor are associated with increased risk of statin-induced myopathy. *Basic Clin. Pharmacol. Toxicol.* 118(3), 214–218 (2016).

48 Pierno S, Camerino GM, Cippone V *et al.* Statins and fenofibrate affect skeletal muscle chloride conductance in rats by differently impairing ClC-1 channel regulation and expression. *Br. J. Pharmacol.* 156(8), 1206–1215 (2009).

•• **This experimental work shows that statin administration downregulates expression of CLC-1 chloride channel in muscle cells. The observation may explain statin muscle toxicity in carriers of pathogenic mutation in *CLCN1*.**

49 Hanai J, Cao P, Tanksale P *et al.* The muscle-specific ubiquitin ligase atrogin-1/MAFbx mediates statin-induced muscle toxicity. *J. Clin. Invest.* 117(12), 3940–3951 (2007).

Large Copy-Number Variations in Patients With Statin-Associated Myopathy Affecting Statin Myopathy-Related Loci

V. STRÁNECKÝ[1], M. NEŘOLDOVÁ[2], K. HODAŇOVÁ[1], H. HARTMANNOVÁ[1], L. PIHEROVÁ[1], P. ZEMÁNKOVÁ[5], A. PŘISTOUPILOVÁ[1], M. VRABLÍK[3], V. ADÁMKOVÁ[4], S. KMOCH[1], M. JIRSA[2]

[1]Institute of Inherited Metabolic Disorders, First Faculty of Medicine, Charles University in Prague, Czech Republic, [2]Laboratory of Experimental Hepatology, Institute for Clinical and Experimental Medicine, Prague, Czech Republic, [3]Third Medical Department, First Faculty of Medicine, Charles University and General Faculty Hospital in Prague, Czech Republic, [4]Preventive Cardiology Department, Institute for Clinical and Experimental Medicine, Prague, Czech Republic, [5]Institute of Biochemistry and Experimental Oncology, First Faculty of Medicine, Charles University in Prague, Czech Republic

Received December 23, 2015
Accepted April 29, 2016
On-line August 19, 2016

Summary

Some patients are susceptible to statin-associated myopathy (SAM) either because of genetic variations affecting statin uptake and metabolism, or because they predispose their carriers to muscular diseases. Among the frequent variants examined using the genome-wide association study approach, *SLCO1B1* c.521T>C represents the only validated predictor of SAM in patients treated with high-dose simvastatin. Our aim was to ascertain the overall contribution of large copy-number variations (CNVs) to SAM diagnosed in 86 patients. CNVs were detected by whole genome genotyping using Illumina HumanOmni2.5 Exome BeadChips. Exome sequence data were used for validation of CNVs in SAM-related loci. In addition, we performed a specific search for CNVs in the *SLCO1B* region detected recently in Rotor syndrome subjects. Rare deletions possibly contributing to genetic predisposition to SAM were found in two patients: one removed *EYS* associated previously with SAM, the other was present in *LARGE* associated with congenital muscular dystrophy. Another two patients carried deletions in *CYP2C19*, which may predispose to clopidogrel-statin interactions. We found no common large CNVs potentially associated with SAM and no CNVs in the *SLCO1B* locus. Our findings suggest that large CNVs do not play a substantial role in the etiology of SAM.

Key words

Statin myopathy • Copy number variations • *SLCO1B*

Corresponding author

M. Jirsa, Institute for Clinical and Experimental Medicine, Building Z1, Vídeňská 1958/9, 140 21 Prague 4 – Krč, Czech Republic. E-mail: miji@ikem.cz

Introduction

Statins acting as HMG-CoA inhibitors decrease total serum and LDL-cholesterol and reduce the risk of ischemic heart disease. Although statins are generally well tolerated, a significant number of patients suffer from various side effects, including muscle pain and weakness. Myalgia without elevated serum creatine kinase (CK) activity and myopathy with elevated serum CK represent the most frequent causes of statin intolerance (Argov 2015). Although very rare, rhabdomyolysis is the most severe form of myopathy and results in muscle breakdown, myoglobinuria, kidney damage and death (Van Staa *et al.* 2014). The frequency of muscle problems increases with the daily dose of statins (Mosshammer *et al.* 2014). The mechanisms contributing to statin-associated myopathy (SAM)

include decreased cholesterol content in muscle cell membranes, decreased production of ubiquinone, decreased prenylation of proteins, increased uptake of cholesterol and plant sterols, impaired metabolism of calcium and decreased production of selenoproteins (Mammen and Amato 2010, Thompson *et al.* 2003, Ucar *et al.* 2000). Moreover, administration of statins may unmask pre-existing myopathy due to heterozygous carrier status for muscle disease causing mutation (Argov 2015).

Family studies suggest the involvement of a strong genetic component in statin-induced muscle toxicity and susceptibility (Hedenmalm *et al.* 2015). Genetic factors predisposing carriers to SAM (Ghatak *et al.* 2010, Mosshammer *et al.* 2014) are divided into several groups – factors affecting 1) blood concentration of statins (variations in genes encoding transporters OATP1B1, OATP1B3, OATP2B1, ABCB1, ABCG2 and enzymes CYP3A4, CYP3A5, CYP2C8, CYP2D6, CYP2D9, CYP1A2, CYP2E1, CYP2A6 and CYP2B6), 2) muscle vascularisation (genes encoding angiotensin receptor 1 (AGTR1) and NOS3 and 3) concentration of statins in muscle cells (genes encoding transporters OATP2B1, MRP1, MRP4 and MRP5). Additional numerous factors play a role in the etiology of primary muscle diseases, classified as 4) rare variants underlying disorders of muscle cell energy metabolism in genes encoding myophosphorylase (*PYGM*), alpha-glucosidase (Stroes *et al.* 2015), carnitine palmitoyltransferase 2 (*CPT2*) and myoadenylate deaminase (*AMPD1*), 5) variants responsible for mitochondrial myopathies, 6) variants affecting production of coenzyme Q10 (genes *COQ10A* and *COQ10B*), 7) variants associated with muscle dystrophy (genes encoding dystrophin (*DMD*), myotilin (*MYOT*), lamin A/C (*LMNA*) and caveolin-3 (*CAV3*)) and 8) factors affecting calcium homeostasis (genes encoding the ryanodine receptor 1 (*RYR1*), Na^+/K^+-ATPase (*ATP1A1, ATP1A2, ATP1B1, ATP1G1*) and Ca^{2+}-ATPase (*ATP2A1*)).

Common genetic variations do not seem to be important determinants of statin-induced muscle toxicity (Hopewell *et al.* 2014), with one exception: the SLC*O1B1* rs4149056 genotype (Link *et al.* 2008). In this study we focused on the potential contribution of large rare copy number variants (CNVs) affecting the above-mentioned candidate genes and/or genes involved in functionally related metabolic pathways. Moreover, since *SLCO1B1* c.521T>C (p.V174A) rs4149056 decreases liver uptake of hydrophilic statins and given that allele c.521C is associated with high-dose simvastatin (as found in the SEARCH Collaborative Study (Link *et al.* 2008)), we chose to examine our patients for the presence of known small deletions (Van De Steeg *et al.* 2012) and insertions (Kagawa *et al.* 2015) in the *SLCO1B* locus on chromosome 12p, found previously in patients with Rotor syndrome.

Methods

Selection of study subjects

Eighty-six patients treated with simva-, atorva- or rosuvastatin for familial or polygenic hypercholesterolemia and suffering from SAM fulfilling the consensual definition of the American College of Cardiology (ACC) / American Heart Association (AHA) / National Heart, Lung and Blood Institute (NHLBI) (Pasternak *et al.* 2002) were enrolled. None of the patients was administered the known inhibitors of *SLCO1B1*/*OATP1B1* – cyclosporine, rifampicin, antibiotics, anticancer drugs, estrogens, oral contraceptives – for at least one month prior to the onset of myopathy. Secondary causes of myopathy (e.g. hypothyroidism and other endocrine diseases, alcohol abuse, drug-induced) were excluded. Pregnancy was ruled out in fertile women. Consecutive patients who developed SAM over the course of the four-year study were included.

Written informed consent was obtained from all the study participants prior to any study-related procedure. The local ethics committee approved the conduct of the study, respecting the rules of the Declaration of Helsinki of 1975.

DNA genotyping and CNV identification

Genomic DNA of all available individuals was extracted from whole blood samples using the Qiagen DNA micro kit (QIAgen, Hilden, Germany). The quantity and quality of the isolated DNA were verified spectrophotometrically using the NanoDrop 2000 (Thermo Fisher Scientific, Prague, Czech Republic). Genotyping was performed using Illumina HumanOmni2.5 Exome BeadChips (San Diego, CA) at The Microarray Facility of The Centre of Applied Genomics of The Hospital for Sick Children in Toronto according to manufacturer protocol. Raw data were uploaded into Illumina GenomeStudio version 2011.1 for genotype calling. All samples with a genotype call rate >99 % were subjected to further analysis. Relatedness of

investigated subjects was assessed from obtained genotypes in PLINK (Purcell *et al.* 2007).

Extended homozygosity regions >3 Mb were detected using the 3.2.0 Illumina cnvPartition CNV Analysis Plug-in within GenomeStudio software.

CNVs were identified using PennCNV (Wang *et al.* 2007) and the above-mentioned cnvPartition CNV Analysis Plug-in. Only gains and losses containing a minimum of 10 probes were reported. Gene content of CNVs of interest was functionally annotated in GeneDistiller (Seelow *et al.* 2008) and population frequencies of the identified changes were assessed in the curated catalogue of human genomic structural variations known as DGV (http://dgv.tcag.ca/dgv/app/home).

Validation of identified CNVs

The existence of selected CNVs was independently assessed in exome sequence data, which were made available for each of the samples. DNA for exome sequencing was enriched using SeqCap V3 (NimbleGen) and sequenced on the Illumina HiSeq 1500 system at the University Hospital in Motol (Prague, Czech Republic) as previously described (Kmoch *et al.* 2015).

The resulting FASTQ files were aligned to the human genome reference (hg19) using NovoAlign (Novocraft Technologies, Selangor, Malaysia). Following genome alignment, conversion of SAM format to BAM and duplicate removal were performed using Picard Tools v.1.129 (http://broadinstitute.github.io/picard/). The Genome Analysis Toolkit (GATK) (3.3) was used for local realignment around indels, base recalibration, variant recalibration and genotyping. CNVs were identified from exome read counts using CONTRA 2.0.6 (Li *et al.* 2012) and CNVkit 0.74 (Talevich *et al.* 2014).

Detection of deletions in the SLCO1B locus found previously in subjects with Rotor syndrome

The 405 kb deletion NCBI37/hg19 g.(21,007,644)_(21,412,242)del(CA)ins, removing exons 3-15 of *SLCO1B3* and the whole gene *SLCO1B1*, and the 7.2 kb deletion NCBI37/hg19 chr12:g.(21,035,810)_(21,043,025)del(N205)ins removing *SLCO1B3* exon 12 were genotyped as described by Van De Steeg *et al.* (2012). The heterozygous state for the 7.2 kb deletion was confirmed by simultaneous amplification of the deleted allele and the *SLCO1B3* exon 12 present in the non-deleted allele. We also screened patients for the presence of recently reported long interspersed element-1 (LINE-1) in intron 5 of *SLCO1B3* (Kagawa *et al.* 2015). For this purpose, we used the PCR-based technique reported by Kagawa *et al.* (2015). Blood DNA samples taken from Rotor subjects homozygous for each of the tested mutations and from their heterozygous parents served as positive controls.

Results

Clinical and laboratory findings

Eighty-six patients (30 males and 56 females) aged 29 to 84 years (median – 65 years, interquartile range – 7 years) were selected from patient databases comprising approximately 2500 patients treated for dyslipidemia at the lipid clinics of the 3rd Department of Medicine, 1st Medical Faculty of Charles University and of the Institute for Clinical and Experimental Medicine in Prague. Of these, 51 patients developed myopathy on atorvastatin on a daily dose of 10-20 mg (only 2 patients were given 40 mg daily), 20 patients developed muscle symptoms on simvastatin (daily dose 20-40 mg) and 12 patients on rosuvastatin (daily dose 10-20 mg, 2 patients were given 40 mg daily). One patient presented with muscle symptoms repeatedly on both atorvastatin and rosuvastatin and 2 patients complained while using simva-, atorva- and rosuvastatin.

Fifty-four patients (22 males and 32 females) met the recently published criteria (Vrablik *et al.* 2014) for definitive diagnosis of SAM, whereas in the remaining 32 patients (8 males and 24 females) myopathy was classified as possible.

The median time between the onset of statin therapy and myopathy, calculated from the data obtained from 78 patients, was 1 month. Later onset of myopathy was recorded between month 4 and month 10 only in 10 patients.

Treatment was temporarily interrupted in all examined patients. The median interval between statin withdrawal and myopathy remission, calculated from the data provided by 71 patients, was 10 days with a maximum of 30 days. No remission was achieved in two patients.

All 58 patients in whom serum activity of CK was measured before statin administration, at the onset of muscle problems and after their cessation, reached the highest CK activity at the onset of the myopathy. However, in 9 patients the peak activity of CK did not exceed the upper normal limit. Serum CK activity was not measured in 28 patients (Table 1). Most patients with

severe CK elevation >20 μkat/l also had a concomitant elevation in serum activity of aspartate aminotransferase (AST). In contrast, none of the patients with CK activity <20 μkat/l had serum AST activity higher than twice the normal level.

Table 1. Clinical and laboratory findings in enrolled patients with statin-induced myopathy grouped according to their serum CK activity levels.

Serum CK activity	No. of patients	Sex (m/f)	Median age (IQR)	Susp/proven diagnosis	Atorva/ Simva/ Rosuva (%)	Fibrate users	SAM type
>5x ULN	12	10/2	60 (53-66)	6 suspect hFH, all 12 polygenic	50/25/25	4 (33 %)	11 (92 %) defin 1 (8 %) prob
1-5x ULN	37	13/24	67 (60-71)	4 suspect hFH, 2 hFH proven 35 polygenic	62/25/13	7 (19 %)	25 (68 %) defin 12 (32 %) prob
<ULN	9	3/6	67 (58-70)	4 suspect hFH, 1 hFH proven 8 polygenic	78/11/11	2 (22 %)	6 (67 %) defin 3 (33 %) prob
not available	28	4/24	63 (58-68)	3 suspect hFH, all 28 polygenic	50/25/25	6 (21 %)	12 (43 %) defin 16 (57 %) prob

ULN – upper limit of normal, IQR – interquartile range, hFH – heterozygous familial hypercholesterolemia, defin – definitive, prob – probable.

Table 2. Rare large deletions leading to heterozygous losses in genes potentially involved in SAM pathogenesis and in clopidogrel-statin interactions.

Patient no.	28	30	41	47
Chromosome no.	10	6	10	22
Begin (GRCh37/hg19)	96443782	65786994	96499710	34265402
End (GRCh37/hg19)	96620554	65815520	96557336	34271782
Size (bp)	176772	28526	57626	6380
Gene name	*CYP2C18, CYP2C19*	*EYS*	*CYP2C19*	*LARGE*
[*]DGV gold std var. frequency (%)	0.9	0.3	3.0	0.1
Potential functional implication	clopidogrel-statin interaction	SAM?	clopidogrel-statin interaction	SAM?

[*]DGV – catalogue of human genomic structural variation.

CNV analysis

DNA genotyping was performed in all 86 subjects. All analyzed samples passed the set genotyping criteria, although one sample had to be excluded from further analysis due to the detection of an abnormally high number of CNVs. Genotype analysis confirmed that all study subjects were genetically unrelated.

In the remaining 85 subjects, we identified a total of 2552 CNVs: 684 losses and 1868 gains. In this set, we searched for CNVs that were longer than 20 kb and located within ± 50 kb of any established gene loci. This analysis retrieved 503 CNVs: 164 losses and 339 gains.

The 164 losses ranging from 20-892 kb were present in 76 subjects. From these losses, 27 were recurrent (i.e. found repeatedly in the patient cohort) and 58 were singletons. The losses affected 205 distinct gene

loci, from which 156 loci were functionally annotated in GeneDistiller (http://www.genedistiller.org/). Among these annotated gene loci, we searched using selected key words for the candidate genes listed in the introduction and the following genes: an additional 10 genes for nemaline myopathy (North and Ryan 2015); 7 genes for centronuclear/core myopathies (*BIN1, CCDC78, CNTN1, DNM2, MTM1, MYF6, MYH7*); 12 genes for congenital muscular dystrophies (Sparks *et al.* 2012); 6 genes underlying the congenital myopathies with prominent contractures (*EMD, FHL1, SEPN1, SYNE1, SYNE2, TMEM43*); 16 genes for limb-girdle muscular dystrophies (Pegoraro and Hoffman 2012); 12 genes for congenital myasthenic syndromes (Abicht *et al.* 2012) and 24 genes associated with metabolic myopathies (*ACADL, ACADM, ACADVL, ACAD9, AGL, C10orf2, CPT1B, GYS1, HADHA, HADHB, LPIN1, OPA1, OPA3, PFKM, PGAM2, PGM1, PHKA1, POLG, POLG2, RRM2B, SLC22A5/OCTN2, SUCLA2, TK2, TYMP*). Moreover, we also considered published associations for each of the 156 annotated genes with myopathy or statin metabolism and their potential involvement in pathways reviewed in Ghatak *et al.* (2010) and Mosshammer *et al.* (2014). Using this approach we defined four singleton candidate deletions, which were confirmed from the exome sequence data (Table 2).

Gains ranging from 20-522 kb were present in 83 subjects. From the 339 identified gains, 41 were recurrent and 115 were singletons. The gains affected 359 distinct gene loci, from which 271 loci were functionally annotated in GeneDistiller and evaluated as above. Among the annotated gains we found no single candidate amplification that was independently confirmed in the exome sequence data.

Targeted genotyping for known Rotor syndrome deletions and insertions affecting *SLCO1B1* and *SLCO1B3* was performed in all 86 studied individuals. None of the investigated patients carried any of these three tested candidate variants.

Discussion

Biological mechanisms and genetic factors contributing to SAM are heterogeneous and remain enigmatic. Previous genetic studies have focused almost exclusively on the role of common genetic variants, mostly single nucleotide polymorphisms, and have identified only a small fraction of the expected heritability (Feng 2014, Vrablik *et al.* 2014).

Copy number variations constitute a substantial fraction of the total genetic variability known to cause, predispose to, and modulate, human diseases (Zarrei *et al.* 2015). The distribution of larger CNVs in the general population remains largely unexplored. Because rare pathogenic copy number variations are often large and contain multiple genes, identification of the underlying genetic drivers has proven difficult. In our analysis, we searched for recurrent or individually rare CNVs that may affect genes involved in drug metabolism and muscle function. We did not find any cases of recurring CNVs that would be present in higher frequencies when compared to the general population reported in the curated catalogue of human genomic structural variation (DGV) and in our internal database. Our findings thus suggest that in addition to common single nucleotide variants, large CNVs do not seem to play a substantial role in the etiology of SAM.

In two studied cases, a rare CNV that could be considered an individually contributing genetic factor was detected. In one patient, we found a 28 kb deletion in intron 12 of *EYS* which may have impaired its splicing pattern. Common variants in *EYS* were found to be associated with SAM in a large study based on the GWAS approach (Isackson *et al.* 2011). However, this finding has not been validated in further studies.

A 6.4 kb deletion located in intron 1 of *LARGE* was detected in the other patient. Pathogenic mutations in *LARGE*, when present on both alleles, are known to cause autosomal recessive dystroglycanopathy, which is considered a subtype of congenital muscular dystrophy. Interestingly, a large intronic deletion in exon 10 of *LARGE* has recently been identified as causing the disease in a consanguineous family from Lebanon (Clarke *et al.* 2011).

In another two patients, we found 176 kb and 57 kb deletions affecting the *CYP2C18/CYP2C19* locus. While one patient completely lacked both *CYP2C18* and *CYP2C19*, the smaller deletion present in the other patient removed only the first five exons of *CYP2C19*. *CYP2C19* is known to metabolize a significant number of drugs except for statins (Hirota *et al.* 2013). However, haploinsufficiency of *CYP2C19* contributes to the altered metabolism of clopidogrel concomitantly used with atorvastatin (Tantry *et al.* 2014).

In conclusion, our findings suggest that the participation of common large CNVs in genetic predisposition to SAM is unlikely, whereas rare CNVs may play some role in SAM pathogenesis.

Conflict of Interest

There is no conflict of interest.

Acknowledgements

The study was supported by grant no. NT-14025-3/2013 from the Internal Grant Agency of the Ministry of Health of the Czech Republic. We wish to thank the Genomic Facility at Motol University Hospital in Prague (OPPK.CZ.2.16/3.100/24022) and The National Centre for Medical Genomics (LM2015091) for their instrumental and technical support with genotyping and WES analyses.

References

ABICHT A, MULLER JS, LOCHMULLER H: Congenital myasthenic syndromes. In*: GeneReviews.* PAGON RA, ADAM MP, ARDINGER HH, WALLACE SE, AMEMIYA A, BEAN LJH, BIRD TD, LEDBETTER N, MEFFORD HC, SMITH RJC, STEPHENS K (eds), University of Washington, Seattle (WA), updated 2012.

ARGOV Z: Statins and the neuromuscular system: a neurologist's perspective. *Eur J Neurol* **22**: 31-36, 2015.

CLARKE NF, MAUGENRE S, VANDEBROUCK A, URTIZBEREA JA, WILLER T, PEAT RA, GRAY F, BOUCHET C, MANYA H, VUILLAUMIER-BARROT S, ENDO T, CHOUERY E, CAMPBELL KP, MEGARBANE A, GUICHENEY P: Congenital muscular dystrophy type 1D (MDC1D) due to a large intragenic insertion/deletion, involving intron 10 of the LARGE gene. *Eur J Hum Genet* **19**: 452-457, 2011.

FENG Q: Approach to clinical and genetic characterization of statin-induced myopathy. *Methods Mol Biol* **1175**: 67-90, 2014.

GHATAK A, FAHEEM O, THOMPSON PD: The genetics of statin-induced myopathy. *Atherosclerosis* **210**: 337-343, 2010.

HEDENMALM K, GRANBERG AG, DAHL ML: Statin-induced muscle toxicity and susceptibility to malignant hyperthermia and other muscle diseases: a population-based case-control study including 1st and 2nd degree relatives. *Eur J Clin Pharmacol* **71**: 117-124, 2015.

HIROTA T, EGUCHI S, IEIRI I: Impact of genetic polymorphisms in CYP2C9 and CYP2C19 on the pharmacokinetics of clinically used drugs. *Drug Metab Pharmacokinet* **28**: 28-37, 2013.

HOPEWELL JC, REITH C, ARMITAGE J: Pharmacogenomics of statin therapy: any new insights in efficacy or safety? *Curr Opin Lipidol* **25**: 438-445, 2014.

ISACKSON PJ, OCHS-BALCOM HM, MA C, HARLEY JB, PELTIER W, TARNOPOLSKY M, SRIPATHI N, WORTMANN RL, SIMMONS Z, WILSON JD, SMITH SA, BARBOI A, FINE E, BAER A, BAKER S, KAUFMAN K, COBB B, KILPATRICK JR, VLADUTIU GD: Association of common variants in the human eyes shut ortholog (EYS) with statin-induced myopathy: evidence for additional functions of EYS. *Muscle Nerve* **44**: 531-538, 2011.

KAGAWA T, OKA A, KOBAYASHI Y, HIASA Y, KITAMURA T, SAKUGAWA H, ADACHI Y, ANZAI K, TSURUYA K, ARASE Y, HIROSE S, SHIRAISHI K, SHIINA T, SATO T, WANG T, TANAKA M, HAYASHI H, KAWABE N, ROBINSON PN, ZEMOJTEL T, MINE T: Recessive inheritance of population-specific intronic LINE-1 insertion causes a rotor syndrome phenotype. *Hum Mutat* **36**: 327-332, 2015.

KMOCH S, MAJEWSKI J, RAMAMURTHY V, CAO S, FAHIMINIYA S, REN H, MACDONALD IM, LOPEZ I, SUN V, KESER V, KHAN A, STRANECKY V, HARTMANNOVA H, PRISTOUPILOVA A, HODANOVA K, PIHEROVA L, KUCHAR L, BAXOVA A, CHEN R, BARSOTTINI OG, PYLE A, GRIFFIN H, SPLITT M, SALLUM J, TOLMIE JL, SAMPSON JR, CHINNERY P, BANIN E, SHARON D, DUTTA S, GREBLER R, HELFRICH-FOERSTER C, PEDROSO JL, KRETZSCHMAR D, CAYOUETTE M, KOENEKOOP RK: Mutations in PNPLA6 are linked to photoreceptor degeneration and various forms of childhood blindness. *Nat Commun* **6**: 5614, 2015.

LI J, LUPAT R, AMARASINGHE KC, THOMPSON ER, DOYLE MA, RYLAND GL, TOTHILL RW, HALGAMUGE SK, CAMPBELL IG, GORRINGE KL: CONTRA: copy number analysis for targeted resequencing. *Bioinformatics* **28**: 1307-1313, 2012.

LINK E, PARISH S, ARMITAGE J, BOWMAN L, HEATH S, MATSUDA F, GUT I, LATHROP M, COLLINS R: SLCO1B1 variants and statin-induced myopathy--a genomewide study. *N Engl J Med* **359**: 789-799, 2008.

MAMMEN AL, AMATO AA: Statin myopathy: a review of recent progress. *Curr Opin Rheumatol* **22**: 644-650, 2010.

MOSSHAMMER D, SCHAEFFELER E, SCHWAB M, MORIKE K: Mechanisms and assessment of statin-related muscular adverse effects. *Br J Clin Pharmacol* **78**: 454-66, 2014.

NORTH KN, RYAN MN: Nemaline myopathy. In*: GeneReviews.* PAGON RA, ADAM MP, ARDINGER HH, WALLACE SE, AMEMIYA A, BEAN LJH, BIRD TD, LEDBETTER N, MEFFORD HC, SMITH RJC, STEPHENS K (eds), University of Washington, Seattle (WA), updated 2015.

PASTERNAK RC, SMITH SC JR, BAIREY-MERZ CN, GRUNDY SM, CLEEMAN JI, LENFANT C: ACC/AHA/NHLBI clinical advisory on the use and safety of statins. *Stroke* **33**: 2337-2341, 2002.

PEGORARO E, HOFFMAN EP: Limb-girdle muscular dystrophy overview. In*: GeneReviews.* PAGON RA, ADAM MP, ARDINGER HH, WALLACE SE, AMEMIYA A, BEAN LJH, BIRD TD, LEDBETTER N, MEFFORD HC, SMITH RJC, STEPHENS K (eds), University of Washington, Seattle (WA), updated 2012.

PURCELL S, NEALE B, TODD-BROWN K, THOMAS L, FERREIRA MA, BENDER D, MALLER J, SKLAR P, DE BAKKER PI, DALY MJ, SHAM PC: PLINK: a tool set for whole-genome association and population-based linkage analyses. *Am J Hum Genet* **81**: 559-575, 2007.

SEELOW D, SCHWARZ JM, SCHUELKE M: GeneDistiller--distilling candidate genes from linkage intervals. *PLoS One* **3**: e3874, 2008.

SPARKS S, QUIJANO-ROY S, HARPER A, RUTOWSKI A, GORDON E, HOFFMAN EP, PEGORARO E: Congenital muscular dystrophy overview. In: *GeneReviews.* PAGON RA, ADAM MP, ARDINGER HH, WALLACE SE, AMEMIYA A, BEAN LJH, BIRD TD, LEDBETTER N, MEFFORD HC, SMITH RJC, STEPHENS K (eds), University of Washington, Seattle (WA), updated 2012.

STROES ES, THOMPSON PD, CORSINI A, VLADUTIU GD, RAAL FJ, RAY KK, RODEN M, STEIN E, TOKGOZOGLU L, NORDESTGAARD BG, BRUCKERT E, DE BACKER G, KRAUSS RM, LAUFS U, SANTOS RD, HEGELE RA, HOVINGH GK, LEITER LA, MACH F, MARZ W, NEWMAN CB, WIKLUND O, JACOBSON TA, CATAPANO AL, CHAPMAN MJ, GINSBERG HN: Statin-associated muscle symptoms: impact on statin therapy - European Atherosclerosis Society Consensus Panel Statement on Assessment, Aetiology and Management. *Eur Heart J* **36**: 1012-1022, 2015.

TALEVICH E, SHAIN AH, BOTTON T, BASTIAN BC: CNVkit: copy number detection and visualization for targeted sequencing using off-target reads. *bioRxiv* 010876, 2014. doi: http://dx.doi.org/10.1101/010876

TANTRY US, JEONG YH, GURBEL PA: The clopidogrel-statin interaction. *Circ J* **78**: 592-594, 2014.

THOMPSON PD, CLARKSON P, KARAS RH: Statin-associated myopathy. *JAMA* **289**: 1681-1690, 2003.

UCAR M, MJORNDAL T, DAHLQVIST R: HMG-CoA reductase inhibitors and myotoxicity. *Drug Saf* **22**: 441-457, 2000.

VAN DE STEEG E, STRANECKY V, HARTMANNOVA H, NOSKOVA L, HREBICEK M, WAGENAAR E, VAN ESCH A, DE WAART DR, OUDE ELFERINK RP, KENWORTHY KE, STICOVA E, AL-EDREESI M, KNISELY AS, KMOCH S, JIRSA M, SCHINKEL AH: Complete OATP1B1 and OATP1B3 deficiency causes human Rotor syndrome by interrupting conjugated bilirubin reuptake into the liver. *J Clin Invest* **122**: 519-528, 2012.

VAN STAA TP, CARR DF, O'MEARA H, MCCANN G, PIRMOHAMED M: Predictors and outcomes of increases in creatine phosphokinase concentrations or rhabdomyolysis risk during statin treatment. *Br J Clin Pharmacol* **78**: 649-659, 2014.

VRABLIK M, ZLATOHLAVEK L, STULC T, ADAMKOVA V, PRUSIKOVA M, SCHWARZOVA L, HUBACEK JA, CESKA R: Statin-associated myopathy: from genetic predisposition to clinical management. *Physiol Res* **63** (Suppl 3): S327-S334, 2014.

WANG K, LI M, HADLEY D, LIU R, GLESSNER J, GRANT SF, HAKONARSON H, BUCAN M: PennCNV: an integrated hidden Markov model designed for high-resolution copy number variation detection in whole-genome SNP genotyping data. *Genome Res* **17**: 1665-1674, 2007.

ZARREI M, MACDONALD JR, MERICO D, SCHERER SW: A copy number variation map of the human genome. *Nat Rev Genet* **16**: 172-183, 2015.

ABCB4 disease mimicking morbus Wilson: A potential diagnostic pitfall

Eva Sticova[a,b,c], Magdalena Neroldova[a,d], Radana Kotalova[e], Iva Subhanova[d], Milan Jirsa[a,d]

Introduction. Progressive familial intrahepatic cholestasis type 3 (PFIC3) is a rare autosomal recessive cholestatic liver disorder caused by genetic deficiency of ATP-binding cassette subfamily B member 4 (ABCB4), a hepatocanalicular floppase translocating phospholipids from the inner to the outer leaflet of the canalicular membrane lipid bilayer. PFIC3 is characterised by production of hydrophilic bile with lithogenic properties which is harmful to the hepatobiliary epithelia. Chronic cholestasis in some patients may be accompanied by excessive accumulation of copper in the liver and by increased urinary copper excretion, the findings mimicking Wilson disease (WD).
Methods and Results. We report an 11 y/o male patient with growth retardation, mild craniofacial dysmorphic features and chronic liver disease, initially diagnosed and treated as WD. Whereas genetic testing for WD was negative, further molecular and histopathological analysis revealed two novel mutations (c.833+1G>T and c.1798T>A) in *ABCB4* and complete absence of the ABCB4/MDR3 protein in the liver, determining PFIC3 as the correct diagnosis.
Conclusion. PFIC3 and WD display pleomorphic and sometimes overlapping clinical and laboratory features, which may pose a differential diagnostic problem. Since the patient management in WD and PFIC3 differs significantly, an early and accurate diagnosis is crucial for optimising of therapeutic approach and prevention of possible complications.

Key words: ABCB4, progressive familial intrahepatic cholestasis type 3, Wilson disease, copper metabolism, ATP7B

Received: September 17, 2019; Revised: October 19, 2019; Accepted: October 22, 2019; Available online: November 15, 2019
https://doi.org/10.5507/bp.2019.054

[a]Institute for Clinical and Experimental Medicine, Videnska 1958/9, Prague 4, 140 21, Czech Republic
[b]Institute of Liver Studies, King's College Hospital NHS Foundation Trust, Denmark Hill, London SE5 9RS, United Kingdom
[c]Department of Pathology, Third Faculty of Medicine, Charles University and University Hospital Kralovske Vinohrady, Srobarova 1150/50, Prague, 100 00, Czech Republic
[d]Institute of Medical Biochemistry and Laboratory Diagnostics, First Faculty of Medicine, Charles University and Faculty General Hospital, U Nemocnice 2, Prague, 128 08, Czech Republic
[e]Department of Pediatrics, Second Faculty of Medicine, Charles University and University Hospital Motol, V Uvalu 84, Prague, 15006, Czech Republic
Corresponding author: Eva Sticova, e-mail: eva.sticova@nhs.net

INTRODUCTION

Progressive familial intrahepatic cholestasis type 3 (PFIC3, OMIM #602347, gene *ABCB4*) is an autosomal recessive cholestatic liver disorder caused by absence of functional multidrug resistance protein 3 (MDR3), also known as ATP-binding cassette (ABC) subfamily B member 4 (ABCB4) (ref.[1]). ABCB4/MDR3 is a hepatocanalicular transporter, "floppase", translocating phosphatidylcholine from the inner leaflet to the outer leaflet of the canalicular membrane lipid bilayer[2-4]. Most of the harmful effects of *ABCB4* deficiency on hepatobiliary system are attributable to "toxic bile" with potent detergent and lithogenic properties. Typical laboratory findings associated with PFIC3 are characterised by predominantly conjugated hyperbilirubinemia and elevated serum γ-glutamyl transferase (GGT) activity[1]. Moreover, chronic cholestasis may be accompanied by increased urinary copper excretion and significant accumulation of copper in the liver, i.e., findings that may be potentially misinterpreted as Wilson disease (WD, gene *ATP7B*) (ref.[5-8]).

In this report, we describe the case of an 11 years old male patient suffering from chronic liver disease with biochemical parameters indicating impairment of copper metabolism and excessive copper accumulation in the liver typical for WD. However, subsequent molecular genetic and histopathological analysis revealed mutations in *ABCB4* and complete absence of canalicular ABCB4/MDR3 protein expression.

CASE REPORT

An 11-year-old male patient was initially referred to the local hospital due to growth retardation and a marked hepatosplenomegaly detected during his periodic preventive health screening. The boy complained of occasional pains in the right upper abdominal quadrant and intermittent pruritus. There was no history of bleeding or significant fatigue and his psychomotor development was normal. His family history was unremarkable in terms of hereditary disorders or liver diseases.

Physical examination revealed hepatomegaly with the enlarged firm liver (+ 10 cm at the midclavicular line) and splenomegaly (+ 8 cm). Moreover, marked hirsutism, a short statue (body height 121.5 cm, 4 SD below the

mean), and mild craniofacial dysmorphia with dolichocephaly and a flattened face, the features not attributable to familial factors, were also of notice.

Laboratory examinations were notable for pathological liver function tests with elevated serum GGT (5.5 μkat/L), alanine aminotransferase (ALT, 1.9 – 7.0 μkat/L), and aspartate aminotransferase (AST, 1.8 – 11.0 μkat/L) activity. Total bilirubin level was 53 - 75 μmol/L with conjugated bilirubin level between 42 and 52 μmol/L. Serum ceruloplasmin, α-1-antitrypsin, and albumin, as well as serum lipid levels were initially within the normal range, while urinary copper output was increased to 178 μg/24h. Serological tests for viral hepatitis, autoantibodies, and endocrine screening were negative. Metabolic screening excluded inborn errors of iron, porphyrin, amino acid, and lipid metabolism. As a part of the diagnostic process, core liver biopsy was performed. Advanced septal fibrosis with periportal ductular reaction and hepatocanalicular cholestasis was found, with copper level of 914 μg/g dry weight. Based on these findings, WD was entertained as the most likely diagnosis and treatment with metalcaptase was initiated. However, subsequent slit lamp examination showed absence of Kayser-Fleischer ring and mutational analysis did not reveal mutations in *ATP7B*, thus calling the diagnosis of WD into question.

Within a few months, the liver disease progressed, along with manifestation of portal hypertension and further deterioration of laboratory parameters: total bilirubin level 99.1 μmol/L (conjugated bilirubin 60.5 μmol/L), GGT 5.77 μkat/L, ALT 17.0 μkat/L, AST 19.8 μkat/L, albumin 32.3 g/L, triacylglycerols 3.1 mmol/L, cholesterol 3.3 mmol/L, ammonia 53.6 μmol/L, and α-fetoprotein 12.4 μg/L. Blood count and coagulation parameters were as follows: haemoglobin 133 g/L, haematocrit 0.402, red blood cell count $4.51x10^{12}$/L, white blood cell count $3.3x10^{9}$/L, platelet count $62x10^{9}$/L, APTT 36.2 s, prothrombin time (PT)-Quick 19.60 s, PT-ratio 1.4, INR 1.71, fibrinogen 2.11 g/L, and antithrombin 54%.

Abdominal ultrasonography and CT scan demonstrated hepatomegaly with several parenchymal nodules up to 15 mm, marked splenomegaly, ascites and portosystemic collateral circulation.

Due to gradual progression of the liver disease with unsatisfactory response to the conservative therapy, the patient was referred to the transplant centre, where he underwent split-liver transplantation.

The liver explant removed at transplantation showed diffuse nodularity of the parenchyma with a green discoloration of the nodules. The liver tissue was fixed in 4% paraformaldehyde and processed for histological examination. Sections cut at 4-6 μm were stained with hematoxylin and eosin, periodic acid-Schiff-diastase reaction, orcein and elastin-van Gieson's method. For immunohistochemical analysis, sections were incubated with the anti-MDR3/ABCB4 rabbit polyclonal antibody (NBP2-30887PEP, Novus Biologicals, Colorado). The EnVision Peroxidase Kit (Dako, Glostrup, Denmark) was used for visualisation and counterstaining with Harris's hematoxylin was performed. Light microscopy revealed predominantly micronodular biliary cirrhosis with a mild residual inflammatory infiltrate within the portal tracts and septa. Moreover, features of chronic cholangiopathy with periportal ductular reaction, as well as morphology of cholestasis with cholestatic liver cell rosettes, bile infarcts, Denk-Mallory hyaline inclusions and copper-associated protein depositions in juxtaportal hepatocytes were also easily discernible. In keeping with CT scan findings, the regenerative nodules up to 15 mm were present in the liver parenchyma but no malignancy was identified. Importantly, immunohistological examination demonstrated complete absence of hepatocanalicular ABCB4/MDR3 expression in the patient's liver tissue (Fig. 1). In accordance with previous findings, excessive accumulation of copper with a level of 1867μg/g dry weight was demonstrated in the liver explant; however, based on the histopathological findings, diagnosis of PFIC3 was suggested.

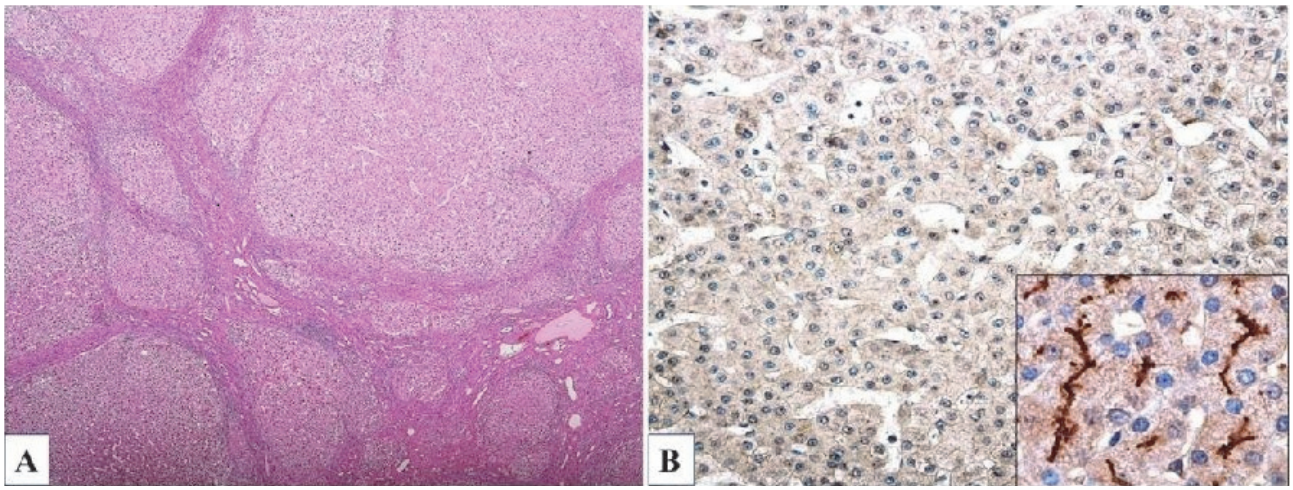

Fig. 1. Histopathology findings in the explanted liver.
(A) Haematoxylin and eosin, original magnification x40, (B) MDR3 immunohistochemistry, original magnification x200 (inset, x400).

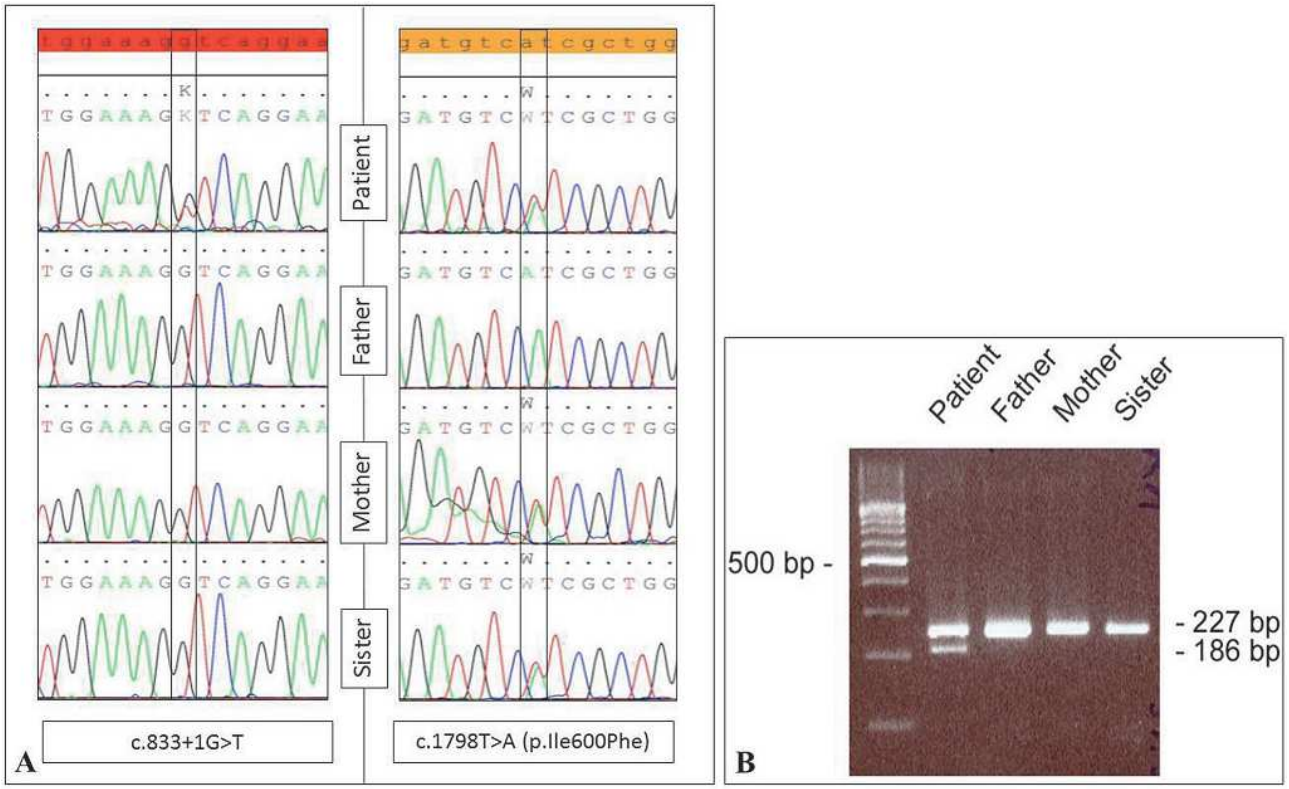

Fig. 2. Family analysis.
(A) Mutations found in the index patient and his first-degree relatives. (B) Detection of the c.833+1G>T mutation using PCR- *Hpy*8I restriction fragment length polymorphism analysis.

Targeted resequencing of *ABCB4* was then indicated to confirm the histopathological diagnosis of PFIC3. Written informed consent was obtained from the patient's legal representatives before genetic testing. *ABCB4* was analysed by direct sequencing of genomic DNA extracted from peripheral leukocytes on an ABI 3130 Genetic Analyser (Applied Biosystems, Foster City, CA). Two novel mutations c.833+1G>T and c.1798T>A in *ABCB4* were detected (Fig. 2).

Whereas pathogenicity of the former splice site mutation is apparent, pathogenicity of the latter, supposed to cause the amino acid substitution p.Ile600Phe, was tested *in silico* using PredictSNP1 (ref.[9]). The substitution located in the first ATP-binding cytoplasmic loop was rated as likely pathogenic with the overall pathogenicity score 87%. Both mutations were detected in heterozygous state. Family analysis revealed that the patient´s mother and sister are heterozygous carriers of the mutation c.1798T>A but none of them carries the mutation c.833+1G>T. The father was shown to be free of both mutations. Therefore, we designed a PCR- *Hpy*8I RFLP method using a combination of a standard forward primer extended with the T7 overhang (5´-*taatacgactcactatag*CAGAGTGCCTTTAAACTTTTCTCC-3´) and a mutated reversed primer extended with the RP overhang (5´-*tgaaacagctatgaccatg*AGTGGCTAAAGAACCTTCgTG-3´, both overhangs are *in italics*) and confirmed that the mutation c.833+1G>T was present exclusively in the index patient (Fig. 2B).

Segregation of both mutations in the family, together with complete absence of MDR3 protein in the liver, strongly suggests that both mutations detected in the proband are located in *trans*. Absence of the splice site mutation in the patient´s father can have multiple explanations including *de novo* mutagenesis or gonadal mosaicism.

DISCUSSION

WD (OMIM #277900) is an autosomal recessive disease caused by mutations targeting the copper transporter ATP7B, characterised by organ copper build up due to impaired copper metabolism and biliary secretion. Clinical manifestations range from asymptomatic course to variable combination of neuropsychiatric and hepatic symptoms including life-threatening liver failure. The diagnosis of WD is based on clinical and biochemical findings, excessive liver copper accumulation and molecular genetic analysis[10-12]. Similarly to WD, PFIC3, caused by almost complete biallelic inactivation of *ABCB4,* also displays pleomorphic clinical and laboratory phenotype, severity of which is affected at least partially by the *ABCB4* allelic status[13-15]. The disease usually occurs in early childhood and is characterised by hepatosplenomegaly with jaundice, pruritus, steatorrhea, and growth retardation[1].

Since liver disease manifests in both WD and PFIC3, differential diagnosis can be complicated. Whereas extrahepatic manifestations such as Kayser-Fleischer ring,

Table 1. Published patients with PFIC3 mimicking Wilson disease.

Age	Sex	Liver copper content (μg/g)	Urinary copper output (μg/24 h)	Serum ceruloplasmin (g/L)	Serum copper conc. (μg/L)	GGT (IU/L)	ABCB4 mutations	Ref.
21	M	NA	1733	0.14	NA	83	NA	8
15	F	1471	342	0.38	1510	734	c.3218G>A (p.C1073Y) c.984T>G (p.Y328*)	7
11	F	860	125	0.27	840	293	c.2563C>T (p.Q855*) c.1283T>C (p.V428A)	6
7	M	863	66	0.45	NA	608	c.490T>G (p.W164G) c.3081+1G>C	6
2	F	248	NA	0.28	1013	405	p.A546D, p.R176W	5

M – *male*, F – *female,* NA – not assessed.
Reference range: liver copper content <250 μg/g dry weight, urinary copper output <60 μg/24 h, serum ceruloplasmin 0.2 – 0.5 g/L, serum copper 750 – 1450 μg/L.

renal tubular acidosis or cardiomyopathy point to WD, growth retardation is more likely linked with chronic cholestasis. Unfortunately, the short statue of our patient was partly explicable by familial factors (mother's height 148 cm, father's height 162 cm). Interestingly, the patient also displayed marked hirsutism and a craniofacial dysmorphia, the features that have not been reported in PFIC3 patients.

The liver plays a central role in copper metabolism, being responsible predominantly for its storage and biliary excretion. Quantification of hepatic copper content provides valuable information for differential diagnosis, and severe copper accumulation is a strong indicator of WD. However, elevated concentrations of copper in the liver tissue as well as increased urinary copper excretion have also been reported in liver disorders not related to WD, especially in patients with prolonged cholestasis[12]. We found only four reports[5-8] documenting abnormal or marginal hepatic copper content in five patients with PFIC3 mimicking WD (Table 1). Four patients had elevated urinary copper excretion, one had also decreased serum ceruloplasmin level. To the best of our knowledge, the value of hepatic copper content 1867 μg/g dry weight on the background of *ABCB4* deficiency is the highest recorded so far (Table 1).

Since histopathological findings associated with both WD and PFIC3 vary widely, sometimes exhibiting morphological overlap, light microscopic analysis of the liver tissue is usually of limited diagnostic importance. However, immunohistochemical evidence of significant reduction or complete absence of the hepatocanalicular MDR3 protein expression, as was demonstrated in our case, may serve as a beneficial but not completely reliable diagnostic tool[16].

Untreated WD and PFIC3 are generally progressive and lethal. Unlike PFIC3, in which patients profit predominantly from administration of ursodeoxycholic acid, WD therapy is based on drugs increasing urinary copper elimination (chelators) or reducing intestinal copper absorption (zinc salts). Interestingly, no beneficial effect of chelation therapy on disease progression has been observed in PFIC3 or other non-WD chronic cholestatic diseases. Liver transplantation remains the ultimate treatment modality for both diseases, especially for rapidly progressive forms and/or for end-stage liver disease[10,11,17].

In summary, PFIC3 and WD display pleomorphic and sometimes overlapping clinical and laboratory features, which may pose a differential diagnostic problem. Since patient management in WD and PFIC3 differs significantly, early and correct diagnosis is crucial for optimising the therapeutic approach, deceleration of pathological processes and prevention of possible complications.

ABBREVIATIONS

ABC, ATP-binding cassette subfamily; ABCB4, ATP-binding cassette, subfamily B, member 4; ATP7B, ATPase, copper transporting, beta polypeptide; ALP, Alkaline phosphatase; ALT, Alanine aminotransferase; AST, Aspartate aminotransferase; GGT, γ-glutamyl transferase; MDR3, Multidrug resistance protein 3; OMIM, Electronic database Online Mendelian Inheritance in Man™; PFIC3, Progressive familial intrahepatic cholestasis type 3; WD, Wilson disease.

Acknowledgements: The authors thank Lucie Budišová for technical assistance. The study was funded by MH CZ - DRO („Institute for Clinical and Experimental Medicine – IKEM, IN 00023001"). ES, MN and MJ were supported by the Ministry of Health of the Czech Republic, grant Nr. NV18-06-00032.

Author contributions: ES, MJ: designed the study and wrote the manuscript; ES: performed histochemical and immunohistological analysis; MN, MJ: carried out mutational analysis; RK: participated in collecting the laboratory and clinical data; IS: performed laboratory evaluation of copper metabolism; All authors revised and edited the draft and are in agreement with the content of the manuscript.

Conflict of interest statement: None declared.

REFERENCES

1. De Vree JML, Jacquemin E, Sturm E, Cresteil D, Bosma PJ, Aten J, Deleuze JF, Desrochers M, Burdelski M, Bernard O, Oude Elferink RP, Hadchouel M. Mutations in the MDR3 gene cause progressive familial intrahepatic cholestasis. Proc Natl Acad Sci 1998;95(1):282-7.
2. Van der Bliek AM, Baas F, Ten Houte de Lange T, Kooiman PM, Van der Velde-Koerts T, Borst P. The human mdr3 gene encodes a novel P-glycoprotein homologue and gives rise to alternatively spliced mRNAs in liver. EMBO Journal 1987;6(11):3325-31.
3. Dean M, Rzhetsky A, Allikmets R. The human ATP-binding cassette (ABC) transporter superfamily. Genome Res 2001;11(7):1156-66.
4. Morita SY, Terada T. Molecular mechanisms for biliary phospholipid and drug efflux mediated by ABCB4 and bile salts. Biomed Res Int 2014;2014:954781.
5. Shneider BL. ABCB4 Disease Presenting with Cirrhosis and Copper Overload-Potential Confusion with Wilson Disease. J Clin Exp Hepatol 2011;1(2):115-7.
6. Ramraj R, Finegold MJ, Karpen SJ. Progressive familial intrahepatic cholestasis type 3: overlapping presentation with Wilson disease. Clin Pediatr 2012;51:689-91.
7. Boga S, Jain D, Schilsky ML. Presentation of progressive familial intrahepatic cholestasis type 3 mimicking Wilson disease: molecular genetic diagnosis and response to treatment. Pediatr Gastroenterol Hepatol Nutr 2015;18(3):202.
8. Bansal N(G), Rastogi M. An Itchy Experience - PFIC 3 Masquerading as Wilson's Disease; Learning from Mistakes. OGH Reports 2017;6(1):67-71.
9. Bendl J, Stourac J, Salanda O, Pavelka A, Wieben ED, Zendulka J, Brezovsky J, Damborsky J. PredictSNP: robust and accurate consensus classifier for prediction of disease-related mutations. PLOS Comput Biol 2014;10(1):e1003440.
10. Rodriguez-Castro KI, Hevia-Urrutia FJ, Sturniolo GC. Wilson's disease: A review of what we have learned. World J Hepatol 2015;7(29):2859-70.
11. Schilsky ML. Wilson Disease: Diagnosis, Treatment, and Follow-up. Clin Liver Dis 2017;21(4):755-67.
12. Lalioti V, Tsubota A, Sandoval IV. Disorders in Hepatic Copper Secretion: Wilson's Disease and Pleomorphic Syndromes. Semin Liver Dis 2017;37(2):175-88.
13. Schatz SB, Jüngst C, Keitel-Anselmo V, Kubitz R, Becker C, Gerner P, Pfister ED, Goldschmidt I, Junge N, Wenning D, Gehring S, Arens S, Bretschneider D,Grothues D, Engelmann G, Lammert F, Baumann U. Phenotypic spectrum and diagnostic pitfalls of ABCB4 deficiency depending on age of onset. Hepatol Commun 2018;2(5):504-14.
14. Davit-Spraul A, Gonzales E, Baussan C, Jacquemin E.The spectrum of liver diseases related to ABCB4 gene mutations: Pathophysiology and clinical aspects. Semin Liver Dis 2010;30(2):134-46.
15. Jacquemin E, DeVree JM, Cresteil D, Sokal EM, Sturm E, Dumont M, Scheffer GL, Paul M, Burdelski M, Bosma PJ, Bernard O, Hadchouel M, Elferink RP. The wide spectrum of multidrug resistance 3 deficiency: from neonatal cholestasis to cirrhosis of adulthood. Gastroenterology 2001;120(6):1448-58.
16. Wendum D, Barbu V, Rosmorduc O, Arrivé L, Fléjou JF, Poupon R. Aspects of liver pathology in adult patients with MDR3/ABCB4 gene mutations. Virchows Arch 2012;460(3):291-8.
17. Van Der Woerd WL, Houwen RHJ, Van De Graaf SFJ. Current and future therapies for inherited cholestatic liver diseases. World J Gastroenterol 2017; 23(5):763-75.

PLOS ONE

RESEARCH ARTICLE

Exome sequencing reveals *IFT172* variants in patients with non-syndromic cholestatic liver disease

Magdaléna Neřoldová[1,2], Elżbieta Ciara[3], Janka Slatinská[1], Soňa Fraňková[1], Petra Lišková[4,5], Radana Kotalová[6], Janka Globinovská[7], Markéta Šafaříková[2], Lucie Pfeiferová[2,8], Hana Zůnová[9], Lenka Mrázová[5], Viktor Stránecký[5], Alena Vrbacká[5], Ondřej Fabián[1,10], Eva Sticová[1], Daniela Skanderová[11], Jan Šperl[1], Marta Kalousová[2], Tomáš Zima[2], Milan Macek[9], Joanna Pawlowska[12], A. S. Knisely[13], Stanislav Kmoch[5], Milan Jirsa[1,2]*

1 Institute for Clinical and Experimental Medicine, Prague, Czech Republic, **2** Institute of Medical Biochemistry and Laboratory Diagnostics, First Faculty of Medicine, Charles University and General University Hospital in Prague, Prague, Czech Republic, **3** Department of Medical Genetics, The Children's Memorial Health Institute, Warsaw, Poland, **4** Department of Ophthalmology, First Faculty of Medicine, Charles University and General University Hospital in Prague, Prague, Czech Republic, **5** Department of Pediatrics and Inherited Metabolic Diseases, First Faculty of Medicine, Charles University and General University Hospital in Prague, Prague, Czech Republic, **6** Department of Pediatrics, Second Faculty of Medicine, Charles University and Faculty Hospital Motol, Prague, Czech Republic, **7** Department of Pediatrics, Hospital Poprad, Poprad, Slovak Republic, **8** Department of Informatics and Chemistry, University of Chemistry and Technology in Prague, Prague, Czech Republic, **9** Department of Biology and Medical Genetics, Second Faculty of Medicine, Charles University and Motol University Hospital, Prague, Czech Republic, **10** Department of Pathology and Molecular Medicine, 3rd Faculty of Medicine, Charles University and Thomayer Hospital, Prague, Czech Republic, **11** Department of Pathology, Faculty of Medicine and Dentistry, Palacky University Olomouc and Faculty Hospital, Olomouc, Czech Republic, **12** Department of Gastroenterology, Hepatology, Nutritional Disorders and Pediatrics, The Children's Memorial Health Institute, Warsaw, Poland, **13** Diagnostik- und Forschungsinstitut für Pathologie, Medizinische Universität Graz, Graz, Austria

* milan.jirsa@ikem.cz

OPEN ACCESS

Citation: Neřoldová M, Ciara E, Slatinská J, Fraňková S, Lišková P, Kotalová R, et al. (2023) Exome sequencing reveals *IFT172* variants in patients with non-syndromic cholestatic liver disease. PLoS ONE 18(7): e0288907. https://doi.org/10.1371/journal.pone.0288907

Editor: Pavel Strnad, Medizinische Fakultat der RWTH Aachen, GERMANY

Received: March 10, 2023

Accepted: July 5, 2023

Published: July 20, 2023

Data Availability Statement: Exome sequencing data contain potentially identifying or sensitive patient and family information. The data are deposited in the General University Hospital in Prague and National Centre for Medical Genomics (https://ncmg.cz/) databases. Access is conditioned by permission from the General University Hospital Ethics Committee (https://www.vfn.cz/en/odbornici/eticka-komise/informace-o-eticke-komisi-vfn/).

Abstract

Background and aim

Gene defects contribute to the aetiology of intrahepatic cholestasis. We aimed to explore the outcome of whole-exome sequencing (WES) in a cohort of 51 patients with this diagnosis.

Patients and methods

Both paediatric (n = 33) and adult (n = 18) patients with cholestatic liver disease of unknown aetiology were eligible. WES was used for reassessment of 34 patients (23 children) without diagnostic genotypes in *ABCB11*, *ATP8B1*, *ABCB4* or *JAG1* demonstrable by previous Sanger sequencing, and for primary assessment of additional 17 patients (10 children). Nasopharyngeal swab mRNA was analysed to address variant pathogenicity in two families.

Funding: MN, ES, and MJ were supported by the Ministry of Health of the Czech Republic (MHCZ, https://www.mzcr.cz/) grants NV18-06-00032 and DRO IKEM IN 00023001. MŠ, LP, MK, and TZ were supported by the MHCZ (https://www.mzcr.cz/) grant DRO VFN IN 00064165, Ministry of Education, Youth and Sports (MEYS, https://www.msmt.cz/) grant LM2018125, and European Regional Development Fund, (https://commission.europa.eu/funding-tenders/find-funding/eu-funding-programmes/european-regional-development-fund-erdf_en) project EF16_013/0001674. HZ and MM were supported by grants DRO FNM IN 00064203 from MHCZ (https://www.mzcr.cz/) and LM2018132 from MEYS (https://www.msmt.cz/). MN and SK were supported by the MEYS (https://www.msmt.cz/) grant SVV 260631. The funders had no role in study design, data collection and analysis, decision to publish, or preparation of the manuscript.

Competing interests: NO authors have competing interests

Abbreviations: ABC, ATP-binding cassette; ACMG, American College of Medical Genetics and Genomics; ALT, alanine aminotransferase; AST, aspartate aminotransferase; BMI, body mass index; BSEP, bile-salt export pump; CCS, circular consensus sequence; CGH, comparative genomic hybridization; COL, collagen; FES, focused-exome sequencing; GGT, gamma-glutamyl transferase; GSD, glycogen storage disease; ID, identifier; IFT, intraflagellar transport; JAG, jagged canonical notch ligand; JAM, junctional adhesion molecule; LP, likely pathogenic; MAF, minor allele frequency; MDR, multiple drug resistance; NCBI, National Centre for Biotechnology Information; NPHP, nephronophthisis; OMIM, Online Mendelian Inheritance in Man; P, pathogenic; PAS, periodic acid-Schiff; PKHD, polycystic kidney and hepatic disease; PKD, polycystic kidney disease; PPOX, protoporphyrinogen oxidase; SNP, single nucleotide polymorphism; SRTD, short-rib thoracic dysplasia; TMEM, transmembrane protein; TNFRSF, tumour necrosis factor receptor superfamily; TP, tumour protein; ULN, upper limit of normal; VP, variegate porphyria; VUS, variant of unknown significance; WES, whole-exome sequencing; ZNF, zinc finger.

Results

WES revealed biallelic variation in 3 ciliopathy genes (*PKHD1*, *TMEM67* and *IFT172*) in 4 clinically unrelated index subjects (3 children and 1 adult), heterozygosity for a known variant in *PPOX* in one adult index subject, and homozygosity for an unreported splice-site variation in *F11R* in one child. Whereas phenotypes of the index patients with mutated *PKHD1*, *TMEM67*, and *PPOX* corresponded with those elsewhere reported, how *F11R* variation underlies liver disease remains unclear. Two unrelated patients harboured different novel biallelic variants in *IFT172*, a gene implicated in short-rib thoracic dysplasia 10 and Bardet-Biedl syndrome 20. One patient, a homozygote for *IFT172* rs780205001 c.167A>C p.(Lys56Thr) born to first cousins, had liver disease, interpreted on biopsy aged 4y as glycogen storage disease, followed by adult-onset nephronophthisis at 25y. The other, a compound heterozygote for novel frameshift variant *IFT172* NM_015662.3 c.2070del p.(Met690Ilefs*11) and 2 syntenic missense variants *IFT172* rs776310391 c.157T>A p.(Phe53Ile) and rs746462745 c.164C>G p.(Thr55Ser), had a severe 8mo cholestatic episode in early infancy, with persisting hyperbilirubinemia and fibrosis on imaging studies at 17y. No patient had skeletal malformations.

Conclusion

Our findings suggest association of *IFT172* variants with non-syndromic cholestatic liver disease.

Introduction

Genetic defects contribute to intrahepatic cholestasis in both children and adults [1]. Using a phenotype-based candidate gene approach, patients can be successfully diagnosed by Sanger sequencing; nonetheless, sequencing of a 66-gene cholestasis panel designed by EGL Genetics in 2017 increased the chance of diagnostic success in infants, children, and young adults, replacing single-gene analysis as a primary diagnostic tool [2]. The Mayo Clinic Laboratories currently offer testing for 112 "cholestasis genes" (test ID: CHLGP); even this is likely not exhaustive.

Limitations imposed by panel size can be overcome by focused-exome sequencing (FES) using capture platforms that target ~5000 genes mutated in Mendelian genetic diseases (Mendeliome) [3] or by whole-exome sequencing (WES). WES is still considered a discovery tool rather than a standard diagnostic procedure although its usefulness has been repeatedly proven in paediatric patients and recently also in adults [4]. The main advantage of WES, coverage of most expressed transcripts, opens the way to unexpected diagnoses, with identification of novel genetic disorders [5–10] and gene-phenotype relationships such as liver manifestations of known extrahepatic diseases without or with secondary liver injury. Whereas the main disadvantageous features of WES–need for excessive data processing and higher cost–have already been overcome, one should keep in mind that, as with FES or panel sequencing, even in WES methodology limitations inhere: Not all exons may be captured, sensitivity for structural variations is low, and WES does not include most non-coding regions [11].

In this study we explored the contribution of WES to molecular diagnosis in 51 patients with intrahepatic cholestasis.

Patients and methods

Patients

Patients with cholestatic liver disease or a history of cholestasis of unknown aetiology documented by detailed medical reports from the referring centre were eligible. Cholestasis was defined as conjugated hyperbilirubinemia accompanied by bilirubinostasis in hepatocytes, canaliculi and Kupffer cells in acinar zone 3, and / or by ductular reaction in acinar zone 1 on histopathologic study, or by elevated serum bile salt level exceeding 10 μmol/l. Patients with extrahepatic bile duct obstruction or autoimmune hepatobiliary disease and those fed only parenterally were excluded. Phenotyping was based on clinical reports and accessible histopathology reports provided by the referring centres (see S1 File). The authors had access to information that could identify individual participants during or after data collection. Where possible, samples from first-degree relatives were obtained for segregation studies. Composed identifiers (IDs) used for index subjects in the results section and tables indicate gender (M—male, F–female), patient age in years at specimen receipt, origin (CE—Central Europe, RO–Roma, PA–Australian Pacific, EA–East Asia, ME–Middle East), and unique number indicating order of specimen receipt. All 18 enrolled adult patients, legal guardians of all 33 enrolled children and all 58 available first-degree relatives who provided DNA samples signed written informed consent for genetic testing approved by the relevant institutional human research committees. The study protocol conforms to the ethical guidelines of the 1975 Declaration of Helsinki as reflected in *a priori* approval by the institution's human research committee of IKEM and Thomayer Hospital in Prague, Czech Republic (Docket No. 17-06-18, date June 28, 2017, study period from July 2017 till December 2022).

Thirty-four enrolled index patients (samples collected between December 2006 and February 2021) represented a subset of 109 patients negatively screened by Sanger sequencing since June 2002 (Fig 1). Most of the remaining 75 patients were lost to clinical follow-up; in a few the diagnosis was re-classified as non-genetic disease. Seventeen index patients with clinically uncertain diagnosis due to various extrahepatic comorbidities such as kidney disease, osteogenesis imperfecta, cutaneous porphyria, orofacial cleft or episodic fever, were examined directly by WES between October 2018 and November 2021.

Histologic and immunohistologic study

Percutaneous liver-biopsy specimens were fixed in 4% paraformaldehyde and routinely processed for histological examination. Paraffin sections cut at 4 μm were stained with haematoxylin and eosin, Weigert-van Gieson with resorcin-fuchsin, periodic acid-Schiff reaction (PAS) with and without diastase pre-digestion, orcein, and Perls' reaction. For immunohistochemical analysis, sections were incubated with anti-cytokeratin 7 antibody at a dilution of 1:100, anti-MDR3/ABCB4 rabbit polyclonal antibody at a dilution of 1:20, and anti-BSEP/ABCB11 rabbit polyclonal antibody at a dilution of 1:200 (details, S1 Table). Primary antibodies were detected by ultraView Universal DAB Detection Kit (Roche Tissue Diagnostics [formerly Ventana Medical Systems], Basel, Switzerland).

DNA isolation. Genomic DNA was extracted from peripheral blood by QIAamp DNA Blood Kit (Qiagen, Hilden, Germany) with standard procedures.

Whole-exome sequencing

After mechanical fragmentation, exome libraries were constructed according to the manufacturer's standard protocol with TruSeq® Exome Kit (Illumina, San Diego, CA). WES was accomplished using the Illumina NextSeq 500 platform. Alignment to the reference sequence

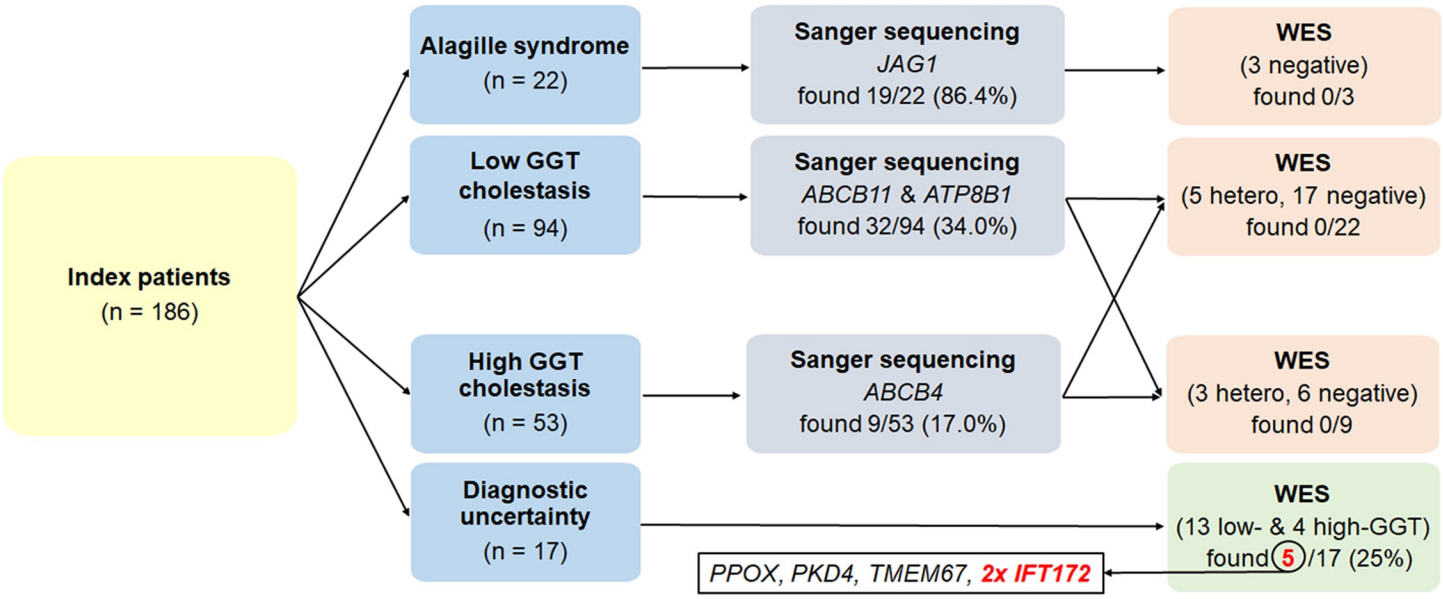

Fig 1. Patient enrolment and sample processing diagramme. Using a phenotype-based candidate gene approach, 169 index patients were screened by Sanger sequencing for variants in *JAG1* (n = 22), *ABCB11* & *ATP8B1* (n = 94), and *ABCB4* (n = 53). The remaining 17 index patients with diagnostic uncertainty were directly examined by WES. Nineteen of the 22 clinically diagnosed Alagille syndrome patients carried monoallelic P, LP or VUS variants in *JAG1* (S3A Table). Forty-one of the 147 patients with non-syndromic cholestasis were homozygotes or compound heterozygotes for P/LP/VUS variants in either *ABCB11* or *ATP8B1* (32 patients with low-GGT cholestasis, S3B Table) or in *ABCB4* (9 patients with high-GTT cholestasis, S3C Table). The 60 patients carrying monoallelic variants in *JAG1* or biallelic variants in *ABCB11*, *ATP8B1* or *ABCB4* were excluded.

https://doi.org/10.1371/journal.pone.0288907.g001

(hg19 build) and variant calling was performed by Qiagen CLC Genomics Workbench 12 (https://digitalinsights.qiagen.com/). Identified variants were selected for annotation and interpretation using a 5% minor allele frequency (MAF) threshold taken from the gnomAD database. IGV Viewer [12] was used to display the data. Exome sequencing data are deposited in the General University Hospital in Prague and National Centre for Medical Genomics databases. Access conditioned by permission from the General University Hospital Ethics Committee.

Sanger sequencing

DNA sequencing of gel-purified PCR products (primer list, S2 Table) was performed by 3.1 Dye Terminator cycle sequencing kit and 3130 Genetic Analyzer electrophoresis (both Thermo Fisher Scientific, Waltham, MA).

Variant classification

Variants were classified according to American College of Medical Genetics and Genomics [ACMG] professional guidelines [13] using the VARSOME tool [14], published literature, variant databases NCBI ClinVar & Human Gene Mutation Database (HGMD), and population frequency information compiled in NCBI dbSNP. Sequence variations were assigned among the 5 categories benign, likely benign, variant of unknown significance (VUS), likely pathogenic (LP), or pathogenic (P). We characterized carriage of one P or LP variant as diagnostic for autosomal-dominant diseases and carriage of P/P, P/LP, or LP/LP variants as diagnostic for autosomal-recessive diseases.

Detection of copy number variations (CNV) and homozygosity regions

The command-line software toolkit CNVkit version 0.9.6CNV was used for CNV analysis of exome-sequencing data. Validation was performed by array comparative genome hybridization (CGH) using the commercially available oligonucleotide platforms GenetiSure Cyto 4x180K and SurePrint G3 CGH+SNP 4x180K (both Agilent Technologies, Santa Clara, CA). The latter platform was also used for detection of homozygosity regions. Data were analysed by CytoGenomics software version 5.1.2.1 (Agilent Technologies). UCSC Genome Browser, DECIPHER, NCBI ClinVar, OMIM, and DGV databases were used for assessment of clinical impacts of deletions and duplications.

Long range PCR and long-range amplicon single strand sequencing

A region containing the variants of interest in *IFT172* was directly amplified from genomic DNA using TaKaRa LA Taq DNA Polymerase with 10x LA PCR Buffer II (TaKaRa, Mountain View, CA) with a two-step PCR protocol (primers, S2 Table). Initial denaturation at 94˚C for 1min was followed by 30 cycles of 98˚C for 10s denaturation and 64.1˚C for 22min and 30s elongation. Final elongation was performed by incubation at 72˚C for 10min. Product length was 22,800 bp. LR-PCR products were purified using SPRI magnetic beads (Beckman Coulter Life Sciences, Brea, CA) according to the manufacturer's protocol, with 2μl used for Qubit 2.0 Fluorometric Quantitation (Beckman Coulter Life Sciences) dsDNA high sensitivity assay. Purified samples were sequenced by Pacific Biosciences Sequel system (PacBio, Menlo Park, CA) according to manufacturer's protocol using SMRTbell Express Template Kit 2.0 and Sequel Sequencing Kit 3.0. To obtain highly accurate reads, Circular Consensus Sequence (CCS) analysis was performed using Pacific Biosciences SMRT Link (v6.0). CCS reads were aligned to human reference genome (hg19) using Minimap2 v. 2.24 [15], sorted with SAMtools and visualized in IGV browser.

Nasopharyngeal swab mRNA analysis

Total RNA was isolated from nasopharyngeal swabs using viRNAtrap and magnetic beads from GeneSpector (Prague, Czech Republic). RNA libraries were prepared using KAPA RNA HyperPrep Kit with RiboErase (Roche, Basel, Switzerland) according to manufacturer's instructions. RNA sequencing (2x100 paired-end reads) was performed in 3 patients and family members using the NovaSeq 6000 system (Illumina, San Diego, CA) at the National Center for Medical Genomics in Prague. The resulting files in FASTQ format were subjected to quality control and trimmed using Atropos v.1.128 [16]. Gene-level abundances were estimated using Salmon v.1.3 [17] with Ensembl based annotation package *EnsDb.Hsapiens.v75*. Normalization and differential expression analyses were performed within the DESeq2 R package [18].

Coding DNA was transcribed from RNA isolated from nasopharyngeal swab using SuperScript™ IV Reverse Transcriptase (ThermoFisher), oligo dT 23VN and random hexamers following manufacturers protocol. A region encompassing *F11R* exons 1–10 was amplified using Phusion Hot Start Flex DNA Polymerase (Thermo Fisher Scientific) with a three step PCR protocol. The 1,052 bp product was purified using SPRI magnetic beads (Beckman Coulter Life Sciences, Brea, CA) and the region of interest was sequenced (primers, S2 Table).

Results

WES was performed in 51 clinically unrelated index subjects and in 58 available family members. Demographic characteristics and laboratory phenotype of the enrolled index subjects are presented in Table 1.

Table 1. Demographic characteristics and phenotypes of enrolled index subjects.

Age at referral (years)	Low-GGT cholestasis		High-GGT cholestasis	
	male	female	male	female
<2	4	3	4	0
2–18	13	2	4	3
≥19	3	8	3	4

Low GGT means serum GGT activity ≤ 1.04 μmol/l for the age category 7wk– 52wk, ≤ 0.39 μmol/l for children aged 1y – 15y, ≤ 0.84 μmol/l for males aged > 15y and ≤ 0.64 μmol/l for females aged > 15y.

https://doi.org/10.1371/journal.pone.0288907.t001

In 26 index subjects (18 children at referral), initial Sanger sequencing had found no aetiologic variants in *JAG1* (OMIM 601920), *ABCB11* (OMIM 603201), *ATP8B1* (OMIM 602397), or *ABCB4* (OMIM 171060). In 8 single heterozygotes (5 children at referral) for P/LP variants in *ABCB11*, *ATP8B1* (S4A and S4B Table) or *ABCB4* (S4A and S4C Table), clinical findings (with disease) were discordant with heterozygosity for just one variant. WES did not reveal genetic causes of liver disease in these 34 patients; however, among the remaining 17 families (10 index patients were children at referral), unexpected molecular findings potentially relevant for genetic liver disease were obtained in 6 patients (Table 2).

In 3 of these patients (ID F48CE680, F9CE723, and M18CE172), molecular diagnoses respectively of variegate porphyria (VP, OMIM #176200), polycystic kidney disease with or without polycystic liver disease 4 (PKD4, OMIM #263200), and nephronophthisis 11 (NPHP11, OMIM #613550, ref. [19]) were established. Two other index subjects harboured biallelic variants in *IFT172* (OMIM 607386):

Patient 1 with biallelic variants in *IFT172*

A Roma man (ID M26RO684, Table 2) aged 26y, living with foster parents and without available birth-family members, had chronic liver disease with hepatomegaly since early childhood.

Table 2. Candidate causative pathogenic / likely pathogenic variants and variants of unknown significance compatible with patient phenotype and type of inheritance.

Patient ID	Clin. dx.	P / LP variants	VUS
F48CE680	PCT, low-GGT cholestasis	***PPOX* rs774663053 c.397G>T p.(Glu133*)**, CM981616, HET	not found
F9CE723 (+ parents)	low-GGT PFIC	***PKHD1* rs760222236 c.8870T>C p.(Ile2957Thr),** CM020500, HET, maternal	***PKHD1* NM_138694.4 c.10768A>T p.(Ile3590Phe),** HET, paternal
M18CE172 (+ parents)	low-GGT PFIC	***TMEM67* rs201893408 c.1843T>C p.(Cys615Ser)**, CM094694, HOM, both unaffected parents HET	not found
M26RO684	glycogenosis, high-GGT PFIC	not found	***IFT172* rs780205001 c.167A>C p.(Lys56Thr)**[a], HOM
M14CE762	low-GGT PFIC	***IFT172* NM_015662.3 c.2070del p.(Met690Ilefs*11)**, HET	***IFT172* rs776310391 c.157T>A p.(Phe53Ile)**, HET ***IFT172* rs746462745 c.164C>G p.(Thr55Ser)**, HET
F1RO453 (+ parents + 2 sisters)	low-GGT PFIC	***F11R* NM_016946.6 c.65-2A>T**, HOM, both unaffected parents HET, unaffected sisters HOM and HET	not found

Variants are classified according to the ACMG criteria [13] were valid in week 20, 2023. Clin. dx.–clinical diagnosis. GGT–gamma-glutamyl transferase, PFIC–progressive familial intrahepatic cholestasis, PCT–porphyria cutanea tarda, rs–dbSNP accession number, CM–HGMD accession number, HET–heterozygous state, HOM–homozygous state.

[a]The Association of Molecular Pathology classification of the marked variant is LP.

https://doi.org/10.1371/journal.pone.0288907.t002

Histopathologic study of a liver-biopsy specimen obtained at age 4y found preserved hepatic lobular and vascular architecture with well-glycogenated hepatocytes and trivial steatosis; fibrosis, inflammation, and accumulations of bile pigment were not seen (Fig 2).

Glycogen storage disease (GSD) was suspected and the patient was repeatedly examined by a specialist in genetic metabolic diseases. Activities of phosphorylase in leukocytes and of phosphorylase kinase and glycogen debrancher enzyme in erythrocytes investigated at age 9y were within normal ranges, leaving mild forms of GSD types I or III still under consideration. Alanine aminotransferase (ALT) and aspartate aminotransferase (AST) activities were elevated

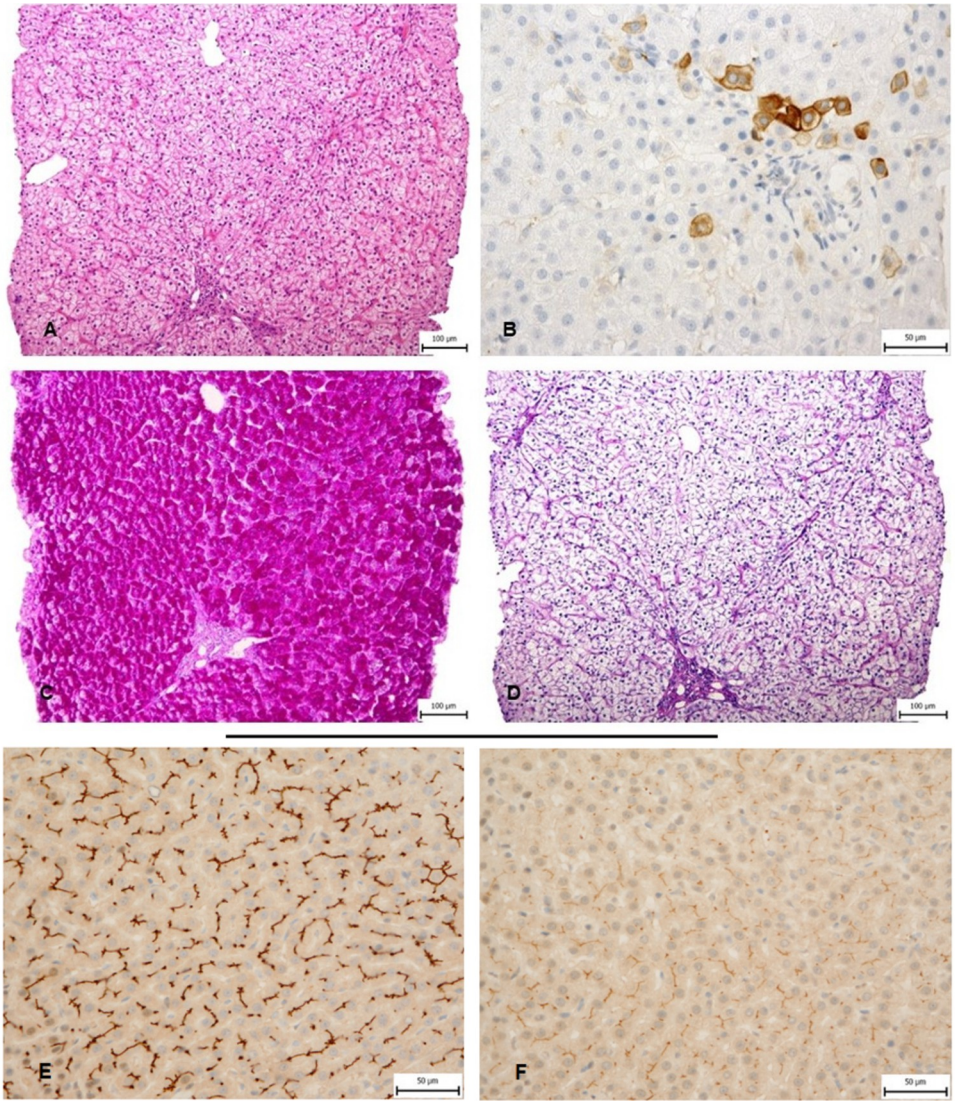

Fig 2. Photomicrographs, liver of patient homozygous for variant c.167A>C p.(Lys56Thr) in *IFT172* (index patient ID M26RO684, aged 4y). (**A**) Preserved lobular architecture with enlarged and pale hepatocytes (haematoxylin and eosin, original magnification 200x). (**B**) Interlobular bile duct deficiency with aberrant CK7 expression in some periportal hepatocytes (anti-CK7 immunostaining—CK7-expressing cells highlighted in brown / negative background blue, original magnification 400x). (**C**) Glycogen accumulation in hepatocytes with diffuse PAS reactivity, (**D**) lacking after diastase pre-digestion (original magnification 200x both). (**E**) Strong diffuse expression of ABCB11 on canalicular membranes of hepatocytes (anti-ABCB11 immunostaining, original magnification 400x). (**F**) Focally attenuated expression of ABCB4 on canalicular membranes of hepatocytes (anti-ABCB4 immunostaining, original magnification 400x).

https://doi.org/10.1371/journal.pone.0288907.g002

(ALT 1.5x upper limit of normal [ULN], AST 2x ULN) without abnormal values for other biomarkers (serum bilirubin, GGT, blood glucose, lactate and lipid profile, renal-function indicators, and erythrocyte glycogen content) at age 11y. Dietary measures were introduced and metabolic-disease specialists supervised the patient till age 25y, when end-stage kidney disease of unknown aetiology requiring initiation of haemodialysis maintenance was diagnosed. Evaluation for renal transplant took place at the Institute of Clinical and Experimental Medicine.

On admission, apart from severely elevated urea and creatinine values, mildly increased serum AST activity (2.7x ULN) and severely increased cholestasis-biomarker enzyme activities (alkaline phosphatase 6.5x ULN, GGT 11.3x ULN) were observed, without hyperbilirubinemia. Ultrasonography revealed bilateral renal atrophy without abnormalities of liver or spleen. Percutaneous liver biopsy was repeated. The light-microscopy finding of mild hepatocellular glycogen deposition was unchanged. In addition, transfusional siderosis and lack of interlobular bile ducts in 5 of 14 portal tracts accompanied by mild features of chronic cholestasis were observed. Portal-tract fibrosis, hamartomatous or cystic bile-duct profiles, and hypoplasia of portal-vein radicles were absent; criteria for diagnosis of ductal plate malformation were not met. Canalicular expression of the homologues BSEP/ABCB11 and MDR3/ABCB4 was preserved, but for the latter was strikingly less prominent than for the former, suggesting *ABCB4* disease. WES was requested to aid in diagnosis.

P/LP variants were detected among neither 66 neonatal/adult cholestasis genes [2] nor 21 genes mutated in GSD [20]. Bioinformatics analysis revealed a homozygous variant, rs780205001 c.167A>C (p.Lys56Thr), in *IFT172*, validated by Sanger sequencing (Fig 3A). The variant, rare in population databases (ExAC 0.0000119, GnomAD_exome 0.0000084, ALFA 0.005%) and not found in 110 unrelated Roma individuals, has not been identifiably reported in *IFT172*-related conditions. The lysine residue is highly conserved and a moderate physicochemical difference between lysine and threonine exists. The available evidence is currently insufficient to determine the role of this variant in disease. Therefore, the variant is classified as VUS in the NCBI ClinVar database (acc. no. VCV001015325.2). However, using the ACMG classification, Varsome suggested "warm" VUS (ACMG/AMP = PS4_supp (1p) + PM2_supp (1p) + PM3_supp (0.5p)+ PP3 (1p)+ PP4 (1p)+ BP1 (-1p) = 3.5points >>VUS (tepid/warm)) and the prediction programmes PredictSNP (all MAPP, PhD-SNP, PolyPhen, SIFT and SNAP) and MutationTaster suggested likely pathogenicity. Accordingly, advanced modelling of protein sequence and biophysical properties (such as structural, functional, and spatial information, amino acid conservation, physicochemical variation, residue mobility, and thermodynamic stability) performed at Invitae (San Francisco, CA) indicates that this missense variant is expected to disrupt IFT172 protein function.

RNAseq of mRNA isolated from nasopharyngeal swabs confirmed that the variant NM_015662.3 r.257A>C was present in all reads from the *IFT172* transcripts, without impact on *IFT172* mRNA expression level, which was within population expression boundaries. No abnormal alternative splicing event in *IFT172* was observed. The impact of the variant on IFT172 protein expression or subcellular localisation in the liver biopsy specimen could not be assessed due to the lack of a suitable antibody.

Parental unavailability precluded confirmation of homozygosity for the *IFT172* variant by analysis of parental DNA samples. To distinguish between true homozygosity and hemizygosity for *IFT172* c.167A>C, CNV analysis focused on the *IFT172* locus ([GRCh37]: chr2: 27667244–27712610) was repeated. Read number did not fall. Moreover, WES data identified the variant as located in a 24.03Mb homozygosity region ([GRCh37], chr2:20440321–44471409). To validate this, we performed genomic hybridisation on two CGH arrays. In line with exomic data, no copy-number changes in the *IFT172* region (2p23.3) or other CNV(s) explaining the proband's phenotype were identified. The CGH SNP array detected loss of

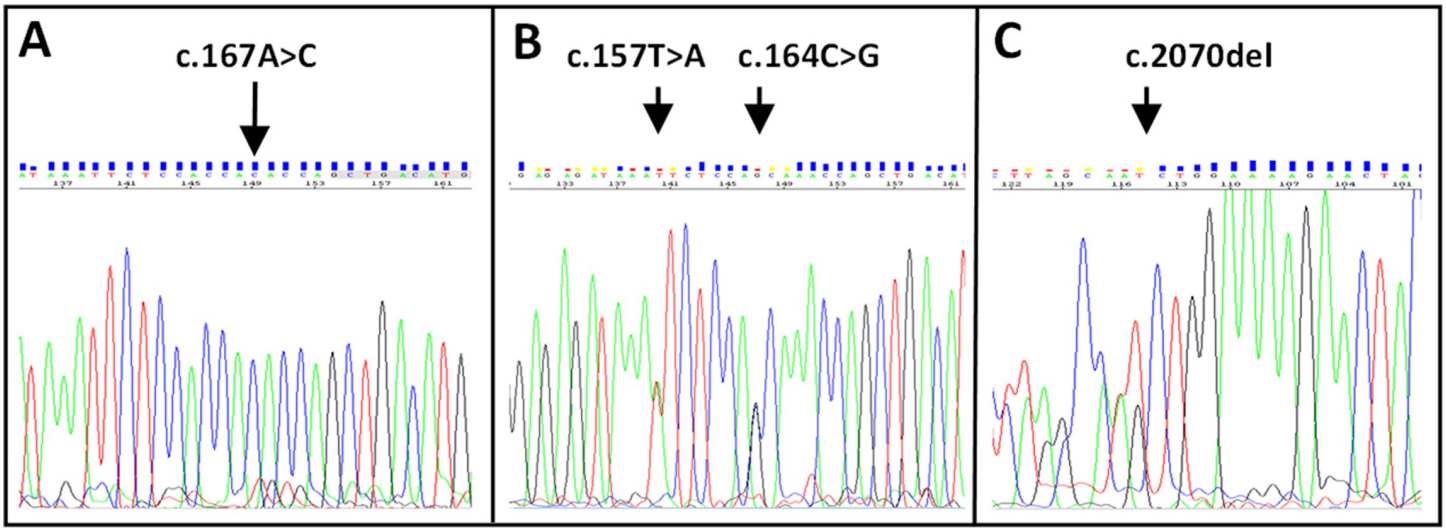

Fig 3. Validation electropherograms of *IFT172* partial genomic DNA sequence of exon 2 from index subjects M26RO684 (**A**) and M14CE762 (**B**), and exon 20 from index subject M14CE762 (**C**).

https://doi.org/10.1371/journal.pone.0288907.g003

heterozygosity of autosomal regions (total range 322Mb; 11.2% of haploid autosomal genome). Coefficient of consanguinity (*f*) of the proband's biological parents was 1/4. We also confirmed that *IFT172* lay in a 27.2Mb homozygosity region (arr[GRCh37] 2p23.3(19824727_47021455) x2 hmz).

Within 1y the patient´s body mass index (BMI) recovered from 27.6 to 33 (obesity grade I). At age 26y the patient was listed for kidney transplantation, performed at age 27y.

The finding of a homozygous c.167A>C p.(Lys56Thr) "warm" VUS in *IFT172* suggested short-rib thoracic dysplasia 10 (SRTD10, OMIM #615630) or Bardet-Biedl syndrome 20 (OMIM #619471). Further physical examination and roentgenograms of the chest, hips, legs, and feet revealed no bone malformations. Nor did ophthalmologic examination identify retinitis pigmentosa, typical in IFT172 deficiency (S1 Fig). Best corrected visual acuity was bilaterally normal (1.0 Snellen decimal values), as was intraocular pressure (19mmHg OD, 15mmHg OS). The patient interestingly had an abnormally thin retinal ganglion cell layer, documented using spectral domain optical coherence tomography (Spectralis, Heidelberg Engineering, Heidelberg, Germany).

Patient 2 with biallelic variants in *IFT172*

A caucasian boy (ID M14CE762, Table 2) born to unaffected parents, manifested severe icterus, hepatosplenomegaly, and coagulopathy aged 2mo, with hyperbilirubinemia (total bilirubin 18x ULN, direct bilirubin 27.3x ULN), abnormal hepatobiliary-injury biomarker values (AST 8.9x ULN, ALT 2.8x ULN), and hypercholanemia (30x ULN). GGT activity was within normal range. Light microscopy of a liver-biopsy specimen found giant-cell change of hepatocytes with cholestasis and fibrosis; steatosis and glycogen accumulation were absent. By age 10mo hyperbilirubinemia was nearly resolved; however, it has persisted (age 18y, total and direct bilirubin 1.4x and 1.1x ULN respectively) and findings on elastography (liver stiffness 9 kPa) indicate liver fibrosis and steatosis. The patient´s BMI is 20.6. Aside from nystagmus, physical-examination and laboratory findings are otherwise unremarkable, with in particular no skeletal malformations and no signs of kidney disease. He carries 3 variants in *IFT172*: On one allele he harbours the novel deletion c.2070del p.(Met690Ilefs*11, Fig 3C), classified as

likely pathogenic (PVS1+PM2 = 9 points), and on the other (*i.e.*, in *trans*) 2 single-nucleotide substitutions, rs776310391 c.157T>A p.(Phe53Ile) and rs746462745 c.164C>G p.(Thr55Ser) (Fig 3B), both classified as VUS according the ACMG guidelines and likely pathogenic based on the Association for Molecular Pathology criteria (c.157T>A: PM2_supp (1p) + PM3_supp (1p) +PP3 (1p) = 3 points >>VUS (tepid), c.164C>G: PM2_supp (1p) + PM3_supp (1p) + BP1 (-1p) + BP4 (-1p) = 0 points >>>VUS (ice cold)). Since both parents refused genetic testing, relative position of the variants was assessed by single strand sequencing of long-range PCR products encompassing all 3 mutated loci.

Carrier of biallelic variant in *F11R*

Finally, in a one-year-old (now 8y) Roma girl (ID F1RO453) with cholestatic cirrhosis, WES revealed a yet unreported homozygous splice-site variant, c.65-2A>T, in *F11R* (OMIM 605721), encoding the tight junction protein JAM1 (Figs 4 and S2).

Both unaffected parents were asymptomatic heterozygotes for the *F11R* c.65-2A>T variant.

Since no liver-biopsy specimen suitable for mRNA analysis was available, we analyzed nasopharyngeal-swab mRNA by RNAseq. Apart from the expected in-frame deletion of 69 base pairs (NM_016946.6 r.144_212del) caused by skipping of exon 2 (confirmed by Sanger sequencing of *F11R* cDNA), RNAseq revealed no P/LP variants. The *F11R* variant is predicted to replace 24 amino-acid residues by serine (p.Cys22_Pro45delinsSer). Such an indel should impair the function of the altered protein, if expressed, by removing the motif Asn43-Asn44--Pro45, involved in *trans*-homophilic interaction of JAM1 *cis*-dimers [21]. Unfortunately, clinical pathogenicity of the variant is uncertain: The same homozygous variant exists in the proband´s sister, aged 7y and unaffected at this writing.

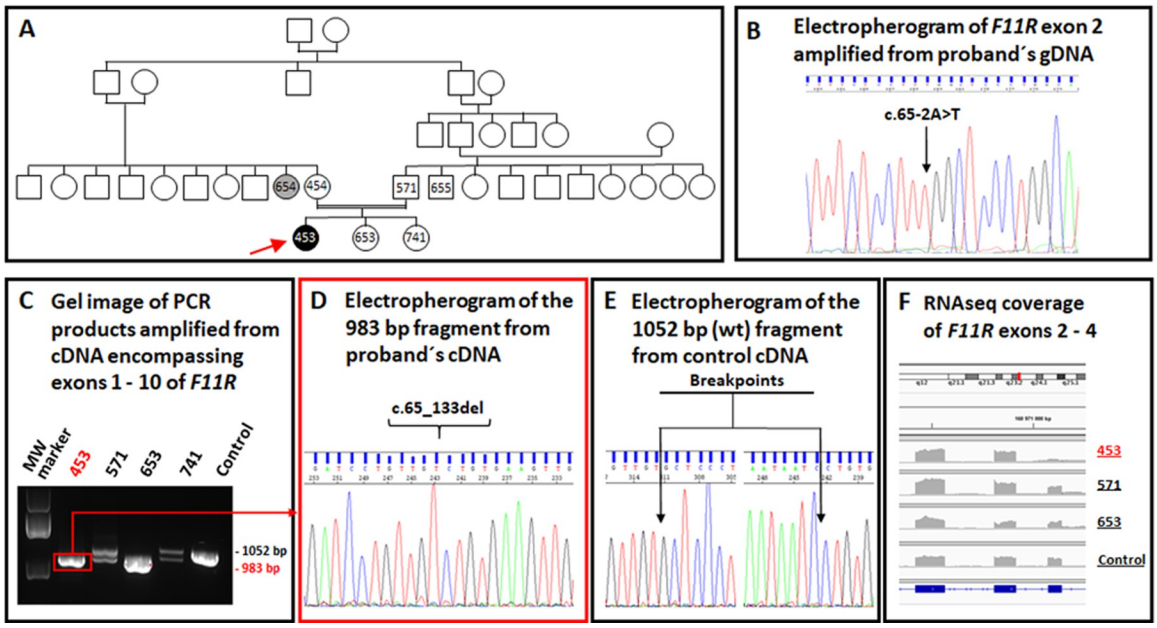

Fig 4. Molecular findings, family with JAM1 deficiency (index patient ID F1RO453). (**A**) Pedigree; arrow, index patient. (**B**) Sanger-sequencing electropherogram of *F11R* exon 2 amplified from the index patient´s gDNA. Arrow, homozygous *F11R* c.65-2A>T splice-site variant. (**C**) Agarose-gel electropherogram of PCR products encompassing exons 1–10 amplified from nasopharyngeal swabs *F11R* cDNA. (**D**) Sanger-sequencing electropherogram of the 983-bp fragment amplified from nasopharyngeal-swab cDNA of proband. Arrow, skipped exon 2. (**E**) Sanger-sequencing electropherogram of the 1052-bp fragment amplified from control nasopharyngeal-swab cDNA (wild-type sequence). Arrows, breakpoints. (**F**) Graphical representation of *F11R* exons 2, 3, and 4 coverage by RNAseq of nasopharyngeal-swab mRNA in IGV Viewer.

https://doi.org/10.1371/journal.pone.0288907.g004

Extrahepatic diseases

Apart from the patients described above, other genetic diagnoses were suggested in another three probands (Table 3). These include osteogenesis imperfecta caused by a recently reported variant in *COL1A2* (OMIM 120160) [22], familial periodic fever associated with a known variant in *TNFRSF1A* (OMIM 191190), and a combination of orofacial cleft with growth and mental retardation contributed by variants in *TP63* (OMIM 603273), *COL2A1* (OMIM 120140), and *ZNF423* (OMIM 604557) [23].

Discussion

In our cohort of 51 enrolled index patients, 34 of whom were extensively pre-screened by targeted gene approach, WES revealed unexpected findings in just 6 patients and other or additional genetic diagnoses in another 3 subjects. Multiple reasons for low efficiency can be adduced. Technical limitations of WES have been touched on; perhaps more important are difficulties with interpretation of variant pathogenicity. Sequencing of individual exomes provides lists of VUS never assessed experimentally. ACMG classification of individual variants is partially based on indirect indicators and *in silico* predictions–these in some situations may be misleading. That ClinVar classifications of numerous variants are equivocal, with several classifications of the same variant proposed, thus is unsurprising.

Concerning the capacity of WES to reveal rare unexpected principal and additional diagnoses, WES is obviously superior to sequencing a single gene or a disease gene panel. In the patient with jaundice associated with cutaneous porphyria (ID F48CE680), WES established the molecular diagnosis of variegate porphyria. This experience illustrates that diagnosis of disorders manifesting as cutaneous porphyria, with cholestasis and a negative family history but without a personal history of neurovisceral attacks, is scarcely possible without molecular-genetic studies.

Whereas congenital hepatic fibrosis was a clinical consideration in the second patient (ID F9CE723) despite the absence of cystic biliary-tract and renal disease detected after establishing the genetic diagnosis, ciliopathy gene variants were unexpected in the other three patients. In two, renal disease did not meet diagnostic criteria for nephronophthisis [19] before renal failure developed. Indeed, associations between liver disease and ciliopathy syndromes, including PKD4 and NPHP11, are published (review, Diamond *et al.* [24]).

The phenotype of IFT172 disease–short rib thoracic dysplasia 10 without polydactylv–varies greatly. It encompasses asphyxiating thoracic dysplasia (Jeune syndrome) [25], Mainzer-Saldino syndrome [25], isolated retinal degeneration [26], Bardet-Biedl syndrome [26, 27], and oral-facial-digital syndrome [28]. Some patients with Jeune or Meinzer-Saldino syndrome have

Table 3. Variants supporting other genetic diagnoses.

Patient ID	Clin. dx.	P / LP variants	Variants of unknown significance
F57CE614 (+ mother)	low-GGT PFIC	***COL1A2* rs67525025 c.767G>T p.(Gly256Val)**, CM062547, HET, non-maternal	not found
F6CE561 (+ parents)	high-GGT PFIC	***TNFRSF1A* rs4149584 c.362G>A p.(Arg121Gln)**, CM012483, HET, maternal	not found
M3RO646 (+ parents)	high-GGT PFIC	***TP63* rs768752805 c.799G>A p.(Val267Ile)**, CM1812821, HET, paternal ***ZNF423* rs548986682 c.3370G>A p.(Glu1124Lys)**, CM1512351, HET, maternal	***COL2A1* rs201675352 c.410G>A p.(Arg137His)**, CM160186, HET, paternal

Variants are classified according to the ACMG criteria [13] valid in week 20, 2023. Clin. dx.–clinical diagnosis. GGT–gamma-glutamyl transferase, PFIC–progressive familial intrahepatic cholestasis, rs–dbSNP accession number, CM–HGMD accession number, HET–heterozygous state, HOM–homozygous state.

https://doi.org/10.1371/journal.pone.0288907.t003

nephronophthisis designated as NPHP17. Liver disease includes bile-duct abnormalities with cystic dilatation and periportal fibrosis. Although liver abnormalities may attract medical attention as the first sign of Jeune syndrome [29], they are considered minor and inconsistent ciliopathy features encountered in Jeune syndrome even with only mild skeletal malformations [30].

Non-syndromic cholestatic liver injury in IFT172 disease without skeletal malformations–and without bile-duct abnormalities–has never been identifiably reported. Our observation of 2 unrelated carriers of biallelic IFT172 variants with unexplained primary cholestatic liver disease, strengthened in the older patient (ID M26RO684) by adult-onset nephronophthisis, location of the homozygous *IFT172* variant in a large homozygosity region inherited from consanguineous parents (cousins) and absence of candidate variants in the other 18 nephronophthisis genes, suggests association. Reduced retinal ganglion cell layer thickness observed in the older patient can be a sign of early pre-perimetric glaucoma [31]; however, given the age of the patient and normal intraocular pressure, a link with *IFT172* cannot be excluded.

What diagnosis to assign to the sixth patient, who harbours a homozygous splice-site variant in *F11R*, remains unclear. F11R deficiency has never been identifiably reported in humans. Since *F11r* $^{-/-}$ mice are highly susceptible to liver injury [32–34] and since deficiency of other tight junction proteins, namely tight junction protein 2 and claudin-1, is associated with cholestatic liver disease [35, 36], to explain the proband´s phenotype as a consequence of JAM1 deficiency tempted us. That the proband´s unaffected sister carries the same *F11R* variant in homozygous state, however, casts doubt on the association. One might invoke incomplete penetrance driven by unknown genetic or environmental factors to explain this phenotypic variation, but studies in more families with JAM1 deficiency are essential to settle the matter.

An important favourable characteristic of genomic analysis technologies in general is that they are non-invasive. The clinical utility of biopsy in genetic liver diseases is limited [1]; in addition, patients or their parents may refuse liver biopsy, considering it unacceptably risky. Broader availability of RNAseq has opened the way to pathogenicity studies of candidate variants in liver-disease–causing genes expressed in extrahepatic epithelial tissues such as those accessible by nasopharyngeal swab (see S5 Table). As demonstrated in our patients with pathogenic variants in *IFT172* and *F11R*, nasopharyngeal-swab mRNA analysis can be more informative than can immunohistologic assessment of expression of a limited panel of proteins in liver-biopsy specimens. Based on this experience, we believe that combined analysis of the whole exome and of nasopharyngeal-swab mRNA will make up for loss of some information hitherto gained in genetic liver diseases via histopathologic study.

In conclusion, we confirm the clinical utility of WES in patients with suspected genetic cholestasis. Combining WES with nasopharyngeal-swab mRNA analysis improves interpretation of WES data. Our findings suggest association of *IFT172* variants with primary cholestatic liver disease which awaits confirmation by additional similar observations.

Supporting information

S1 File. List of referring centres.
(DOCX)

S1 Table. Antibodies.
(DOCX)

S2 Table. Sequence based reagents.
(DOCX)

S3 Table. Variants detected by initial Sanger sequencing in 60 excluded patients.
(DOCX)

S4 Table. Clinical diagnosis and variants found by initial Sanger sequencing in 34 enrolled patients.
(DOCX)

S5 Table. Nasopharyngeal swab expression of cholestasis and ciliopathy genes.
(DOCX)

S1 Fig. Retinal findings in patient homozygous for the *IFT172* c.167A>C variant.
(PDF)

S2 Fig. Molecular findings, family with JAM1 deficiency.
(PDF)

S1 Checklist. STROBE statement—checklist of items that should be included in reports of observational studies.
(DOCX)

Acknowledgments

We thank Lucie Budišová for excellent technical assistance, Natálie Rysková for analysis of control Roma exomes and genomes, and all physicians who referred their patients for genetic testing.

Author Contributions

Conceptualization: Milan Jirsa.

Data curation: Markéta Šafaříková, Hana Zůnová, Lenka Mrázová, Alena Vrbacká.

Formal analysis: Elżbieta Ciara, Lucie Pfeiferová, Hana Zůnová, Lenka Mrázová, Viktor Stránecký.

Funding acquisition: Tomáš Zima, Milan Macek, Stanislav Kmoch, Milan Jirsa.

Investigation: Magdaléna Neřoldová, Elżbieta Ciara, Petra Lišková, Markéta Šafaříková, Hana Zůnová, Lenka Mrázová, Alena Vrbacká, Ondřej Fabián, Eva Sticová, A. S. Knisely.

Project administration: Milan Jirsa.

Resources: Janka Slatinská, Soňa Fraňková, Radana Kotalová, Janka Globinovská, Daniela Skanderová, Jan Šperl, Joanna Pawlowska.

Supervision: Marta Kalousová, Tomáš Zima, Milan Macek, Stanislav Kmoch, Milan Jirsa.

Validation: Magdaléna Neřoldová.

Visualization: Magdaléna Neřoldová, Petra Lišková.

Writing – original draft: Magdaléna Neřoldová.

Writing – review & editing: Elżbieta Ciara, Petra Lišková, Marta Kalousová, A. S. Knisely, Stanislav Kmoch, Milan Jirsa.

References

1. Ibrahim SH, Kamath BM, Loomes KM, Karpen SJ. Cholestatic liver diseases of genetic etiology: Advances and controversies. Hepatology. 2022; 75(6):1627–46. https://doi.org/10.1002/hep.32437 PMID: 35229330
2. Karpen SJ, Kamath BM, Alexander JJ, Ichetovkin I, Rosenthal P, Sokol RJ, et al. Use of a comprehensive 66-gene cholestasis sequencing panel in 2171 cholestatic infants, Children, and Young Adults. J

Pediatr Gastroenterol Nutr. 2021; 72(5):654–60. https://doi.org/10.1097/MPG.0000000000003094 PMID: 33720099

3. Pengelly RJ, Ward D, Hunt D, Mattocks C, Ennis S. Comparison of Mendeliome exome capture kits for use in clinical diagnostics. Sci Rep. 2020; 10(1):3235. https://doi.org/10.1038/s41598-020-60215-y PMID: 32094380
4. Hakim A, Zhang X, DeLisle A, Oral EA, Dykas D, Drzewiecki K, et al. Clinical utility of genomic analysis in adults with idiopathic liver disease. J Hepatol. 2019; 70(6):1214–21. https://doi.org/10.1016/j.jhep.2019.01.036 PMID: 31000363
5. Luan W, Hao CZ, Li JQ, Wei Q, Gong JY, Qiu YL, et al. Biallelic loss-of-function ZFYVE19 mutations are associated with congenital hepatic fibrosis, sclerosing cholangiopathy and high-GGT cholestasis. J Med Genet. 2021; 58(8):514–25. https://doi.org/10.1136/jmedgenet-2019-106706 PMID: 32737136
6. Gao E, Cheema H, Waheed N, Mushtaq I, Erden N, Nelson-Williams C, et al. Organic solute transporter alpha deficiency: A disorder with cholestasis, liver fibrosis, and congenital diarrhea. Hepatology. 2020; 71(5):1879–82. https://doi.org/10.1002/hep.31087 PMID: 31863603
7. Unlusoy Aksu A, Das SK, Nelson-Williams C, Jain D, Ozbay Hosnut F, Evirgen Sahin G, et al. Recessive mutations in KIF12 cause high gamma-glutamyltransferase cholestasis. Hepatol Commun. 2019; 3(4):471–7. https://doi.org/10.1002/hep4.1320 PMID: 30976738
8. Maddirevula S, Alhebbi H, Alqahtani A, Algoufi T, Alsaif HS, Ibrahim N, et al. Identification of novel loci for pediatric cholestatic liver disease defined by KIF12, PPM1F, USP53, LSR, and WDR83OS pathogenic variants. Genet Med. 2019; 21(5):1164–72. https://doi.org/10.1038/s41436-018-0288-x PMID: 30250217
9. Gonzales E, Taylor SA, Davit-Spraul A, Thebaut A, Thomassin N, Guettier C, et al. MYO5B mutations cause cholestasis with normal serum gamma-glutamyl transferase activity in children without microvillous inclusion disease. Hepatology. 2017; 65(1):164–73. https://doi.org/10.1002/hep.28779 PMID: 27532546
10. Gomez-Ospina N, Potter CJ, Xiao R, Manickam K, Kim MS, Kim KH, et al. Mutations in the nuclear bile acid receptor FXR cause progressive familial intrahepatic cholestasis. Nat Commun. 2016; 7:10713. https://doi.org/10.1038/ncomms10713 PMID: 26888176
11. Burdick KJ, Cogan JD, Rives LC, Robertson AK, Koziura ME, Brokamp E, et al. Limitations of exome sequencing in detecting rare and undiagnosed diseases. Am J Med Genet A. 2020; 182(6):1400–6. https://doi.org/10.1002/ajmg.a.61558 PMID: 32190976
12. Robinson JT, Thorvaldsdottir H, Winckler W, Guttman M, Lander ES, Getz G, et al. Integrative genomics viewer. Nat Biotechnol. 2011; 29(1):24–6. https://doi.org/10.1038/nbt.1754 PMID: 21221095
13. Richards S, Aziz N, Bale S, Bick D, Das S, Gastier-Foster J, et al. Standards and guidelines for the interpretation of sequence variants: a joint consensus recommendation of the American College of Medical Genetics and Genomics and the Association for Molecular Pathology. Genet Med. 2015; 17(5):405–24. https://doi.org/10.1038/gim.2015.30 PMID: 25741868
14. Kopanos C, Tsiolkas V, Kouris A, Chapple CE, Albarca Aguilera M, Meyer R, et al. VarSome: the human genomic variant search engine. Bioinformatics. 2019; 35(11):1978–80. https://doi.org/10.1093/bioinformatics/bty897 PMID: 30376034
15. Li H. Minimap2: pairwise alignment for nucleotide sequences. Bioinformatics. 2018; 34(18):3094–100. https://doi.org/10.1093/bioinformatics/bty191 PMID: 29750242
16. Didion JP, Martin M, Collins FS. Atropos: specific, sensitive, and speedy trimming of sequencing reads. PeerJ. 2017; 5:e3720. https://doi.org/10.7717/peerj.3720 PMID: 28875074
17. Patro R, Duggal G, Love MI, Irizarry RA, Kingsford C. Salmon provides fast and bias-aware quantification of transcript expression. Nat Methods. 2017; 14(4):417–9. https://doi.org/10.1038/nmeth.4197 PMID: 28263959
18. Love MI, Huber W, Anders S. Moderated estimation of fold change and dispersion for RNA-seq data with DESeq2. Genome Biol. 2014; 15(12):550. https://doi.org/10.1186/s13059-014-0550-8 PMID: 25516281
19. Otto EA, Tory K, Attanasio M, Zhou W, Chaki M, Paruchuri Y, et al. Hypomorphic mutations in meckelin (MKS3/TMEM67) cause nephronophthisis with liver fibrosis (NPHP11). J Med Genet. 2009; 46(10):663–70. https://doi.org/10.1136/jmg.2009.066613 PMID: 19508969
20. Ellingwood SS, Cheng A. Biochemical and clinical aspects of glycogen storage diseases. J Endocrinol. 2018; 238(3):R131–R41. https://doi.org/10.1530/JOE-18-0120 PMID: 29875163
21. Steinbacher T, Kummer D, Ebnet K. Junctional adhesion molecule-A: functional diversity through molecular promiscuity. Cell Mol Life Sci. 2018; 75(8):1393–409. https://doi.org/10.1007/s00018-017-2729-0 PMID: 29238845

22. Ju M, Bai X, Zhang T, Lin Y, Yang L, Zhou H, et al. Mutation spectrum of COL1A1/COL1A2 screening by high-resolution melting analysis of Chinese patients with osteogenesis imperfecta. J Bone Miner Metab. 2020; 38(2):188–97. https://doi.org/10.1007/s00774-019-01039-3 PMID: 31414283

23. Karaca E, Harel T, Pehlivan D, Jhangiani SN, Gambin T, Coban Akdemir Z, et al. Genes that affect brain structure and function identified by rare variant analyses of mendelian neurologic disease. Neuron. 2015; 88(3):499–513. https://doi.org/10.1016/j.neuron.2015.09.048 PMID: 26539891

24. Diamond T, Nema N, Wen J. Hepatic ciliopathy syndromes. Clin Liver Dis (Hoboken). 2021; 18(4):193–7. https://doi.org/10.1002/cld.1114 PMID: 34745577

25. Halbritter J, Bizet AA, Schmidts M, Porath JD, Braun DA, Gee HY, et al. Defects in the IFT-B component IFT172 cause Jeune and Mainzer-Saldino syndromes in humans. Am J Hum Genet. 2013; 93(5):915–25. https://doi.org/10.1016/j.ajhg.2013.09.012 PMID: 24140113

26. Bujakowska KM, Zhang Q, Siemiatkowska AM, Liu Q, Place E, Falk MJ, et al. Mutations in IFT172 cause isolated retinal degeneration and Bardet-Biedl syndrome. Hum Mol Genet. 2015; 24(1):230–42. https://doi.org/10.1093/hmg/ddu441 PMID: 25168386

27. Schaefer E, Stoetzel C, Scheidecker S, Geoffroy V, Prasad MK, Redin C, et al. Identification of a novel mutation confirms the implication of IFT172 (BBS20) in Bardet-Biedl syndrome. J Hum Genet. 2016; 61 (5):447–50. https://doi.org/10.1038/jhg.2015.162 PMID: 26763875

28. Yamada M, Uehara T, Suzuki H, Takenouchi T, Fukushima H, Morisada N, et al. IFT172 as the 19th gene causative of oral-facial-digital syndrome. Am J Med Genet A. 2019; 179(12):2510–3. https://doi.org/10.1002/ajmg.a.61373 PMID: 31587445

29. Whitley CB, Schwarzenberg SJ, Burke BA, Freese DK, Gorlin RJ. Direct hyperbilirubinemia and hepatic fibrosis: a new presentation of Jeune syndrome (asphyxiating thoracic dystrophy). Am J Med Genet Suppl. 1987; 3:211–20. https://doi.org/10.1002/ajmg.1320280525 PMID: 3130856

30. Schmidts M. Clinical genetics and pathobiology of ciliary chondrodysplasias. J Pediatr Genet. 2014; 3 (2):46–94. https://doi.org/10.3233/PGE-14089 PMID: 25506500

31. Lehmann P, Hohberger B, Lammer R, Mardin C. Extended ganglion cell layer thickness deviation maps with OCT in glaucoma diagnosis. Front Med (Lausanne). 2021; 8:684676. https://doi.org/10.3389/fmed.2021.684676 PMID: 34150817

32. Rai RP, Liu Y, Iyer SS, Liu S, Gupta B, Desai C, et al. Blocking integrin alpha4beta7-mediated CD4 T cell recruitment to the intestine and liver protects mice from western diet-induced non-alcoholic steatohepatitis. J Hepatol. 2020; 73(5):1013–22. https://doi.org/10.1016/j.jhep.2020.05.047 PMID: 32540177

33. Gupta B, Liu Y, Chopyk DM, Rai RP, Desai C, Kumar P, et al. Western diet-induced increase in colonic bile acids compromises epithelial barrier in nonalcoholic steatohepatitis. FASEB J. 2020; 34(5):7089–102. https://doi.org/10.1096/fj.201902687R PMID: 32275114

34. Rahman K, Desai C, Iyer SS, Thorn NE, Kumar P, Liu Y, et al. Loss of junctional adhesion molecule A promotes severe steatohepatitis in mice on a diet high in saturated fat, fructose, and cholesterol. Gastroenterology. 2016; 151(4):733–46 e12. https://doi.org/10.1053/j.gastro.2016.06.022 PMID: 27342212

35. Sambrotta M, Strautnieks S, Papouli E, Rushton P, Clark BE, Parry DA, et al. Mutations in TJP2 cause progressive cholestatic liver disease. Nat Genet. 2014; 46(4):326–8. Epub 2014/03/13. doi: ng.2918 [pii] 10.1038/ng.2918. https://doi.org/10.1038/ng.2918 PMID: 24614073

36. Hadj-Rabia S, Baala L, Vabres P, Hamel-Teillac D, Jacquemin E, Fabre M, et al. Claudin-1 gene mutations in neonatal sclerosing cholangitis associated with ichthyosis: a tight junction disease. Gastroenterology. 2004; 127(5):1386–90. https://doi.org/10.1053/j.gastro.2004.07.022 PMID: 15521008